Appendix B

"Modeling of Wake-vortex Aircraft Encounters"

A Maters Thesis

Submitted to

The Department of Mechanical Engineering

Howard University

April 16, 1999

ABSTRACT

There are more people passing through the world's airports today than at any other time in history. With this increase in civil transport, airports are becoming capacity limited. In order to increase capacity and thus meet the demands of the flying public, the number of runways and number of flights per runway must be increased. In response to the demand, the National Aeronautics and Space Administration (NASA), in conjunction with the Federal Aviation Administration (FAA), airport operators, and the airline industry are taking steps to increase airport capacity without jeopardizing safety.

Increasing the production per runway increases the likelihood that an aircraft will encounter the trailing wake-vortex of another aircraft. The hazard of a wake-vortex encounter is that heavy load aircraft can produce high intensity wake turbulence, through the development of its wing-tip vortices. A smaller aircraft following in the wake of the heavy load aircraft will experience redistribution of its aerodynamic load. This creates a safety hazard for the smaller aircraft. Understanding this load redistribution is of great importance, particularly during landing and take-off.

In this research wake-vortex effects on an encountering 10% scale model of the B737-100 aircraft are modeled using both strip theory and vortex-lattice modeling methods. The models are then compared to wind tunnel data that was taken in the 30' x 60' wind tunnel at NASA Langley Research Center (LaRC). Comparisons are made to determine if the models will have acceptable accuracy when parts of the geometry are removed, such as the horizontal stabilizer and the vertical tail. A sensitivity analysis was also performed to observe how accurately the models could match the experimental data if there was a 10% error in the circulation strength. It was determined that both models show accurate results when the wing, horizontal stabilizer, and vertical tail were a part of the geometry. When the horizontal stabilizer and vertical tail were removed there were difficulties modeling the sideforce coefficient and pitching moment. With the removal of only the vertical tail unacceptable errors occurred when modeling the sideforce coefficient and yawing moment. Lift could not be modeled with either the full geometry or the reduced geometry attempts.

TABLE OF CONTENTS

LIST OF TABLES

LIST OF FIGURES

LIST OF SYMBOLS

b	wing span, ft
C_d	drag coefficient
C_l	rolling moment coefficient
c_{l_α}	2-dimensional lift curve slope, $\partial c_l / \partial \alpha$
C_L	lift coefficient
C_m	pitching moment coefficient
C_n	yawing moment coefficient
C_Y	sideforce coefficient
N_{strips}	total number of strips
R	radius from vortex center, ft
S	planform reference area, ft^2
S_i	reference area of strip i, ft^2
u	velocity component along X axis, ft/s
U	total velocity, ft/s
v	velocity component along Y axis, ft/s
V_θ	vortex tangential velocity, ft/s
w	velocity component along Z axis, ft/s
x	coordinate along X axis, ft
y	coordinate along Y axis, ft
Y	lateral axis
z	coordinate along Z axis, ft
Z	vertical axis
α	angle of attack, deg
α_N	angle of attack in a plane normal to the planform, rad
α_S	strip angle of incidence, rad
θ	pitch angle, rad
ψ	yaw angle, rad
ϕ	roll angle, rad
δ	dihedral angle, rad
β	sideslip angle, deg
Γ	vortex circulation strength, ft^2/s

Subscripts

b	reference to body axis system
$c/4$	reference to strip ¼ chord point
i	reference to strip i
L	reference to left or port vortex
R	reference to right or starboard vortex
w	wake-induced component
∞	free-stream component

CHAPTER 1: INTRODUCTION

1.1 Purpose of Study

There are more people passing through the world's airports today than at any other time in history and with this increase in civil transport, airports are becoming capacity limited. In order to increase capacity and thus meet the demands of the flying public the number of runways and the number of flights per runway must be increased. During Visual Meteorological Conditions (VMC), it is the pilot's responsibility to maintain safe separation. Under these conditions the separation distance between aircrafts during landing and takeoff are significantly lower than the distances used under Instrument Meteorological Conditions (IMC). When the aviation weather service indicates IMC there is low visibility, and it is the controller's responsibility to maintain safe separation. One way to increase production per runway is to decrease the separation distances during IMC, and research programs are underway to determine how this can be implemented safely. It has been predicted that with the new separation distances, airport capacity could be increased by 10-15 percent.

The Federal Aviation Administration (FAA), airline operators, and the National Aeronautics and Space Administration (NASA) are joining together in an effort to determine new separation distances. Present separation distances are listed in Table 1. Dunham et. al. [1] states that in order to obtain new separation distances during landing and take-off under IMC, a metric that defines an acceptable wake-vortex encounter must be developed for use in automated air-traffic-control systems. This metric is a matrix of

Table 1: U.S. wake-vortex separation standards, distances in nautical miles. [10]

Following Aircraft	Leading Aircraft		
	Heavy	Large	Small
Heavy ≥ 300,000 lb.	4	3	3
Large > 12,500 lb. and < 300,000 lb.	5	3	3
Small ≤ 12,500 lb.	6	4	3

safe distances for several leader-aircraft/follower-aircraft pairs and meteorological conditions. Before implementing the air traffic control system, the wing-tip vortices that are created during flight must also be understood. This is due to the hazardous upset that an aircraft experiences when encountering a trailing wake of a preceding larger aircraft. This wake – encounter redistributes the aerodynamic load of the aircraft and often results in loss of control. In order to develop this metric it must be understood how wing-tip vortices react under different atmospheric conditions, and what are the characteristics of a vortex generated by different aircrafts. This data must then be incorporated into simulations of wake-vortex/aircraft encounters.

In response to these factors NASA has launched the Terminal Area Productivity (TAP) program. This program consists of four areas: Air Traffic Management, Aircraft/Air Traffic Control Systems Integration, Low-Visibility Landing and Surface Operations, and Reduced Spacing Operations [2]. The Reduced Spacing Operations (RSO) component of TAP will use wind tunnel testing, piloted and unpiloted simulations, flight testing, and computational analysis [1] to develop the metric for an

acceptable wake-vortex/aircraft encounter. An Aircraft Vortex Spacing System (AVOSS) is also under development as part of the Reduced Spacing Operations. This system will account for atmospheric effects on the transport and decay of the wake. The system will also take in to account vortex sensor data and operational definitions of acceptable strengths for wake-vortex/aircraft encounters. In return the system will give separation distances between aircrafts [3].

1.2 Literature Review

During the 1970's and 1980's simulations from simple one-degree-of freedom, roll-upset models to multi-degree-of-freedom, vortex-lattice and Navier-Stokes solutions were utilized to model the effect of a vortex-wake on an encountering airplane. However, limited experimental data from wind tunnels or flight tests was available to validate the simulations. Simulation validation was provided through subjective pilot evaluation, which was used to determine hazardous conditions [2]. For example, Sammonds et. al. [4] performed a study where simulator cabs were equipped with instruments for both instrument flight rules and visual flight rules landing approach tasks. Strip theory was used to calculate the forces and moments due to the wake-vortex. Four pilots were used in this study to give their assessment of the two simulations. All pilots agreed that the simulations were comparative to actual wake-vortex encounters, although pitch, yaw, and acceleration were underrepresented. This was not seen as a major concern since the important parameter in a wake-vortex/aircraft encounter is roll. It was also found that the turbulence model produced greater intensity than would actually be experienced due to atmospheric conditions and increased decay. For validation of hazard

criteria each pilot was asked to assess the wake encounters as hazardous or nonhazardous. From this assessment it was found that bank angle gave an acceptable boundary for hazardous conditions. Ultimately, an upset of 7 degrees in bank angle was considered hazardous at low altitudes. A piloted simulation was tested by Jenkins and Hackett [5] under eighty flight conditions for approach encounters at low speeds. Vortex-lattice modeling was used and adjustments were made to simulate real flight conditions as observed by pilots using the simulator. It was found that as the wake-vortex strength increased at a fixed radius, the pilot's opinion of the realism of the encounter decreased. Further, the pilots found that by increasing pitch and yaw encounter angles the simulator better reproduced real flight conditions. They determined the simulator to be an inexpensive and effective way to study wake encounters. Hastings and Keyser [6] also did simulator testing. Encounters were determined to be acceptable or unacceptable by looking at altitude dependent bank angle and flight path deviation. It was found that the initial upset was less when the encounter was moved laterally or vertically away from the vortex center. The severity of the encounter was greatly effected by aging in ground effect. Vicroy [2] stated that the criteria involved in earlier studies like those mentioned above included: maximum bank angle, encounter altitude, vortex strength, and encounter angle. This metric was used for determining hazardous conditions, but was not be suitable for determining acceptable conditions. In later work a batch simulation was run using a simulation of a B737-100 airplane to develop an acceptable wake encounter boundary. A simple wake model that was proposed by Burnham [7] was used to model the vortex from the generating airplane. Strip theory was then used to determine the aerodynamic effect on the encountering airplane. He found that at or below 150 feet the

horizontal boundary became a limiting criteria; above 150 feet the maximum bank angle is the limiting criteria. A sensitivity study was also performed to determine the effects of using incorrect input data. It was found that mis-modeling of the vertical stabilizer has the greatest effect on the boundary values [8].

In order to model the effect a wake has on an encountering aircraft, an accurate model of the wake itself must first be developed. Greene [9] developed a simple model that was used to determine how density stratification, turbulence, and Reynolds number effect the wake decay. Due to ambient pressure with altitude, the wake is compressed as it descends. Results of Greene's model were compared to flight test measurements as well as ground test measurements and were found to be in good agreement. He also found that in the absence of stratification or turbulence the Reynolds number can account for the difference between the model and flight data. Present separation distances are for "standard atmosphere" conditions, but if there are static atmospheric conditions the wake lingers around close to two times longer than accounted for by the FAA; if there is extreme turbulence or stratification the wake decays quicker than what has been accounted for by the FAA.

A study by Stuever and Greene [10] looked at the initial wake that is created by typical aircrafts. They also looked at how the wake decays under different atmospheric conditions before finally looking at the effect the wake-vortex has on a following aircraft. This study included twenty-two aircraft models. Greene's model was used for wake strength, and strip theory was used to calculate the forces and moments experienced by the following aircraft. Hazardous boundaries, which were determined by research done for a previous piloted-simulation study, were used as the hazard criteria. The

results showed that setting separation distances due to only the weight of the leading aircraft would not give the best separation distances. Atmospheric effects play an important role in the separation and Crow instability appears to help relieve the vortex hazard. Crow instability is a process of decay where the wake takes on a sinusoidal appearance and the vortex cores begin to come together to form rings before finally dissipating [11]. They also found that the roll control inputs might prove useless when encountering a wake due to the wake's speed and strength.

Another computational model by Kandil et. al. [12] was developed which solved the three-dimensional Reynolds averaged Navier-Stokes equation and the dynamic equation for rolling motion. This program was used to determine the effects of the trailing wake vortex from a 747 generating wing on a following 747 wing. The program was run for both turbulent and laminar flows. Initially the following wing was stationary and data was collected. Then the following wing was allowed to react to the wake. It was determined that when the following wing was located in the vortex center it incurred a large rolling moment, and when the following wing was located between the vortices it incurred a loss in lifting force. Both the laminar and turbulent flow cases showed an initial flow separation on the upper and lower surfaces of the following 747 wing; the separation being smaller for the turbulent case. As the roll was increased the separation on the upper surface of the following wing increased and it was also increased for the turbulent case at which time wing tip vortex shedding occurred. Where the turbulent case exhibits a higher roll angle, the laminar case has higher decay in lift coefficient. Stewart [13] used an analytical approach to examine the effects of a wake vortex on an encountering aircraft. A single vortex was used to interact with a following wing, and

strip theory was implemented to calculate the roll effects on the encountering wing. Conservation of momentum was used to calculate the interaction. By extracting the angular momentum from the vortex they found that the rolling moment was decreased. The more momentum that is extracted the more the rolling moment is decreased up to a maximum of 30%.

Rossow and Tinling [14] studied how much a wake must decay to obtain a separation distance of 2 nautical miles. The objective here was to determine how much the wake must decay before it can be considered safe for an encountering aircraft. Previous flight simulator research was used to determine how much control capability is required to overcome a vortex interaction. After it was determined how much control was present, then a percentage was added in for aircraft maneuvers, flight-path corrections, etc. Finally, the maximum wake intensity that can safely be encountered was determined. Rossow found the criteria to be based on the ratio of the vortex-induced acceleration in roll to the aileron-induced acceleration. The vortex-to-aileron rolling moment must be less than approximately 0.5 before the wake is at an acceptable encounter magnitude, and the wake-vortex induced rolling moment coefficients must be less than 0.03. A number of possible wake alleviation schemes have been suggested, but past tests have determined that other constraints on aircraft performance must be considered.

Dunham [1] introduced models that have been utilized in the present study of trailing wakes and encountering aircraft. The models used include linear rotary approximation and Munk's transverse flow method. These models are not useful in modeling the encountering airplane, but are good for estimates of the relative order of

magnitude of the wake-vortex. Dunham also used the strip theory method which suffers from a reliance on two-dimensional aerodynamic sectional characteristics. He discussed the vortex-lattice and panel methods but although these are the preferred models, he dismissed them as more complex.

Margason et. al. [15] made an assessment of six panel methods. These methods were: Hess, VSAERO (Vortex Separation Aerodynamics Program), QUADPAN (Quadrilateral Panel Aerodynamics Program), MCAERO, vortex-lattice, and PAN AIR (Paneled Aerodynamics). Five wing-alone and two wing-body configurations were tested using these panel methods. The vortex-lattice method was not tested on all of the configurations due to its inability to represent thick surfaces. It is the simplest of the methods and utilizes linearized boundary conditions. The wing of the model configuration is separated into both chordwise and spanwise panels to form horseshoe vortices. Control points are located on each panel, and have a no flow boundary condition. The velocities are found using the Biot-Savart Law. A summation of all velocities is used to find a set of linear algebraic equations whose solution gives the horseshoe vortex strengths.

For the Hess method, prescribed chordwise vorticity distributions on lifting panels are used to model lifting configurations. The doublet strength is constant in the spanwise direction for each panel, and the Kutta condition is satisfied in order to determine the pressure. VSAERO (Vortex Separation Aerodynamics Program) and QUADPAN (Quadrilateral Panel Aerodynamics Program) are both surface singularity panel methods that use quadrilateral panels to represent three-dimensional configurations. The Neuman boundary condition is applied for panel source strengths, and Dirichlet

boundary conditions are applied internally at the panel centers. The doublet strength of the upper and lower surfaces corresponds to the net doublet strength of the wake. MCAERO and PAN AIR are two high-order Morino class methods. These methods use quadrilateral panels that are subdivided into eight triangular sub-panels. MCAERO includes Green's identity to determine a unique source-doublet specification and uses high order doublet singularities. Internal Dirichlet boundary conditions are applied at each control point. The PAN AIR code allows prediction of subsonic or supersonic linearized potential flow, and general boundary conditions can be used with this method. Margason's results showed that the panel methods were in good agreement with experimental results, but were limited by their requirement of large amounts of computer time which ultimately effects cost. The higher order panel methods had the same limitations, although they could provide accurate solutions with fewer panels. PMARC, which is described as a low order panel method was investigated by Walden et. al. [16] to determine its usefulness in modeling the forces and moments encountered by a following aircraft encountering a trailing wake-vortex. A rectangular wing was used as the wake generator and a business jet was used as the following aircraft, and the results were compared with experimental data. It was determined that the best wake technique to use with PMARC is the streamline-based wake technique. This technique integrates valid vortex velocity distributions on the following aircraft and also can model wake roll-up and trajectory. PMARC showed good agreement with experimental results at low angles of attack. The code can not model wake decay and since it is an inviscid code, can not model viscous effects.

Rossow [17] shows that most theoretical wake models assume are taken to have

zero diameter cores and infinite velocities at their centers. Consequently, results from strip theory and vortex-lattice methods are unrealistic. Rossow, therefore developed a model in which there is a flat wing which creates a wake that remains undisturbed and does not roll up. It also assumes that the vortex, which is being encountered, can not penetrate either the wing or its wake. This follows Munk's transverse flow method and simple closed form solutions could be obtained. These results are in good agreement with vortex-lattice methods for a flat plate with an aspect ratio less than two. For locations where maximum values of lift and rolling moment are located, corrections are required since the wing does not completely turn the flow of the vortex.

Brandon et. al.[18] presents the setup and method of the wind tunnel testing for this study. The purpose was to determine the feasibility of using free flight test techniques to study wake-vortex/aircraft encounters. There were five people used in this test flight: the roll and yaw pilot, the safety cable operator, the tunnel operator, the pitch pilot, and the thrust pilot. Each person was located at a position along the axis that they were operating which proved useful since their only objective was to deal with motion of the model in that direction. In the experiment, the strength of the vortex was adjusted by changing the angle of attack of the generating wing. Lasers were placed at the forward, middle, and aft positions of the vortex to enhance the axis of the vortex for accurate positioning of the following aircraft. Dynamic sensors were placed in the tunnel and on the model to obtain flight data such as: angular rates, normal-axial acceleration, side-force acceleration, angle of attack, sideslip, control-surface position, and pressure. The results proved that wind tunnel experiments could be used for studying vortex encounters, although the conditions must be well controlled. It was determined that

vertical trajectories are demanding for the pilot-operator with high-strength vortices and lateral penetration is demanding with low-strength vortices.

For years researchers have studied the trailing wake to better understand how and why it decays and how an encountering aircraft reacts to it. The creation of smaller yet safe separation distances is dependent upon the understanding of this phenomenon. Acceptable and hazardous wake-vortex/ aircraft encounter conditions must be determined. The detailed simulation information used when studying a wake-vortex encounter on a single aircraft may not be practical for fleet analysis. Simulation analysis and hazard metrics must be developed for the commercial aircraft fleet. Simple simulation models will likely be used and the errors associated with these models must be understood [2]. The present research provides the first validation of the strip theory and vortex-lattice modeling techniques. In previous research these models were not compared to experimental data. Previously they have been largely used in work utilizing simulators and they were altered according to the pilot's assessment of the realism of the encounter. Now it must be determined how accurate these models are in actual wake-vortex/aircraft encounter situations. To accomplish this task, static test data that was taken by the Vehicle Dynamics Branch at NASA's Langley Research Center in their 30'x 60' wind tunnel for a generating wing and a 10% scale model of the B737-100 as the follower aircraft will be used.

1.3 Contribution

As stated in the previous section both the strip theory model and the vortex-lattice model have been in existence for years, and over time, modifications have been made to

improve their realism. The vortex-lattice model was originally developed by Margason and Lamar [20], and at the time it could only handle uniform flow and a limited number of planforms. The vortex-lattice and strip theory models, which will be used for this research, can deal with nonuniform flow and the three planforms that will be used in this study.

To date strip theory and vortex-lattice models have been used to determine the reaction an aircraft will have when encountering a wake. As stated in the literature review, section 1.2, for these studies researchers have used pilots in a simulator to ascertain these reactions. The simulation was run and the pilots were asked to give their opinion on the realism of the simulation. If the pilot's comments were negative, modifications would be made to either the strip theory model or the vortex-lattice model; whichever was being utilized for that particular study. At that time this was the best method for studying vortex/aircraft encounters and developing a separation criteria. Researchers did not have experimental data to validate the methods against. With the increase in the number and size of aircrafts in use today it is imperative that we find a more scientific approach to determining the validity and accuracy of these models. We can no longer depend on someone's opinion for validation. This is the purpose of this research. It will give a means of determining the accuracy of the models by comparing them to a scientifically controlled experiment. This will be the first step in validating the models. Since civil transport does not operate in a controlled environment, further validation will need to be required, but this is the first step.

There are three objectives to the present research. The first is to determine the accuracy of the strip theory and vortex-lattice methods using all three planforms (wing,

horizontal stabilizer, vertical tail). Next comparisons will be made with experimental data to determine if the models still have acceptable accuracy when parts of the geometry such as the horizontal stabilizer and the vertical tail are removed. Finally a determination will be made of how dramatic the difference between the models and the experiment will be if the models have a 10% error in its circulation.

For the first objective the models should prove to be fairly accurate. Problems may occur at high angles of attack due to flow separation. When looking at the geometrical contribution if we remove both the horizontal stabilizer and the vertical tail there may be problems with pitching moments since the horizontal stabilizer compensates for pitch control. There may also be a significant difference in yawing moment since the vertical tail controls the yawing motion. It will need to be determined if the reduction in accuracy due to the removal of the planforms is significant enough to cause modeling problems, and thus cause detrimental inaccuracies in a metric for separation distances.

CHAPTER 2: METHODOLOGY

2.1 Overview of Research

The problem with developing new separation distances for aircraft is the trailing wing-tip vortices that are created in the wake. When an aircraft flies through the air it experiences a pressure difference between the top and bottom of the wing, at which time streamwise vortices develop across the span of the wing and subsequently roll-up into two wing-tip vortices. The circulation strength of the trailing vortices is a function of the aerodynamic load of the aircraft, its speed, and wingspan. If a trailing aircraft flies through the wake of a heavy-load proceeding aircraft then the aerodynamic load across the wing of the trailing aircraft will be redistributed. This redistribution of the load can produce forces and moments that cause the pilot to lose control. With the increase in the number and size of civil transport aircraft we must further our understanding of the trailing wake-vortex, its decay, and its upset potential. The decay is the process of the wake dying down and the flow returning to its initial state prior to the disturbance created by the aircraft. Several atmospheric phenomena influence the decay of the wake. For instance, the wake decays at a faster rate if there are temperature and pressure gradients in the atmosphere than if the atmosphere is stagnant. Modeling the decay of a trailing vortex in a non stratified, uniform wind field would not cause a great deal of problems, but the task is to create an accurate decay model for a turbulent wind field. The decay of the vortices is not by simple diffusion when dealing with a turbulent wind field. Instead they can be seen to go through a series of stages before decay. Initially the vortices wrap

up out of the vortex sheet leaving the trailing edge. They then go through a slow, symmetric, somewhat sinusoidal instability. The vortex cores then recede and form a wavy pattern until eventually the cores come together to form rings. After the rings have formed the wake dissipates. This behavior is known as Crow instability [10].

There are primarily two aerodynamic prediction methods used for the study and simulation of wake effects on encountering aircrafts. These methods are strip theory and vortex-lattice. Over the years they have been modified to handle turbulent wind fields, however up to now the methods have never been validated against experimental data. The strip theory and vortex-lattice methods must be validated for accuracy if they are to be used to determine the metric for acceptable encounter and thereby safe separation distances. For validation the methods will be compared to experimental data. Static tests were performed in NASA Langley's 30' x 60' wind tunnel. The static experiments measured the forces and moments of an aircraft encountering a trailing vortex. The minimum amount of geometrical information needed for acceptable accuracy of the models will also be determined. Finding the accuracy will be accomplished by comparing experimental results to model results when the vertical tail is removed from the model. Then a comparison will be made when both the horizontal stabilizer and the vertical tails have been removed from the models. The objective for this part of the study is to determine the least amount of geometrical information required for accurate results. This information will be useful to determine the least amount of geometry information required for feet wide analysis. Finally a sensitivity study of the models will be performed. With this study will be able to determine how accurate data has to be that is inputted into the models.

2.2 Approach

The approach is to compare the strip theory and vortex-lattice prediction methods to the wind tunnel data. For the wind tunnel experiment, baseline data was determined when the generating wing was removed from the wind tunnel. This data was taken to determine how the aircraft behaves in the absence of a vortex, and to determine flowfield changes inside the tunnel. The baseline data will be used in determining the difference in the forces and moments of the aircraft with and without a trailing wake encounter. Computationally, the circulation of the wake will be set equal to zero to simulate the generating wing being removed from the wind tunnel. Similar to the experiment, the change in the forces and moments will be determined by taking the data when circulation equals zero, and subtracting it from the data when the circulation is not equal to zero. A comparison of the experimental baseline data to the strip theory and vortex-lattice baseline data will be made to determine if there are any initial disturbances inside the wind tunnel. The experiment was run for both a large generating wing and a small generating wing. Several locations around the vortex including its center, have been chosen as data points. For both the experiment and the models there is an alpha sweep where the sideslip angle has been held constant and the angle of attack is varied. There is also a beta sweep where the angle of attack is held constant and the sideslip angle is varied. The sideslip angle is the angle at which the nose of the aircraft is rotated on the yaw axis from the primary flow direction. For the models these variables will be altered in a test file. The test file will also allow for changes in location around the vortex, free stream velocity, and Euler angles. The airelon flaps are set equal to zero for this research. Comparisons will be made

between the two models and the experiment for an alpha sweep when all panels are a part of the geometry. The same will then be done for a beta sweep. Data will be compared for an alpha sweep where the horizontal stabilizer and vertical tails have been removed for both models and the experimental aircraft. In the next comparison only the vertical tail will be removed. This will help to test the accuracy of the models. At this point the minimum geometry required for accurate results will be determined. In order to determine if the tails can be removed and still receive accurate results, the alpha sweep with all tails on for the experiment will be compared to the alpha sweep of the two models where the horizontal stabilizer and vertical tail are removed. Finally the beta sweep of the experiment when all tails are on will be compared to the beta sweep of the two models where the vertical tail is off.

2.3 Wind Tunnel Test

A ten-percent scaled down model of Boeing's B737-100 aircraft was used for the static test. The experiment was performed in NASA LaRC's 30'x 60' wind tunnel. The aircraft model was placed on a static mount that was used to measure the forces and moments the aircraft encountered due to the wake. The Kruger flaps were set to zero degrees. Figures 1 and 2 are pictures of the experimental setup used inside the wind tunnel. Smoke generators was utilized to aid in the visualization of the wake-vortex. The model was constructed of fiberglass and aluminum. During the experiment, both the wing and the following aircraft were inverted and measurements were resumed. This was done because a bounce back effect was noticed when the generating wing was lower than the model. Data was also taken when the horizontal stabilizer and the vertical tail

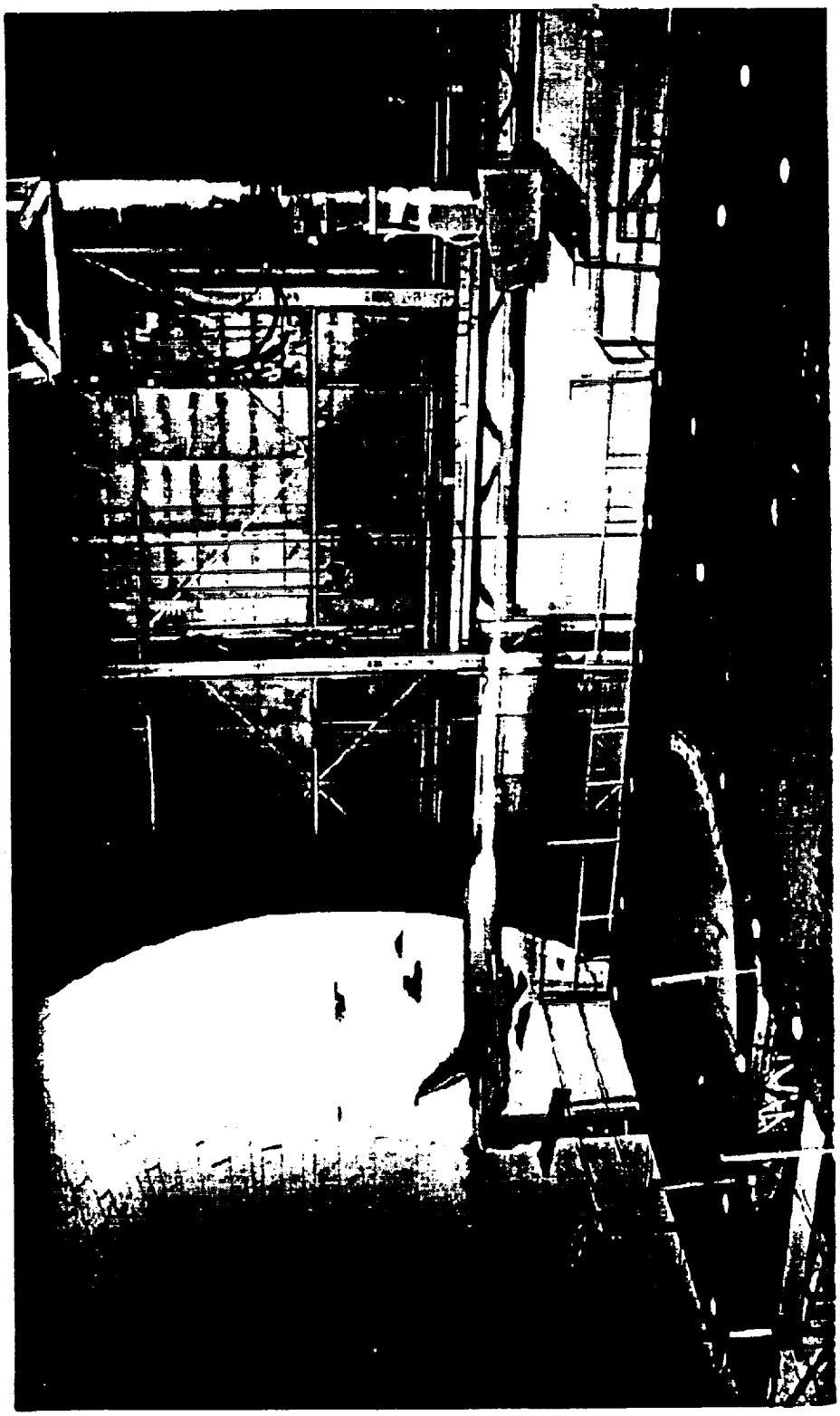

Figure 1: Photo of 30'x60' wind tunnel static test

Figure 2: Photo of 30'x60' wind tunnel static test

were removed from the aircraft model, and when only the vertical tail was removed from the model. Pressure measurements were taken with a 1/8" diameter 5-hole pressure probe. The model was removed and replaced by the probe for the pressure measurements.

Locations analyzed in this research are shown in Figure 3. Data was recorded for

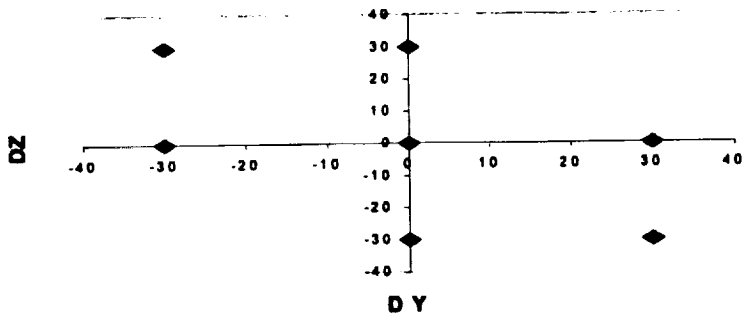

Figure 3: Locations analyzed throughout experiment

an alpha sweep when the angle of attack is varied, and a beta sweep, when the sideforce coefficient is varied. Angles for the alpha sweep are –6, -4, -2, 0, 2, 4, 6, 8, 10, and 15 degrees and for the beta sweep angles utilized are –10, -4, -2, 0, 2, 4, and 10 degrees. These angles were measured with an accelerometer that was mounted on the model. For the removal of the horizontal stabilizer and vertical tail, only the alpha sweep was taken, and for the removal of the vertical tail, only the beta sweep data was taken. Force and moment information obtained was sideforce coefficient, lift coefficient, drag coefficient, rolling moment, yawing moment, and pitching moment.

2.3.1 Generating Wing

Two separate NACA 4412 airfoil sections was used for the generating wings in experiment. These wings were simple wings without flaps to enable large variations in vortex strengths. The first wing had a span of 9.3 ft. and lift coefficient of 0.56. The second wing had a span of 18.6 ft and lift coefficient of 0.28. The angle of attack of the wing determines the circulation strength of the induced vortex. The lift coefficient is directly proportional to the circulation strength. For the large wing the circulation strength was set to 0.28 and for the small wing it was set to 0.56. The wing had a constant distance of 300 in. from the following aircraft. It was mounted on a movable tunnel survey carriage. Smoke generators were placed on the sides of the wing so that the wing-tip vortices created could be seen. The carriage was then positioned at various locations for placement of the vortex with respect to the following aircraft. The center of the vortex was location (0,0).

2.4 Strip Theory

Strip theory modeling utilizes the wing planforms to measure the aerodynamic forces and moments which an aircraft experiences during a wake encounter. Each wing is separated into chordwise strips, and each strip is modeled as a two dimensional airfoil (Figure 4). The strips are defined by their area, dihedral angle, angle of incidence, lift curve slope, quarter chord and three quarter chord point at the midspan of each strip. When running the strip theory program, a number of files are needed. There is an input file, a wake file, and a test file. To begin Computer Aided Design, drawings of the 10% scale model along with detailed drawing of the B737-100 received from Boeing were used to

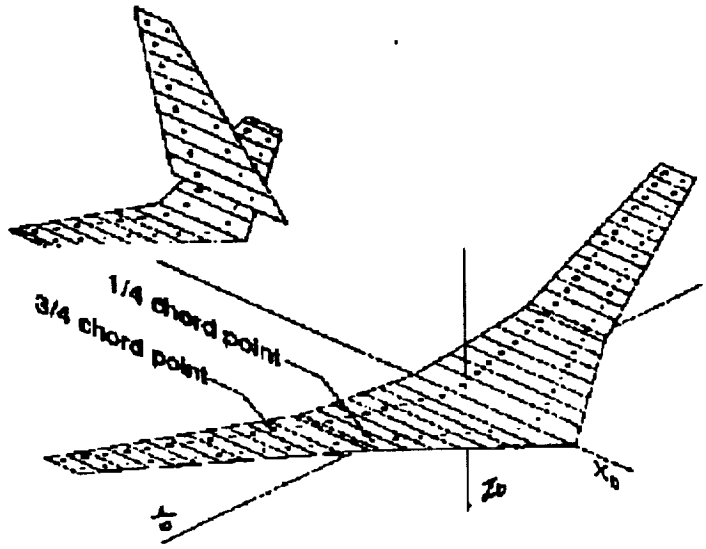

Figure 4: Strip model of B737-100. [8]

determine the correct dimensions of the following aircraft. Once all dimensions are verified, the number and sizes of the chordwise strips is calculated. The input file is then created which lists the number of planforms, the reference area, the reference chord length, and the wing span. The number of strips per planform is also listed for each planform. For each strip, the ¼ chord point, the ¾ chord point, the y-coordinate, the z-coordinate, the reference area, the dihedral angle, the lift curve slope, and the strip angle of attack are recorded. The wake file contains the information about the vortex, which will be explained in more detail later. The test file is the file which allows us to change our location and orientation of the following aircraft.

Reimer and Vicroy [19] describe the method used in strip theory to calculate the

forces and moments. They begin by finding the freestream velocity and local wind velocity at the three-quarter-chord point of each strip. They use the following transformation to translate the inertial velocities to velocities relative to the body axis.

$$\begin{pmatrix} u_b \\ v_b \\ w_b \end{pmatrix} = \begin{pmatrix} \cos\theta\cos\psi & \cos\theta\sin\psi & -\sin\theta \\ \sin\phi\sin\theta\cos\psi - \sin\psi\cos\phi & \sin\psi\sin\theta\sin\phi + \cos\psi\cos\phi & \sin\phi\cos\theta \\ \cos\psi\cos\phi\sin\theta + \sin\psi\sin\phi & \sin\psi\cos\phi\sin\theta + \cos\psi\sin\phi & \cos\phi\cos\theta \end{pmatrix} \begin{pmatrix} u_i \\ v_i \\ w_i \end{pmatrix} \quad 2.4.1$$

Where θ is the pitch angle, ψ is the yaw angle, and ϕ is the roll angle. The local velocity is found by summing the freestream velocities, denoted by ∞, and the wake induced velocities of each strip:

$$\begin{aligned} u_i &= u_\infty + u_{w_i} \\ v_i &= v_\infty + v_{w_i} \\ w_i &= w_\infty + w_{w_i}. \end{aligned} \quad 2.4.2$$

The local angle of attack normal to the planform is then computed for the right half of the planforms, which lie in the horizontal direction,

$$\alpha_{N_i} = \alpha_{s_i} + \tan^{-1}\left(\frac{w_i\cos\delta_i - v_i\sin\delta_i}{u_i}\right) \quad 2.4.3$$

and for the left half of the planforms which lie in the horizontal direction.

$$\alpha_{N_i} = \alpha_{s_i} + \tan^{-1}\left(\frac{w_i\cos\delta_i + v_i\sin\delta_i}{u_i}\right) \quad 2.4.4$$

For the planforms which lie in the vertical direction, the dihedral, δ, is set to 90°, and the angle of attack is the negative of the sideslip angle. Incremental lift and sideforce coefficients can now be computed by:

$$C_{L_i} = \frac{S_i}{S} c_{l_i} \alpha_{N_i} \cos\delta_i \qquad 2.4.5$$

$$C_{Y_i} = \frac{S_i}{S} c_{l_i} \alpha_{N_i} \sin\delta_i \qquad 2.4.6$$

Where S is the planform reference area, and S_i is the reference area of strip i, and c_{l_i} is the two-dimensional lift curve slope of each strip i. Finally, the incremental forces and moments can be summed:

$$C_L = \sum_{i=1}^{N_{strips}} C_{L_i} \qquad 2.4.7$$

$$C_Y = \sum_{i=1}^{N_{strips}} C_{Y_i} \qquad 2.4.8$$

$$C_l = \frac{1}{b} \sum_{i=1}^{N_{strips}} \left(C_{L_i} y_{c/4_i} + C_{Y_i} z_{c/4_i} \right) \qquad 2.4.9$$

$$C_m = \frac{1}{c} \sum_{i=1}^{N_{strips}} C_{L_i} x_{c/4_i} \qquad 2.4.10$$

$$C_n = \frac{1}{b} \sum_{i=1}^{N_{strips}} C_{Y_i} x_{c/4_i} . \qquad 2.4.11$$

Where $x_{c/4_i}$, $y_{c/4_i}$, and $z_{c/4_i}$ are the coordinates of the quarter-cord point. Drag is neglected in this model.

The objective is to determine the forces and moments that act on each incremental panel then to sum all the contributions to determine the reaction over the entire aircraft. To determine the effect the wake has on the aircraft, the change in the forces and moments are computed by taking the difference in the results which include an encountering wake from the calculation when the is no encountering wake.

$$\Delta C_{L_w} = C_{L_{wake}} - C_{L_{nowake}} \qquad 2.4.12$$

2.5 Vortex-Lattice Model

Changes have been made to the vortex-lattice program, which was developed by Margason and Lamar [20] to account for nonuniform flow and an increased number of planforms. A detailed description of the calculations and approach for the vortex-lattice model can be found in [21] by D. Vicroy. This method is the same as that of the strip theory method since only the wing sections are utilized for the geometry and thickness is neglected. The sections of each wing are separated into both chordwise and spanwise directions to form many elemental panels. The vortex-lattice model must satisfy a no-flow boundary condition at the ¾-chord point. This means that at the ¾-chord of each panel the flow can not flow perpendicular to the plane of the panel and match the angle of attack of the ¾-chord point. A horseshoe vortex is also associated with each panel. A vortex filament is located in the spanwise direction at the ¼-chord point and a vortex filament extends from the ¼-chord point on both sides of the panel and extends in the

chordwise direction to infinity, this is illustrated in Figure 5. The Kutta-Joukowski theorem is then used to determine the lift associated with each panel. A summation of the lift across the entire planform is performed and the information is used to determine the aerodynamic characteristics of the encountering aircraft. As in the strip theory model, three files are used to run the vortex-lattice model, the geometry file, the wake file, and the test file. The geometry file is setup in the same manner as the strip theory geometry file, but there will be more panels to deal with since the panels are separated in both spanwise and chordwise directions. The other two files will be used in the same manner as they were used in the strip theory model.

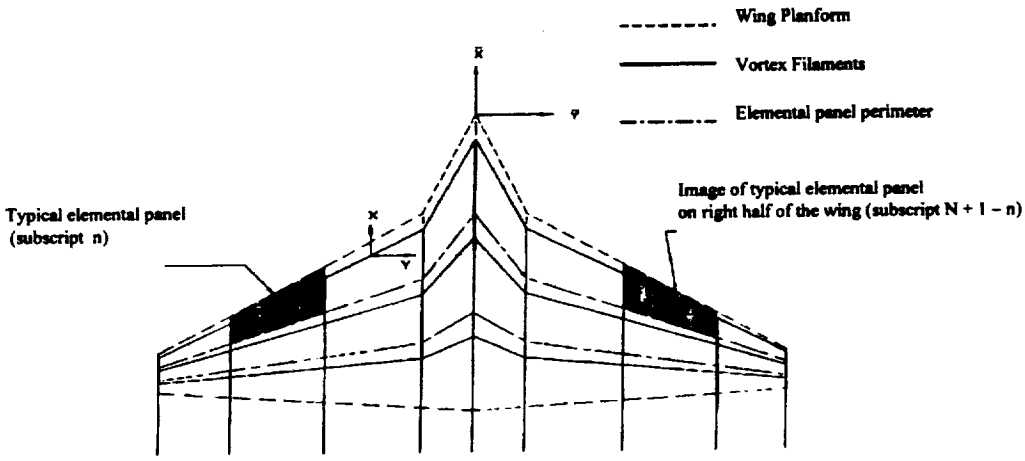

Figure 5: General layout of axis systems, elemental panels, and horseshoe vortices for a typical wing planform. [20]

2.6 Wake-Vortex Model

The wake file that is used in the model programs contains information about the

circulation of the vortex which is defined by

$$\Gamma = \frac{2C_L U_\infty^2 S}{\pi b}. \qquad 2.6.13$$

Where C_L is the lift coefficient, U_∞ is the freestream velocity, S is the planform area, and b is the wing span. The model also utilizes information about the core radius and location (y,z) of the two counter-rotating vortices. The wake model used was originally presented by Burnham [7]. The main idea is to match actual measured velocity data of airplane wakes. In our case the model will fit the velocity measurements that were taken during the wind tunnel experiment. The velocity measured at numerous points during the experiment will be used as input for the wake program which will then return the vortex location and strength. Figure 6 shows a drawing of the vortex model. This model defines the tangential velocity in a single vortex, and also shows the downwash and

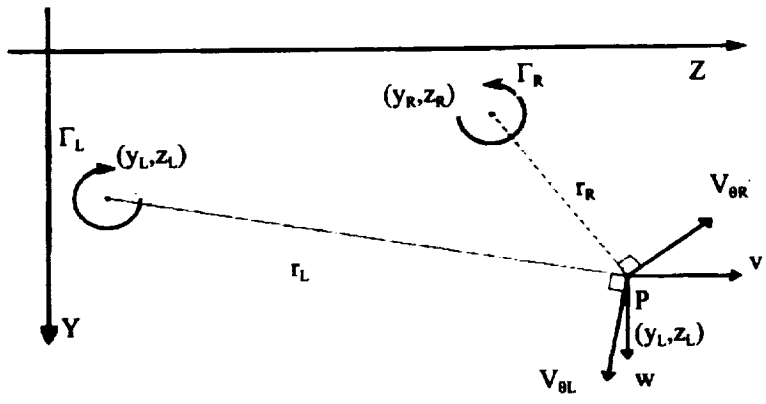

Figure 6: Two dimensional wake model. [8]

sidewash velocity components. Figures 7 and 8 shows the experimental, model, and error in the sidewash and downwash velocity distribution for the large generating wing. Figures 9 and 10 shows the experimental, model, and error in the sidewash and downwash velocity distribution for the small generating wing. For both cases the experimental velocity and model velocity are in good agreement as can be seen by the error.

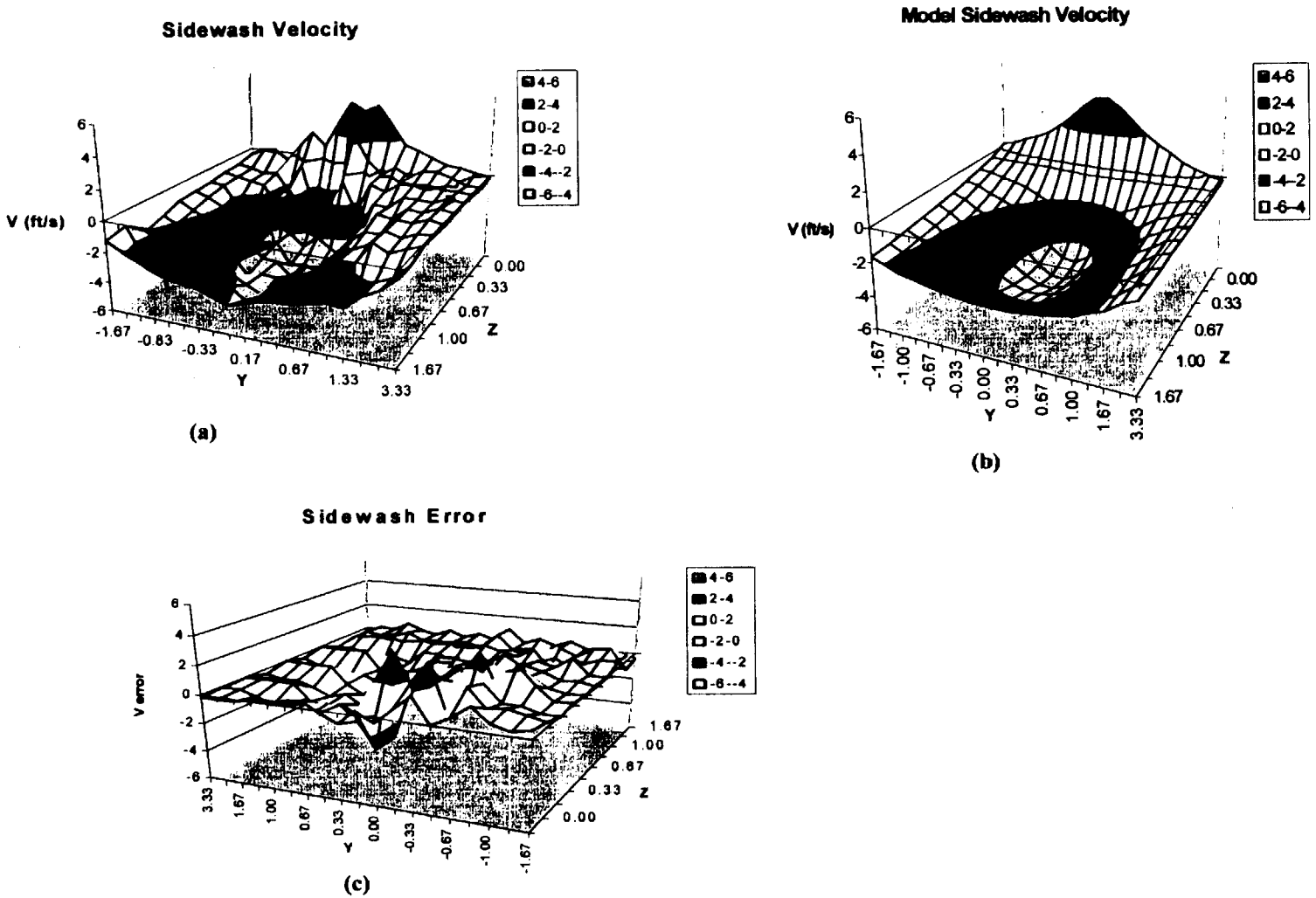

Figure 7: Large Generating Wing Lift Coefficient (CL) = 0.56. (a) Experimental Sidewash Velocity Data (b) Model Sidewash Velocity (c) Model Sidewash Velocity Error Data

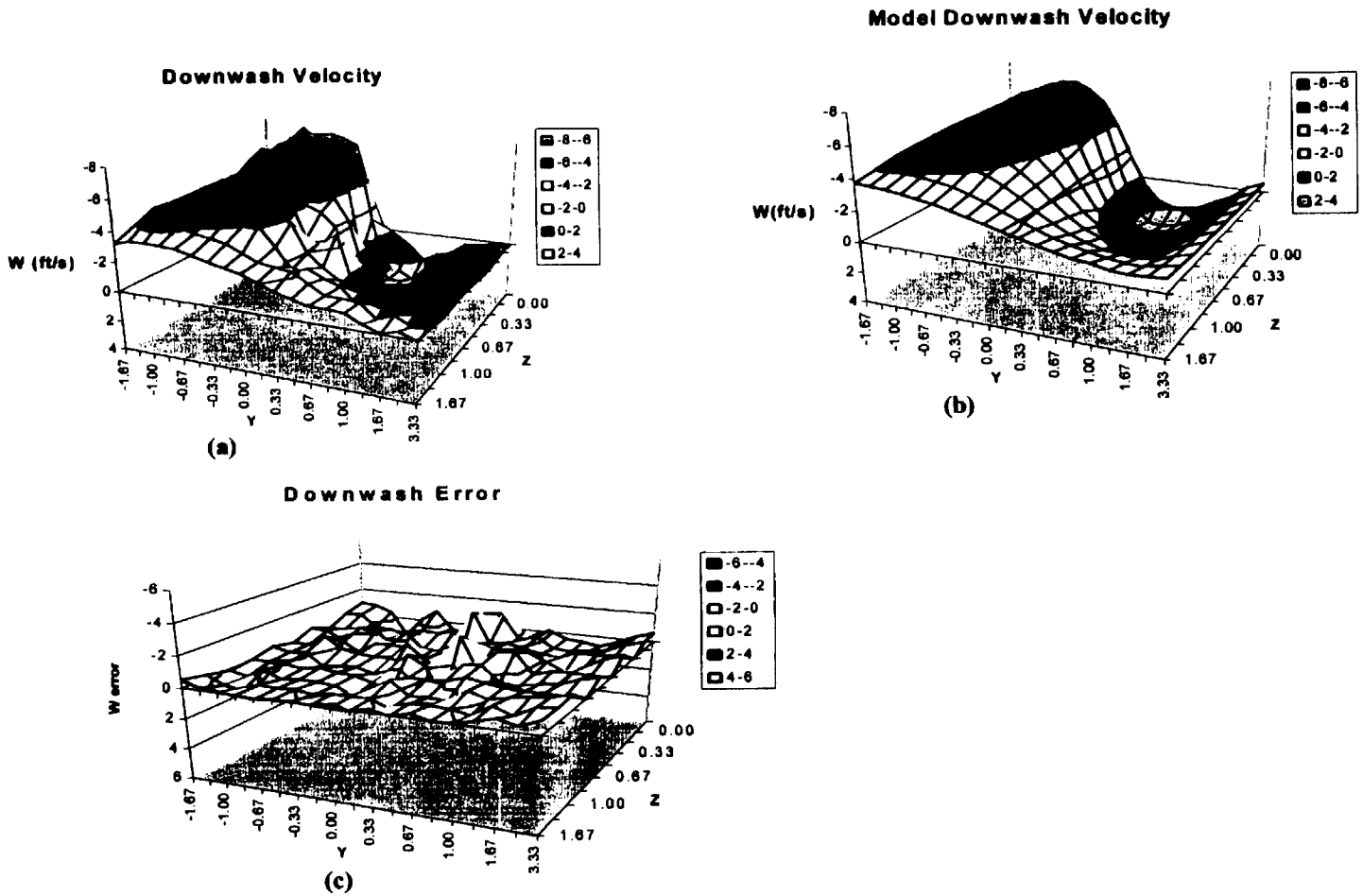

Figure 8: Large Generating Wing Lift Coefficient (CL) = 0.56. (a) Experimental Downwash Velocity Data (b) Model Downwash Velocity (c) Model Downwash Velocity Error Data

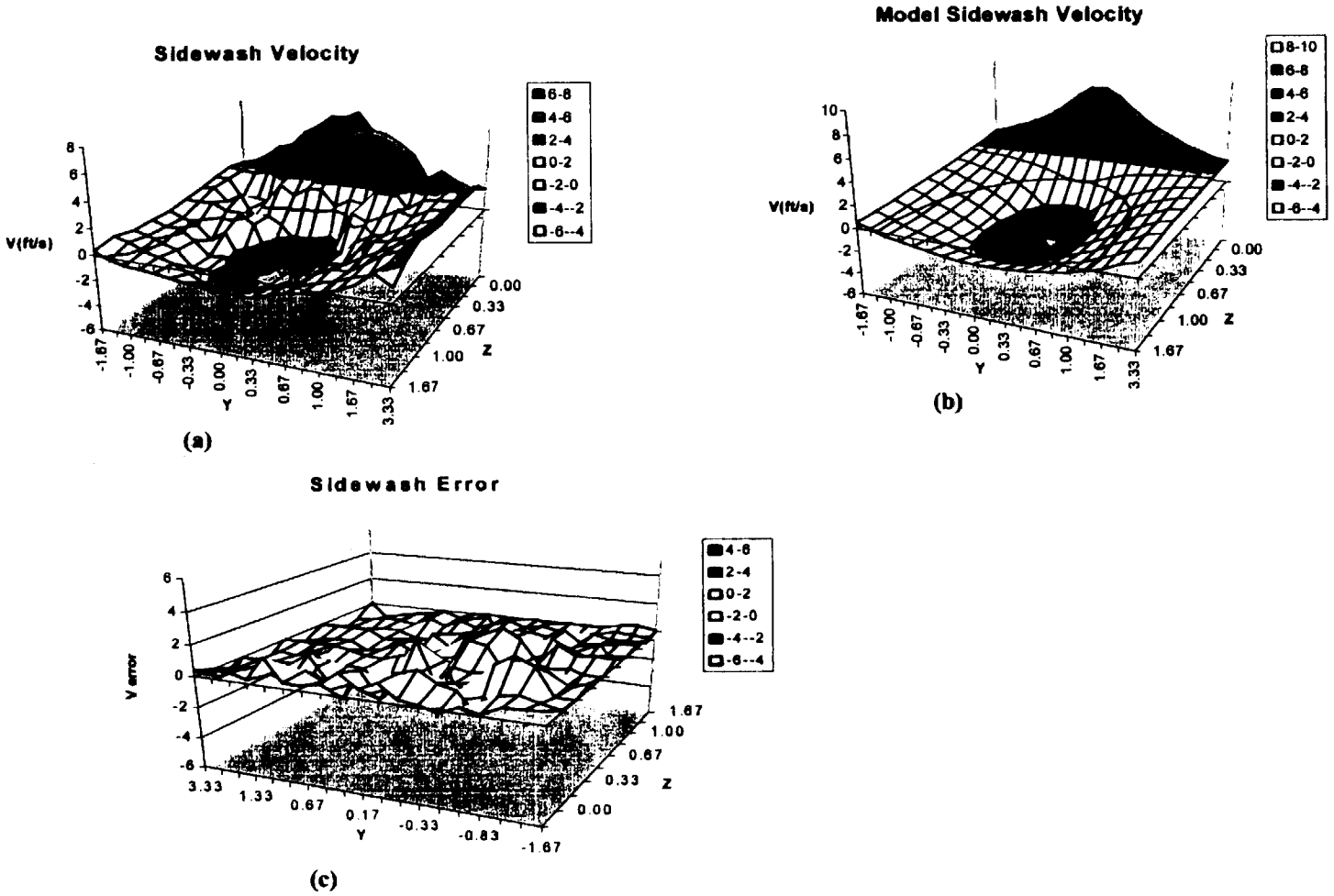

Figure 9: Small Generating Wing Lift Coefficient (CL) = 0.28. (a) Experimental Sidewash Velocity Data (b) Model Sidewash Velocity (c) Model Sidewash Velocity Error Data

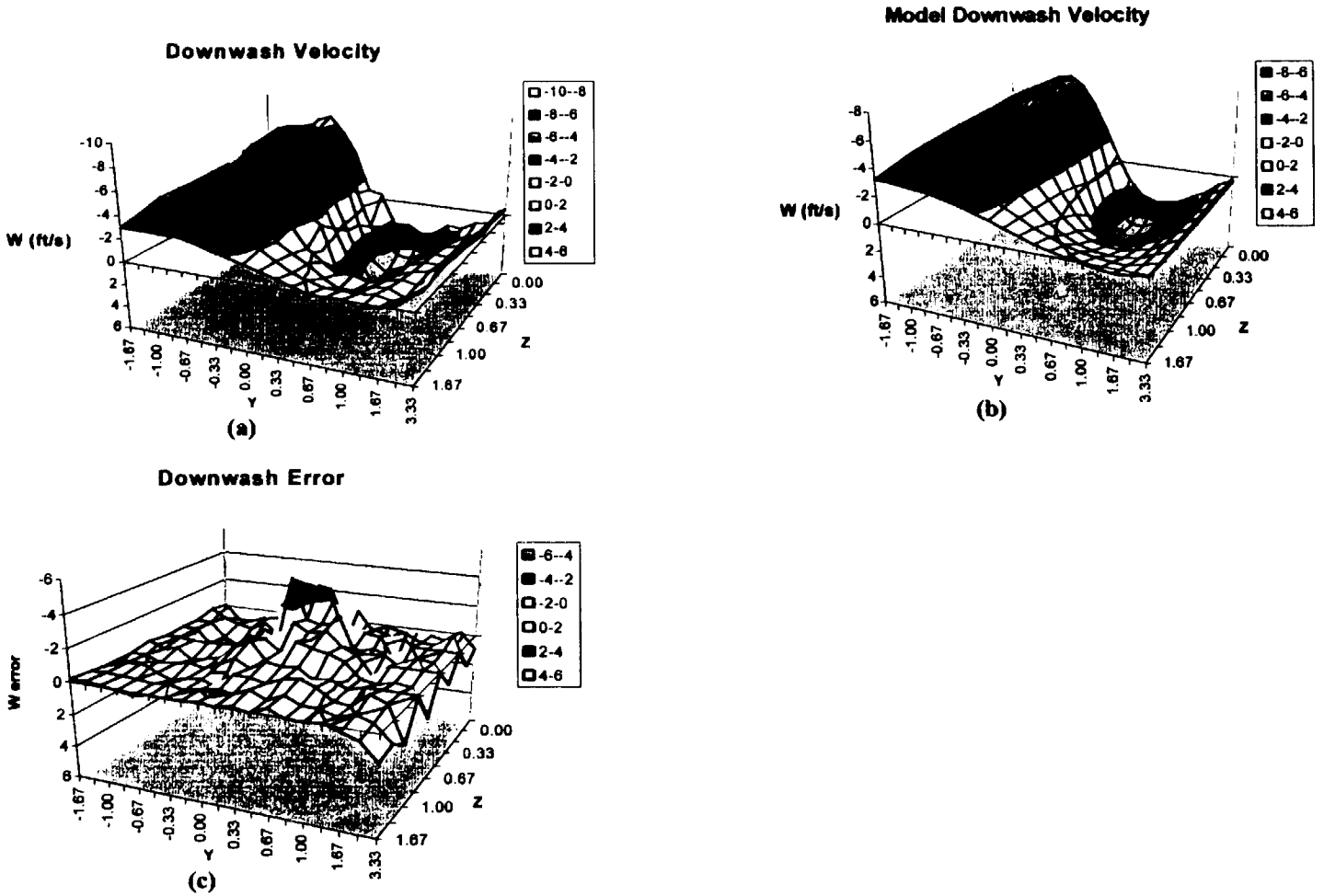

Figure 10: Small Generating Wing Lift Coefficient (CL) = 0.28. (a) Experimental Downwash Velocity Data (b) Model Downwash Velocity (c) Model Downwash Velocity Error Data

CHAPTER 3: RESULTS

There are three objectives in predicting wake-vortex induced forces and moments on an encounter airplane:

a) Assess the accuracy of strip theory and vortex-lattice methods.

b) Assess the accuracy of strip theory and vortex-lattice methods when reduced geometry is used.

c) Assess the accuracy of strip theory and vortex-lattice methods when a sensitivity study is performed.

Using strip theory modeling and vortex-lattice modeling, it is to be determined if the two models will be able to accurately regenerate the reactions an aircraft will have when encountering a wake-vortex. For this part of the project an alpha sweep, when the angle of attack varies, and a beta sweep, when the sideslip angle varies, will be analyzed for each force and moment for both the large generating wing and the small generating wing. The geometry will consist of the wing, horizontal stabilizer, and vertical tail for both models and the experiment. The changes in forces and moments will be calculated by the formula:

$$\text{Change (F\&M)} = (\text{F\&M})_{\text{Wake}} - (\text{F\&M})_{\text{No Wake}} \qquad 3.0.14$$

where (F&M) denotes the forces and moments. This change measures how the aircraft is reacting to its encounter with the wake-vortex.

The second part of the project consists of determining the minimum geometrical information required to give accurate results. First the horizontal stabilizer and the vertical tail will be removed, next data will be taken when removing only the vertical tail. The models will be compared to the experimental data taken with full geometry (e.g. geometry includes wing, horizontal stabilizer, vertical tail). Also shown in the results will be the experimental data when the respective geometry was removed. For the models the changes in the forces and moments will be calculated in a similar manner using the alpha sweep and the beta sweep. Although, since we want to know how the aircraft is reacting to the wake due to the removal of the tails we must relate our change (F&M) to the full geometry of the aircraft. Therefore, we will change equation (14) to:

$$\text{Change (F\&M)} = (\text{F\&M})_{\text{Wake (Partial Geom.)}} - (\text{F\&M})_{\text{No Wake (Full Geom.)}}. \qquad 3.0.15$$

Now we are able to analyze how the aircraft is reacting due to the removal of the tails, and make a comparison to the experimental data where all tails are on. As the last part of the project, a sensitivity analysis will be done to determine if there will be any mis-modeling if the data is ±10 percent.

Initially, it will be determined if there is a difference between the data for the small and large generating wings. If there is no difference in the model results between the two generating wings then only information for the large generating wing will be analyzed. For comparison, only the alpha and beta sweeps will be observed for full geometry situations. For the alpha sweep, only the change in sideforce coefficient, rolling moment, lift coefficient, and pitching moment will be viewed. For the beta sweep

the change in pitching moment, sideforce coefficient, lift coefficient, and pitching moment will be viewed. These forces and moments were chosen because they show the largest disturbance due to the wake-vortex for both cases.

Looking at Figure 11 it can be seen that for location (-30,30) the strip theory and vortex-lattice models for the large wing more closely match the experimental data for both the large and small generating wing. This is also the case for (0,30). At (-30,0) there is a difference between the large and small experimental data. The models more accurately model its respective experimental data, which is also the case for (30,0). At the vortex center the large and small experimental data again shows differences, and the vortex-lattice models accurately model its respective experimental data while the strip theory model shows less accuracy for both wings. Location (0,-30) shows that the experimental data is similar, but all models in this case are inaccurate. In (30,-30) the large and small experimental data has significant differences and the models for the large generating wing along with the vortex-lattice model for the small wing, more closely model the small wing experimental data. In Figure 12 for all locations the experimental data for both wings match up well. The model data for both cases also matches well except for location (0,30). Looking at the change in lift coefficient, Figure 13, it can be seen that the large and small experimental data again matches well; although, for all locations it appears that all the models overpredict the experimental data. For Figure 14 the experimental data matches for all locations except (0,30). All models, except for (-30,30) and (0,30), are also in good agreement, although they seem to predict the experimental data for the small wing better. At (-30,30) the models are not in agreement and at (0,30) the models agree between the large and small experimental data. Observing

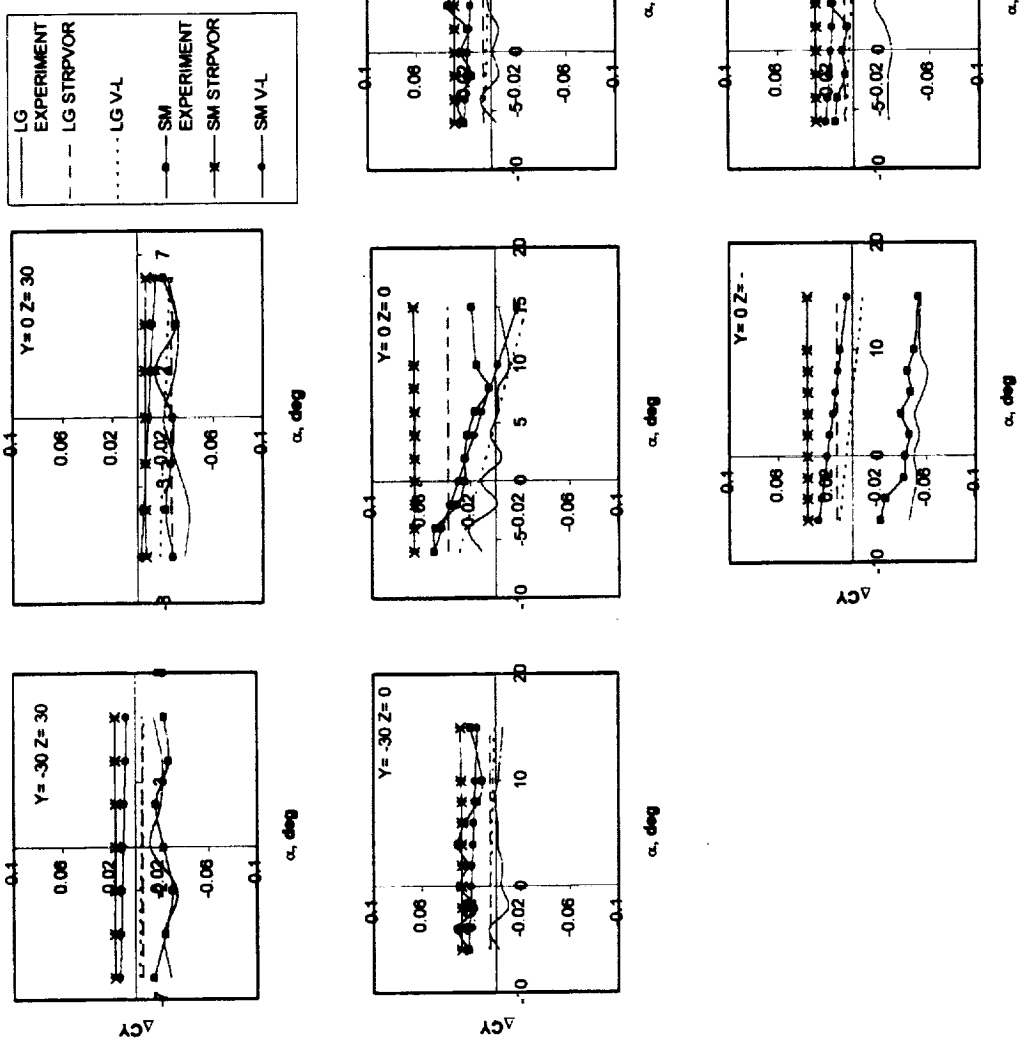

Figure 11: Change in Sideforce Coefficient - large wing and small wing comparison 30'x60' static test (β=0)

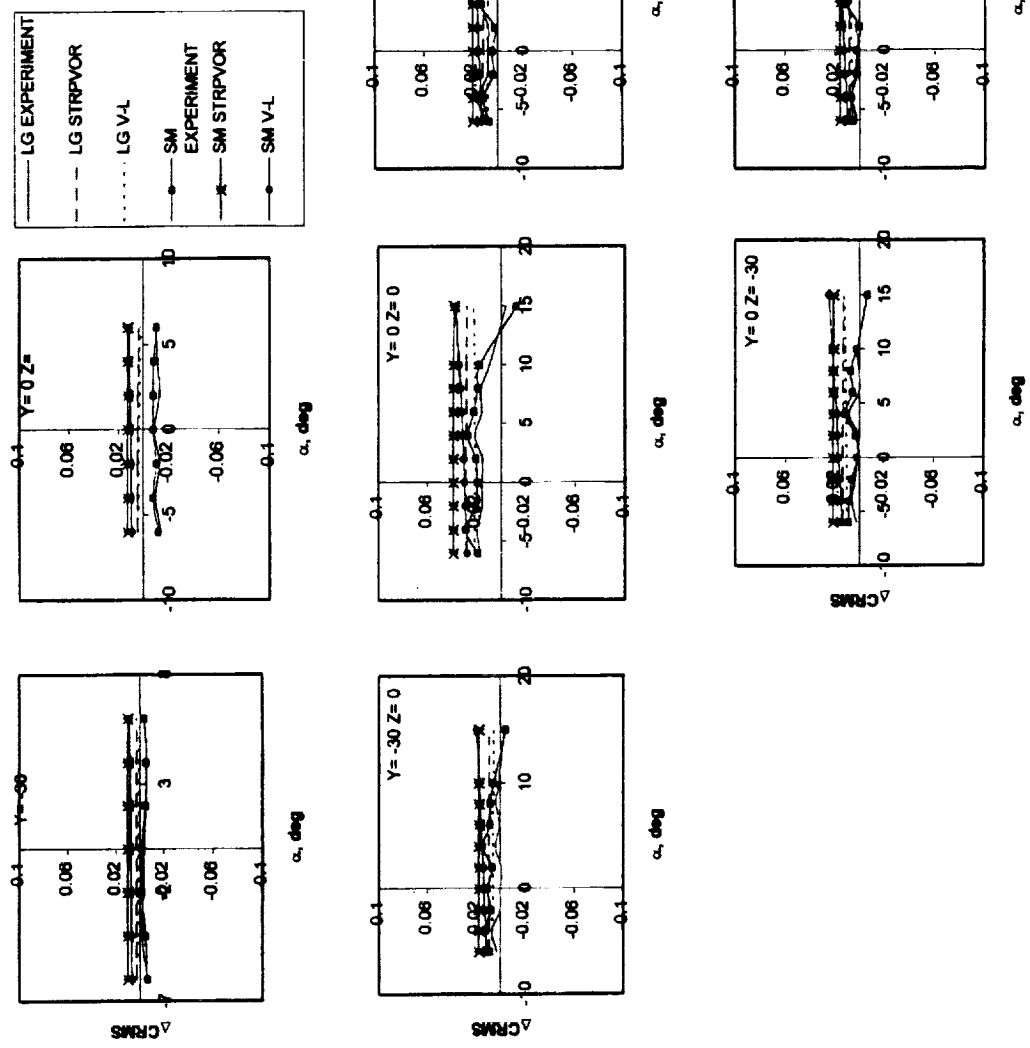

Figure 12: Change in Rolling Moment - large wing and small wing comparison 30'x60' static test (β=0)

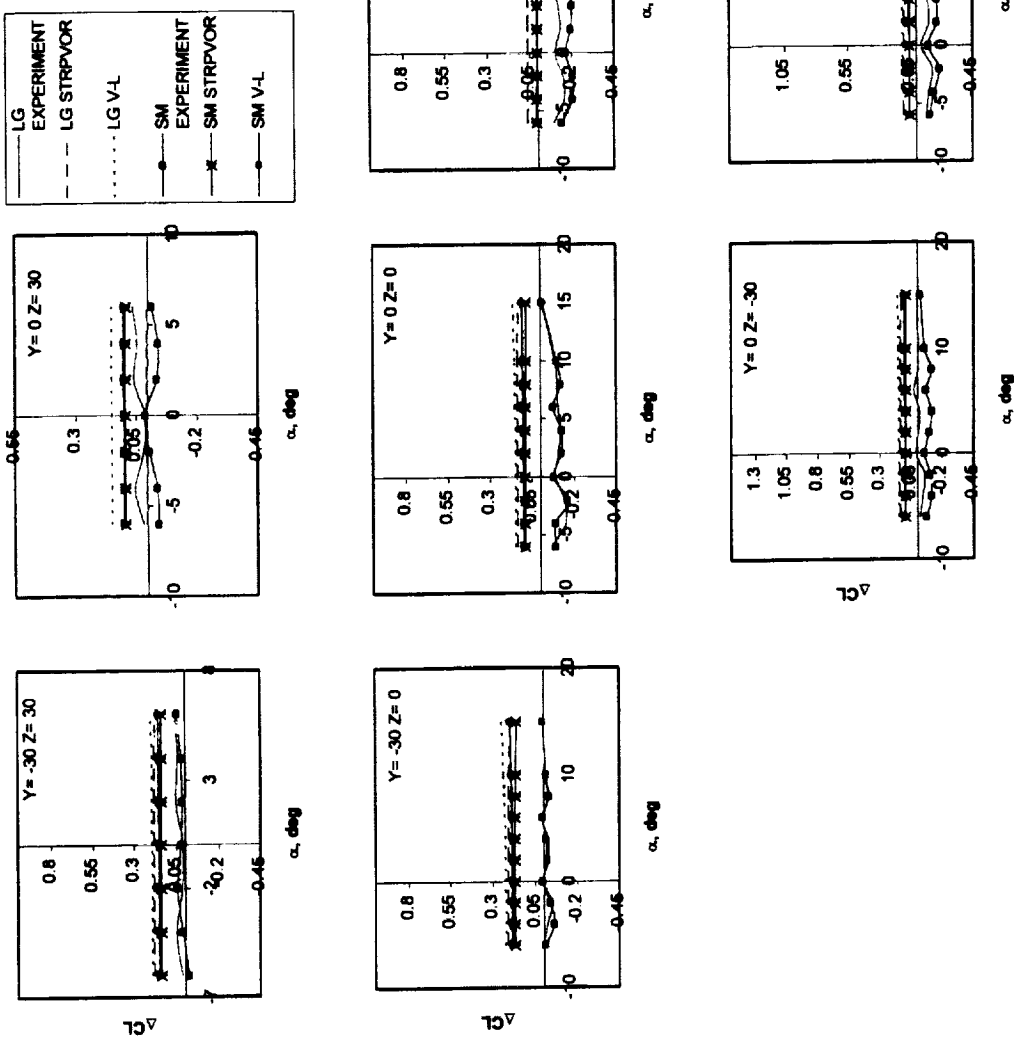

Figure 13: Change in Lift Coefficient - large wing and small wing comparison 30'x60' static test (β=0)

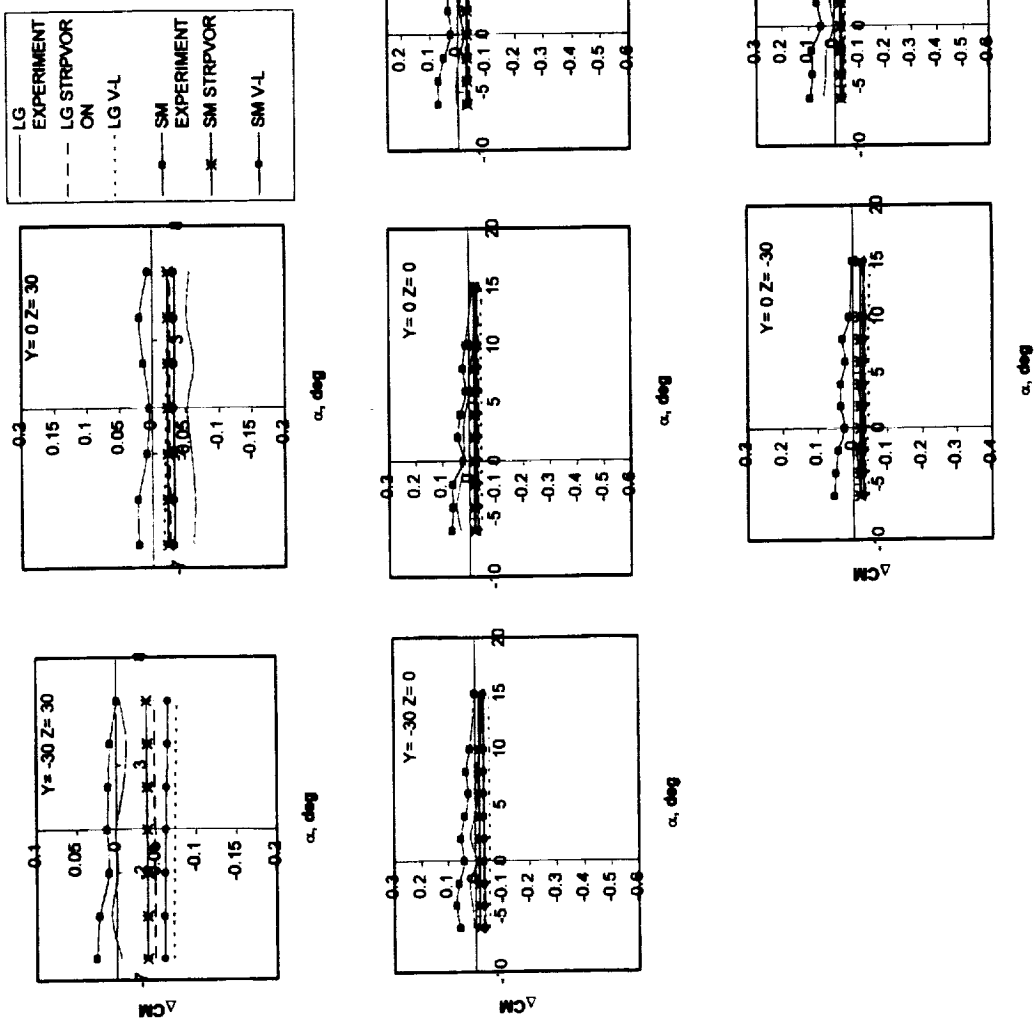

Figure 14: Change in Pitching Moment - large wing and small wing comparison 30'x60' static test (β=0)

Figure 15 the change in the sideforce coefficient for the beta sweep is similar to that of the alpha sweep except for location (0,30) and the vortex center. For (0,30) the strip theory model more accurately represent the experimental data and for (0,0) the large wing models match with the small wing experimental data. In Figure 16 the experimental data matches for both wings except at (0,30), but all models at all locations show significant differences in the results. Looking at the changes in pitching moment shown in Figure 17 it can be seen that the only locations where the experimental data resemble each other is at the vortex center and (30,0). For (-30,30), (0,30), and (-30,0) the models more closely predict the large wing data. For the remaining locations there are significant differences in the predictions of the models.

From the results described above, it appears that the data for the large and small wings are inconclusive and show no real relation to each other. The same also appears to be true for the models of the generating wings. Therefore both large and small generating wing information will be examined separately. The models will be compared to their respective generation wing to fully understand the results for its experiment.

3.1 Large Wing

Figure 18 shows the alpha sweep for the sideforce coefficient. Location (0,0), which is at the center of the vortex, shows a disturbance in the sideforce coefficient. Disturbances can also be seen at (0,-30) and (30,-30). These areas will be dominated by the crossflow (sidewash) which would be the cause of the disturbance. Location (0,30) will also have a large amount of cross flow. When comparing the models to the experiment it can be seen that at (0,0) the strip theory model deviates from the

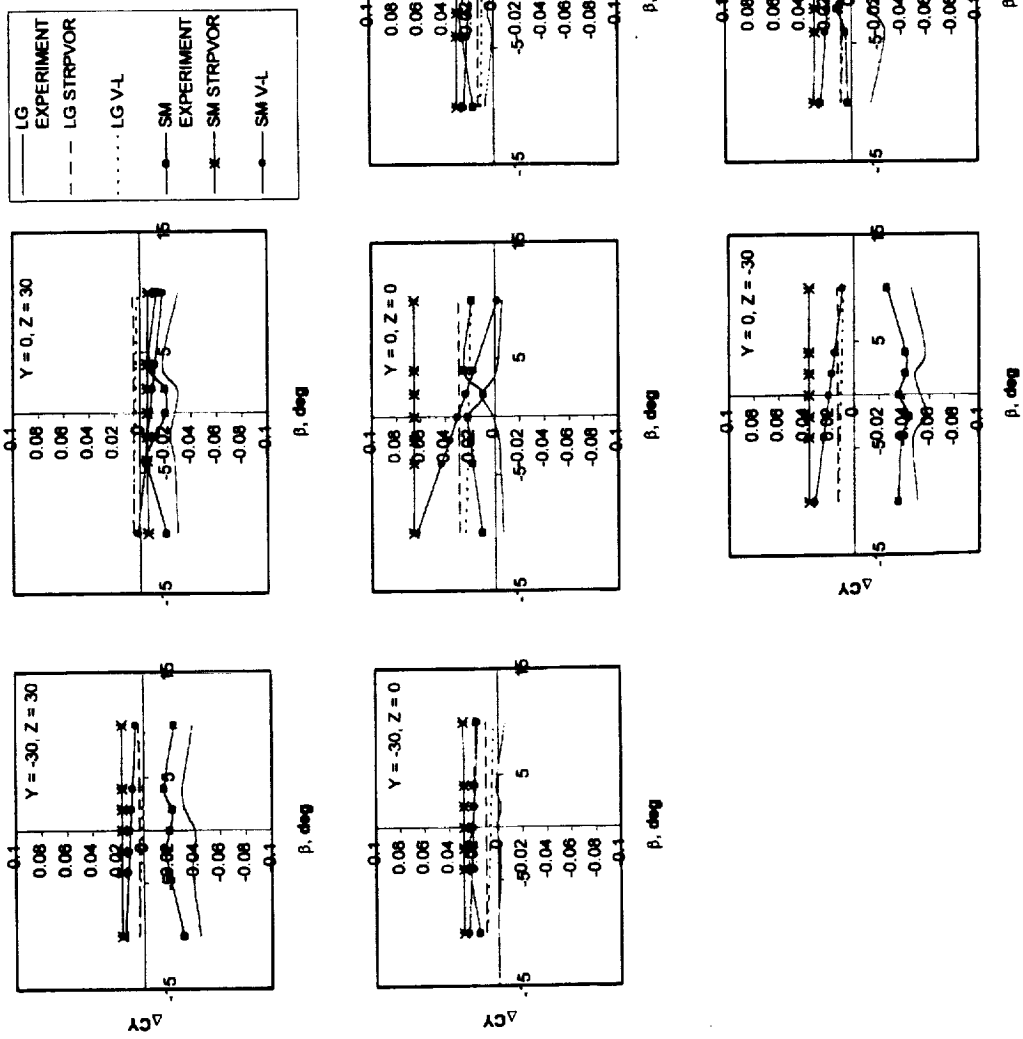

Figure 15: Change in Sideforce Coefficient -large wing and small wing comparison 30'x60' static test ($\alpha = 4$)

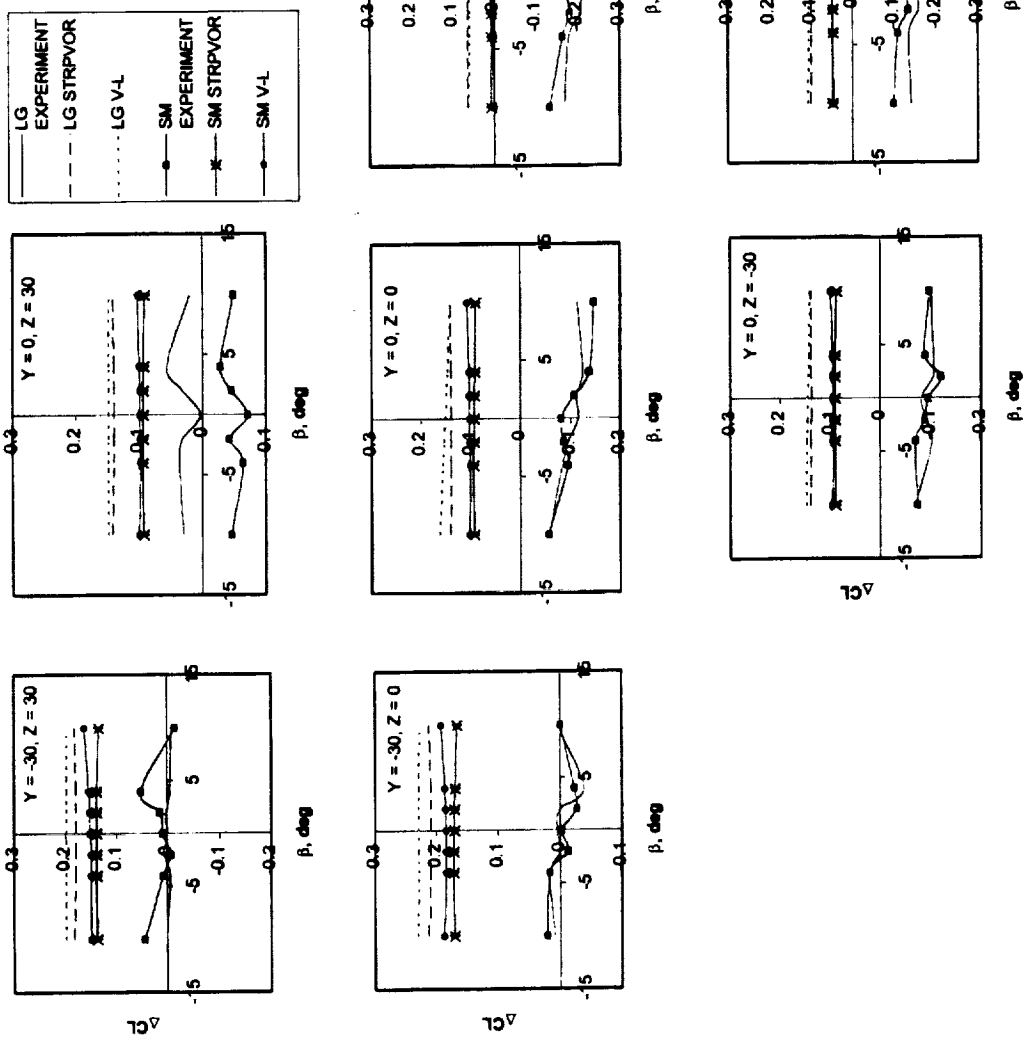

Figure 16. - Change in Lift Coefficient - large wing and small wing comparison 30'x60' static test ($\alpha = 4$)

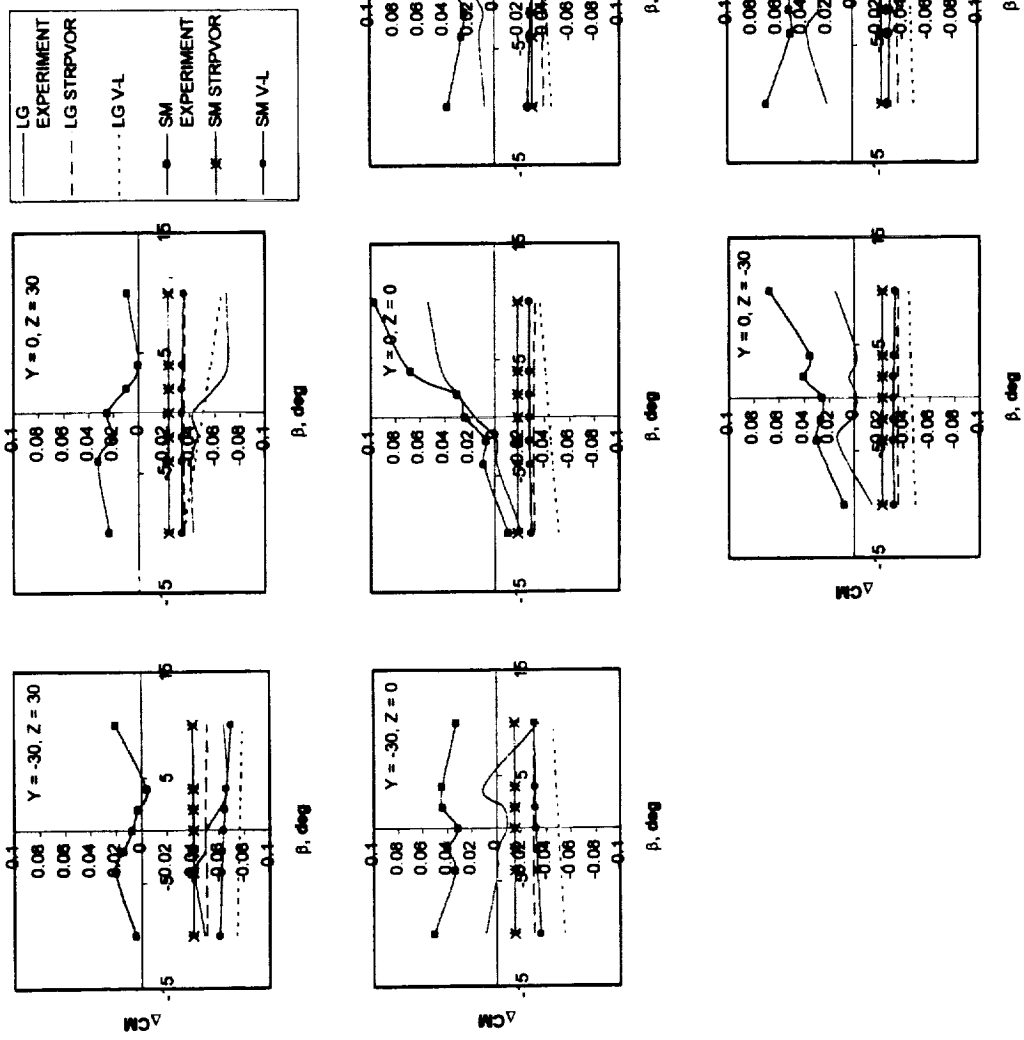

Figure 17: Change in Pitching Moment - large wing and small wing comparison 30'x60' static test ($\alpha = 4$)

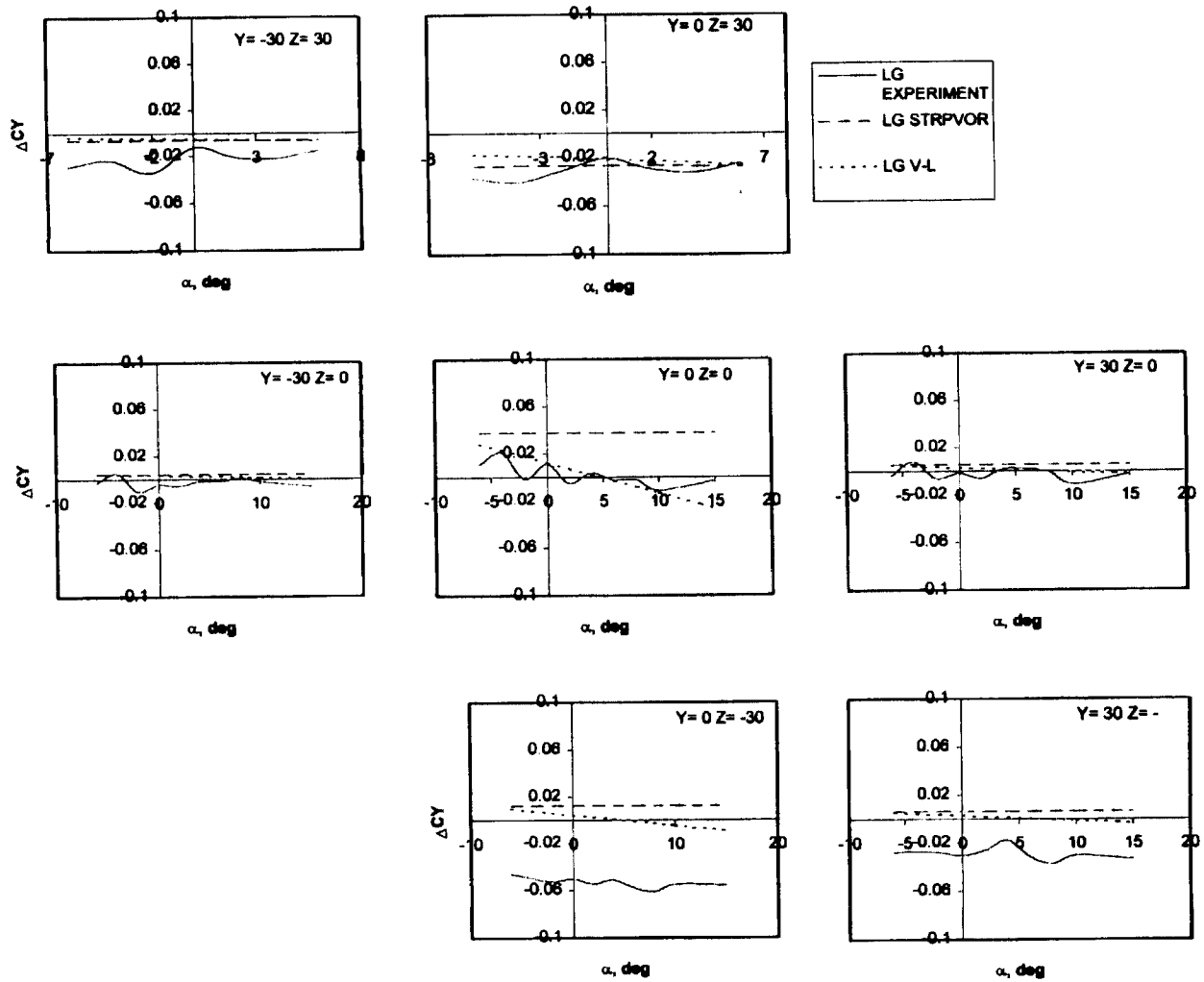

Figure 18: Change in Sideforce Coefficient - large wing 30'x60' static test (CL = 0.28, $\beta = 0$)

experiment while the vortex-lattice model appears to show results that resemble the experimental results. Locations (0,-30) and (30,-30) show that the strip theory model and the vortex-lattice model deviate from the experimental results. The models show virtually no change in the sideforce coefficient whereas the experiment shows that there is a difference. At all other locations the model results are fairly accurate when compared to the experimental data. Most disturbances seen in the sideforce coefficient are along the y-axis, and both models appear to be less accurate in this direction.

In Figure 19 there is very little disturbance in the experimental data. All changes in pitching moment appear to be approximately zero. In comparison, both models seem to accurately represent the change in pitching moment. Location (-30,30) is the only location that shows a minor loss in accuracy. It appears that the two models can accurately model the pitching moment.

Looking at the change in lift coefficient, Figure 20, we see that the experimental data for all locations show that there is virtually no change except at the center of the vortex and directly to the right of the vortex. Directly to the right of the vortex is the area dominated by downwash due to the counter-rotating vortices. Both models have approximately the same results and at all locations the models have a slightly higher magnitude than the experimental data. The only variation is at (0,30) where the change in the strip theory model is in good agreement with the experimental data, but the vortex-lattice data is still slightly higher.

Figure 21 shows that all changes in the drag coefficient are similar. Recalling that drag was not computed for the strip theory model the only data used for comparison is the vortex-lattice model. The experimental data is once again showing that the change

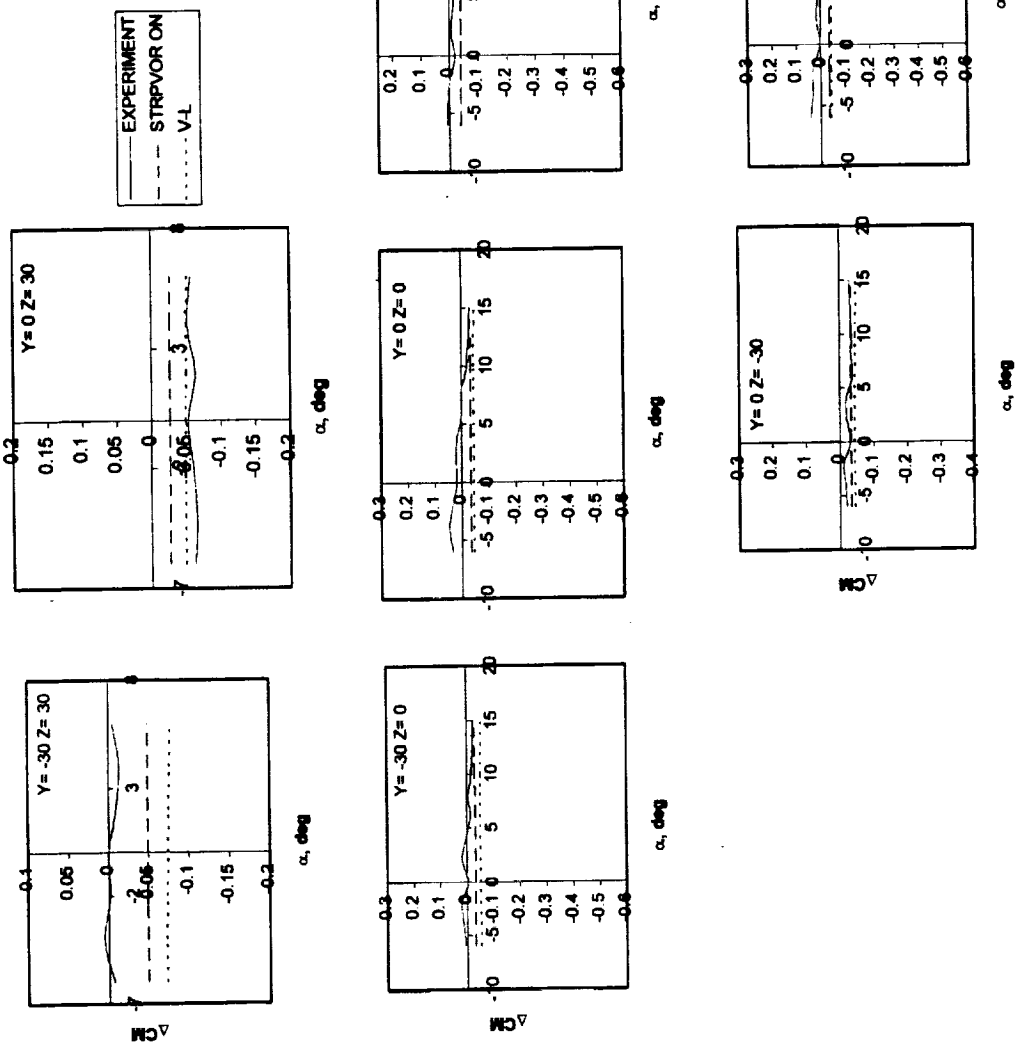

Figure 19: Change in Pitching Moment - large wing 30'x60' static test (CL = 0.28, β = 0)

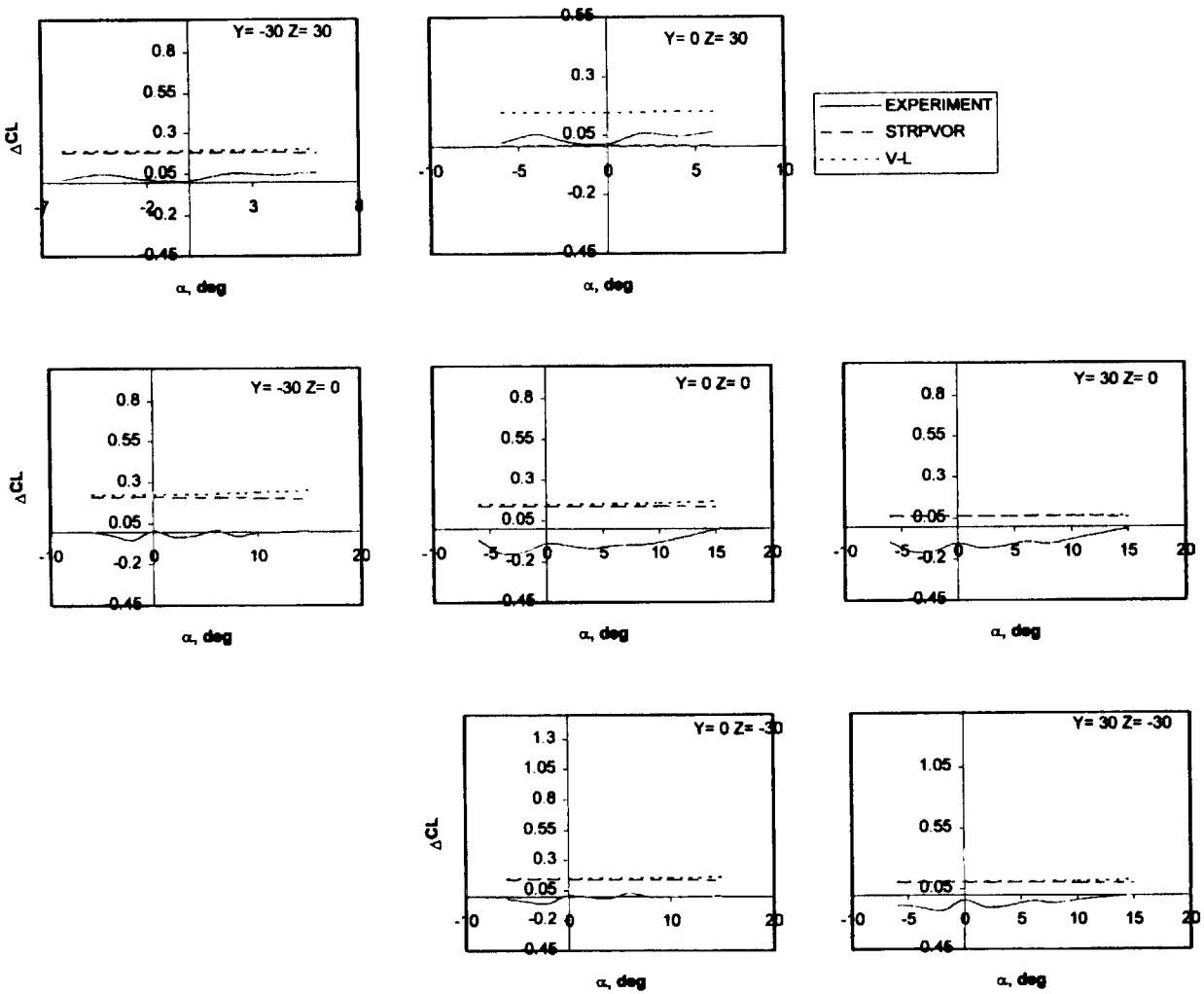

Figure 20: Change in Lift Coefficient - large wing 30'x60' static test (CL = 0.28, $\beta = 0$)

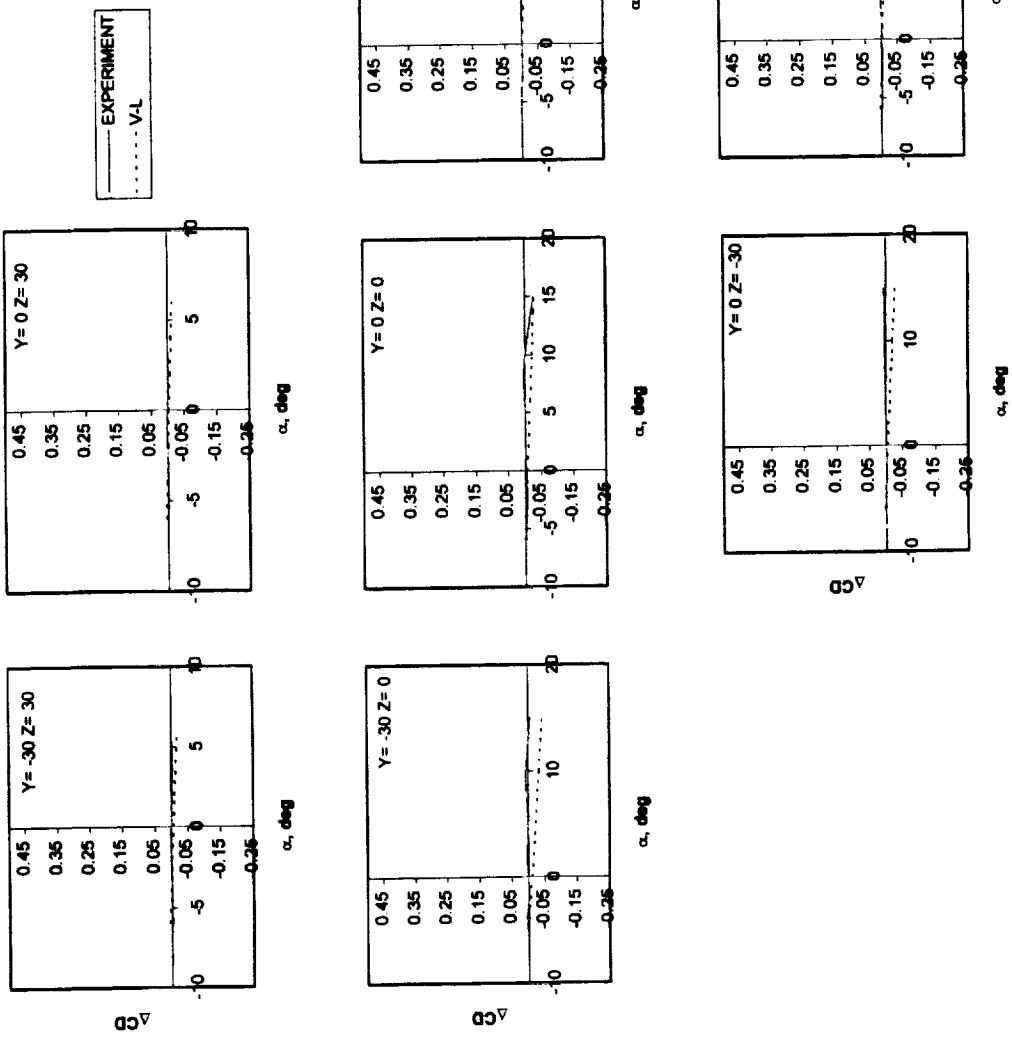

Figure 21: Change in Drag Coefficient - large wing 30'x60' static test (CL = 0.28, $\beta = 0$)

in drag coefficient is zero. The vortex-lattice model demonstrates a high accuracy when compared to the experimental data. There is a deviation in the results at high angles of attack, but this may be due to the separation in the flow.

The experimental data for the rolling moment, Figure 22, shows that the change appears to be zero. Magnitudes do increase slightly along the y-axis. Both models show good agreement with the experimental results. Location (0,0) shows the greatest discrepancy between results. Although both models appear to give approximately the same result the vortex-lattice model appears to give a more accurate solution than strip theory model.

Figure 23 shows the results for the change in yawing moment. Locations (-30,0) and (-30,30) show both models to be in good agreement with experimental data. For (0,0) the vortex-lattice model shows a high amount of accuracy. The strip theory shows a decrease in accuracy, although the magnitude of the difference between strip theory model and the experimental data is very small. Location (30,0) shows the same behavior, but there seems to be a slight increase in accuracy for the strip theory model. Locations (0,-30) and (30,-30) shows a slight margin of error between both models and the experiment. The change in the yawing moment for the experiment increased where the models show a zero change in the moment. Yawing moment has shown the greatest disturbance at locations below the vortex. Once again the vortex-lattice model has proven to be more accurate than the strip theory model.

Now we will take a look at the beta sweep and how changing the sideforce coefficient effects the accuracy of the strip theory and vortex-lattice models. The change in sideforce coefficient, as shown in Figure 24, at location (0,0) shows that the models

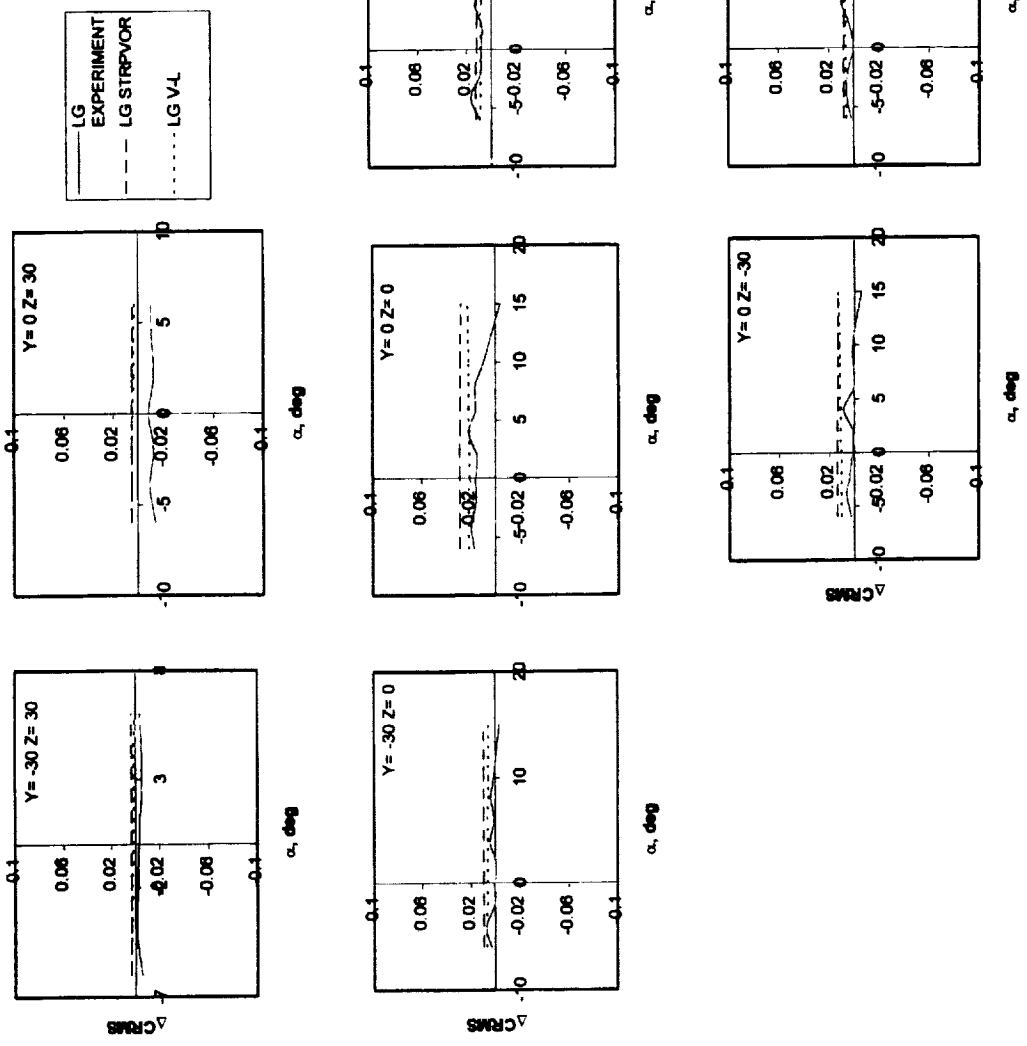

Figure 22: Change in Rolling Moment - large wing 30'x60' static test (CL = 0.28, β = 0)

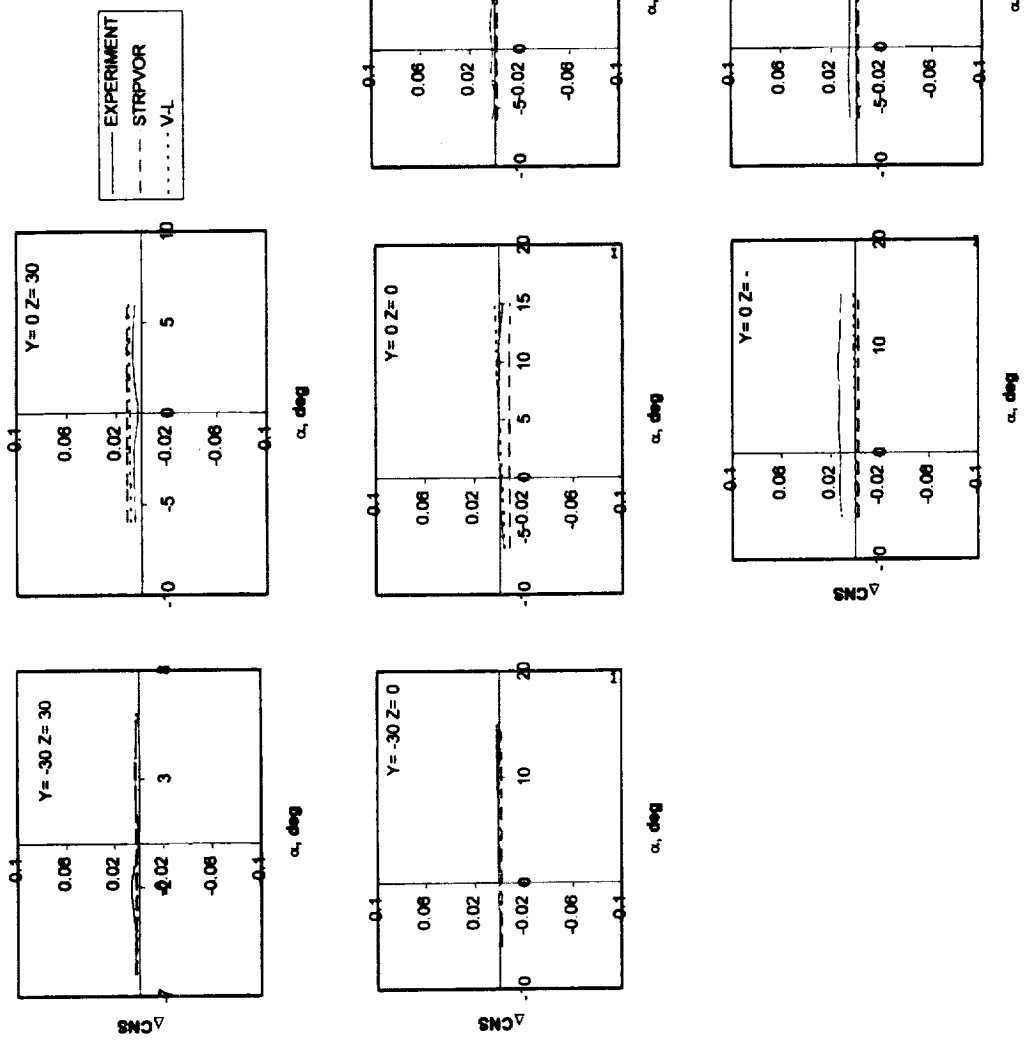

Figure 23: Change in Yawing Moment - large wing 30'x60' static test (CL = 0.28, β = 0)

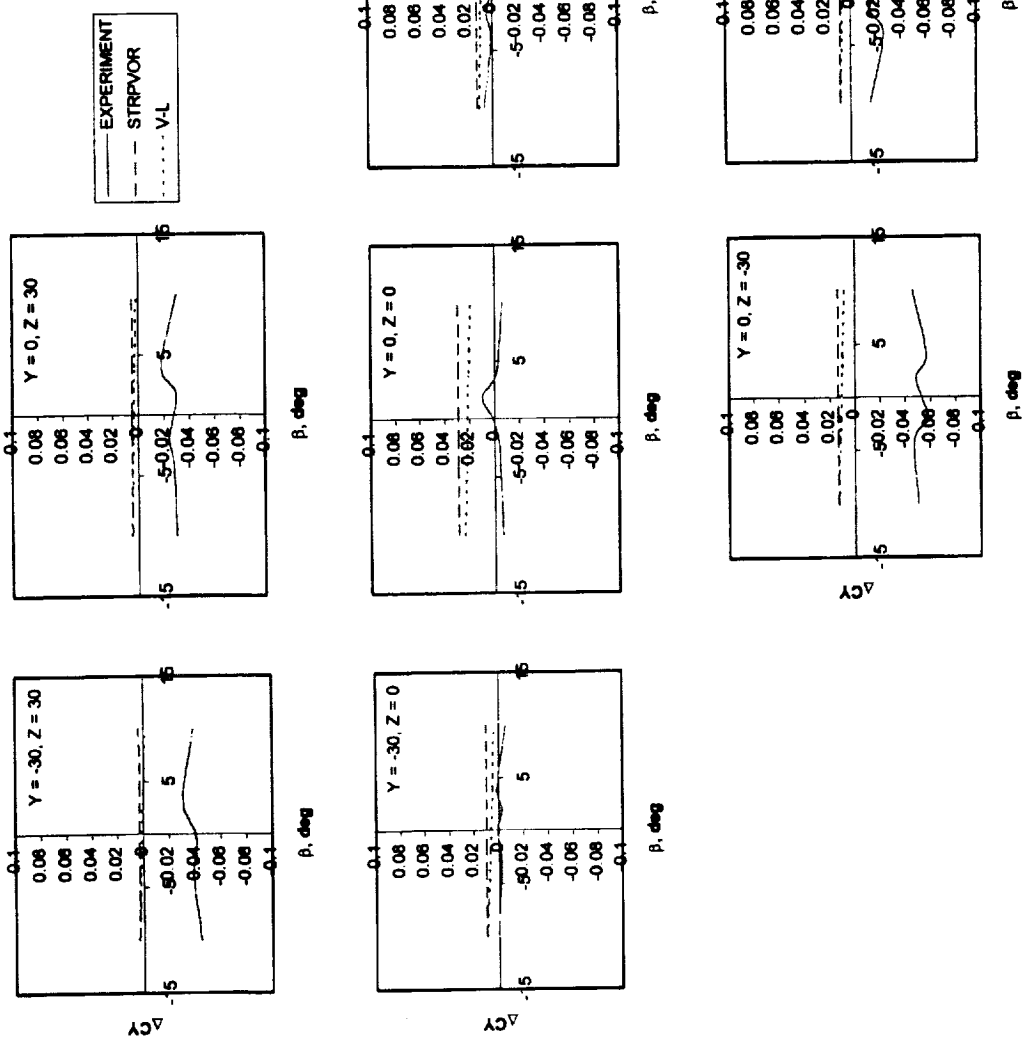

Figure 24: Change in Sideforce Coefficient - large wing 30'x60' static test (CL=0.56, $\alpha = 4$)

deviate from the experimental data. Both the strip theory model and the vortex-lattice model show that the models are inaccurate at (0,30). This is an area dominated by the cross flow. The models show that there is no change in the sideforce coefficient, which is not the case for the experiment. The same applies to locations (30,-30) and (-30,30) as for (0,-30). For the remaining locations both models prove to have a high amount of accuracy.

Figure 25 shows the graph of the change in pitching moment. Location (0,30) shows the vortex-lattice model to be in good agreement with experimental data, and location (-30,30) appears to be in good agreement with the strip theory model. All other locations appear to have some significant differences between the models and the experiments. Looking at the changes in lift coefficient, Figure 26 for all locations the models show inaccuracies.

Deviation in the change in rolling moment between the models and experiment appears at (0,30) and (-30,30). As shown in Figure 27. All other locations show that the models and experiment are in agreement, and that the strip theory model is less accurate than the vortex-lattice model. Changes in yawing moment, in Figure 28, appear to be in good agreement between the models and the experimental data. Of the two models the strip theory model looks to be less accurate than the vortex-lattice model. In Figure 29 there is a consistency at all locations for the change in drag. The strip theory model and vortex-lattice model are in excellent agreement with each other. When comparing the models to the experimental data we see that the models do not accurately model the experimental data. It appears that the difference between the models and the experiment remains constant throughout all locations.

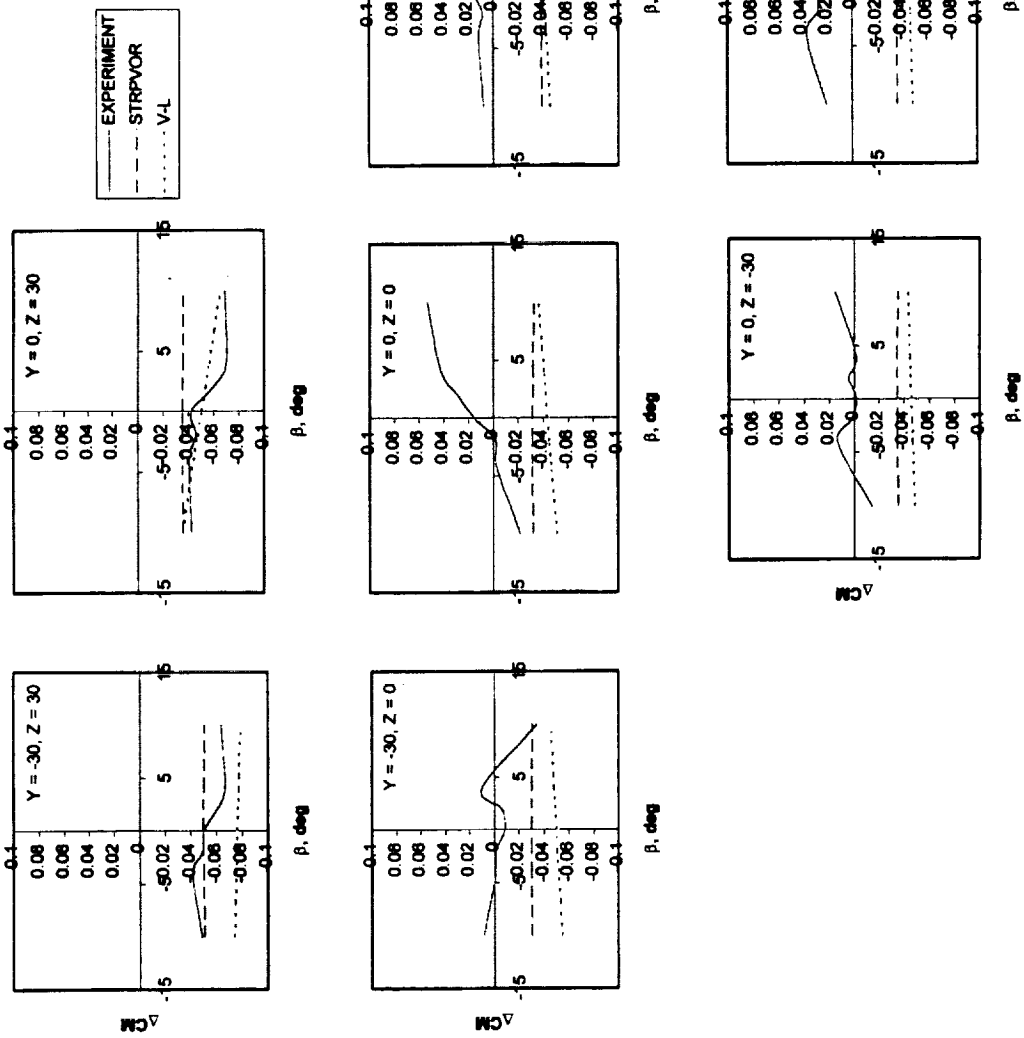

Figure 25: Change in Pitching Moment - large wing 30'x60' static test (C_L=0.56, $\alpha = 4$)

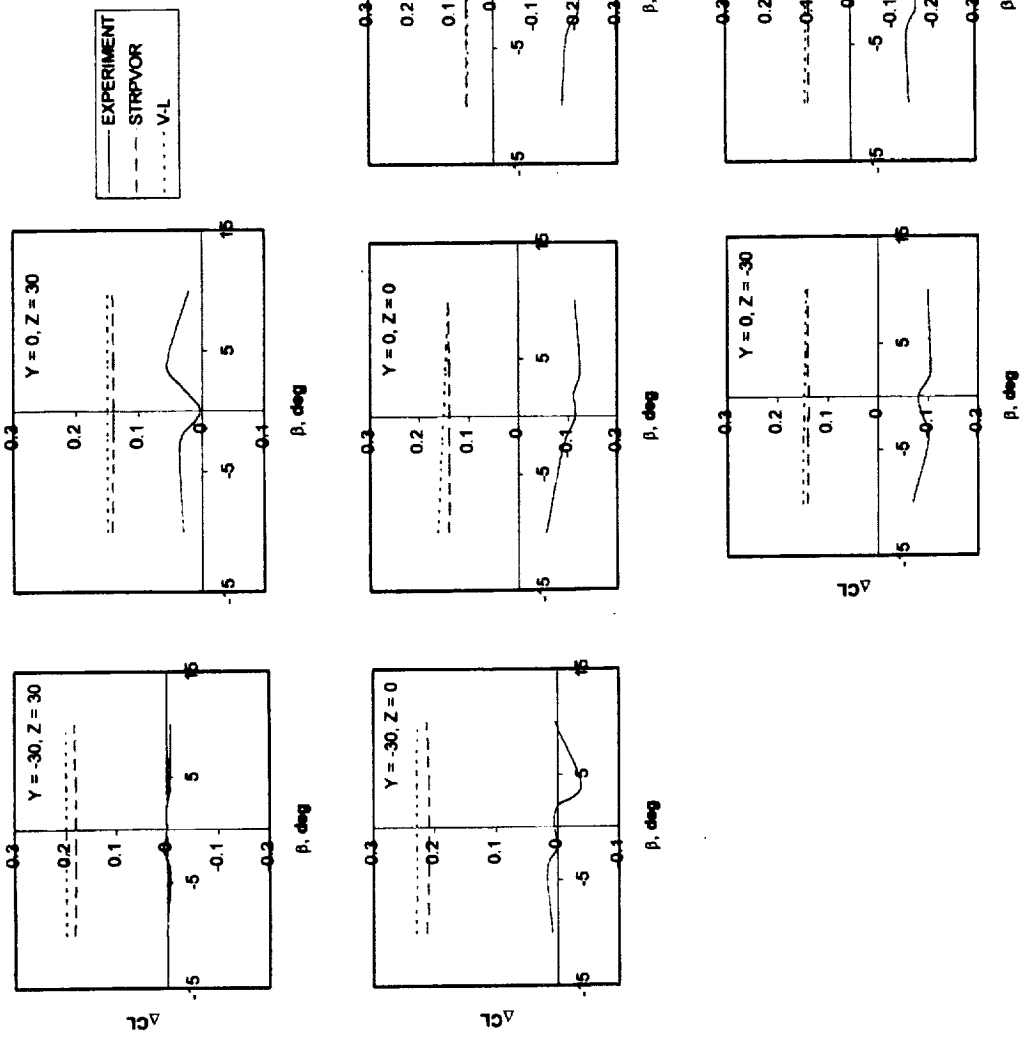

Figure 26: Change in Lift Coefficient - large wing 30'x60' static test (CL=0.56, $\alpha = 4$)

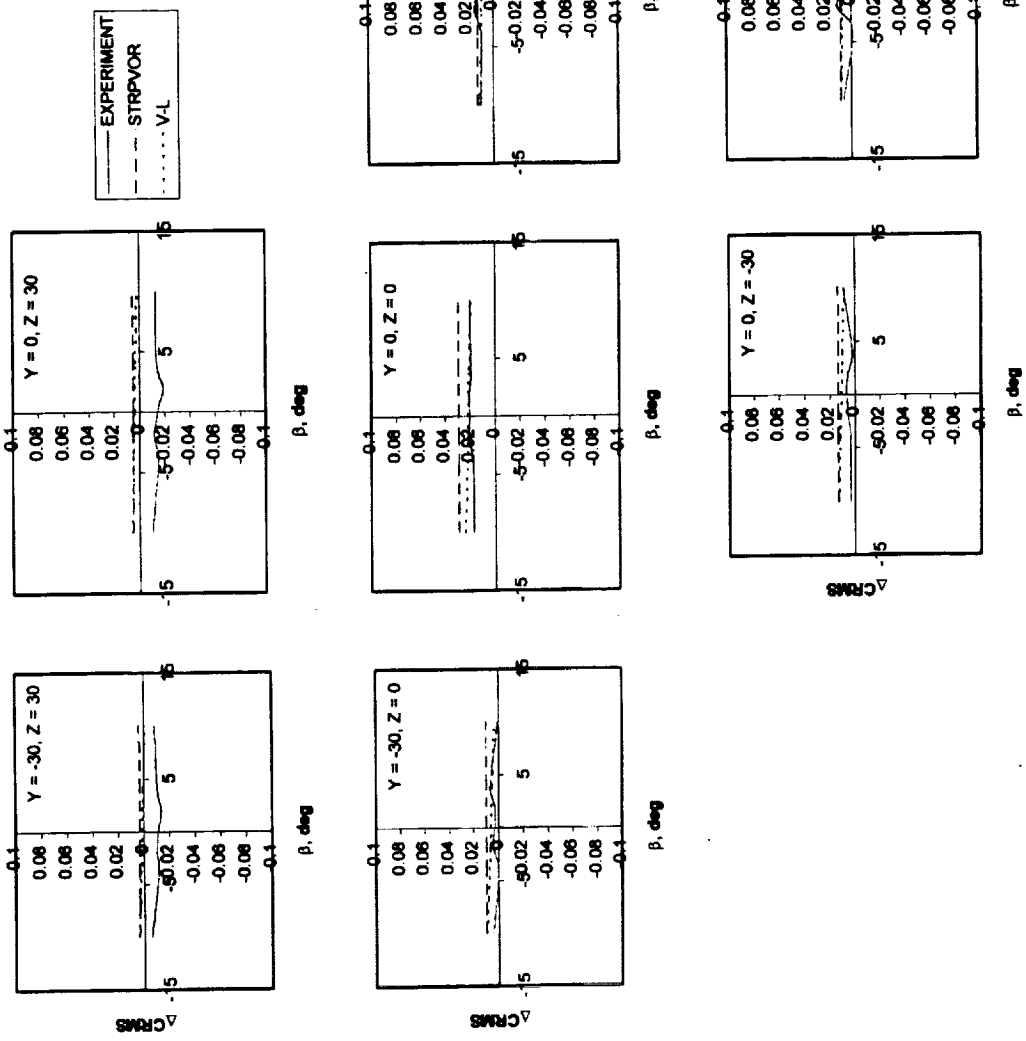

Figure 27: Change in Rolling Moment - large wing 30'x60' static test (CL=0.56, $\alpha = 4$)

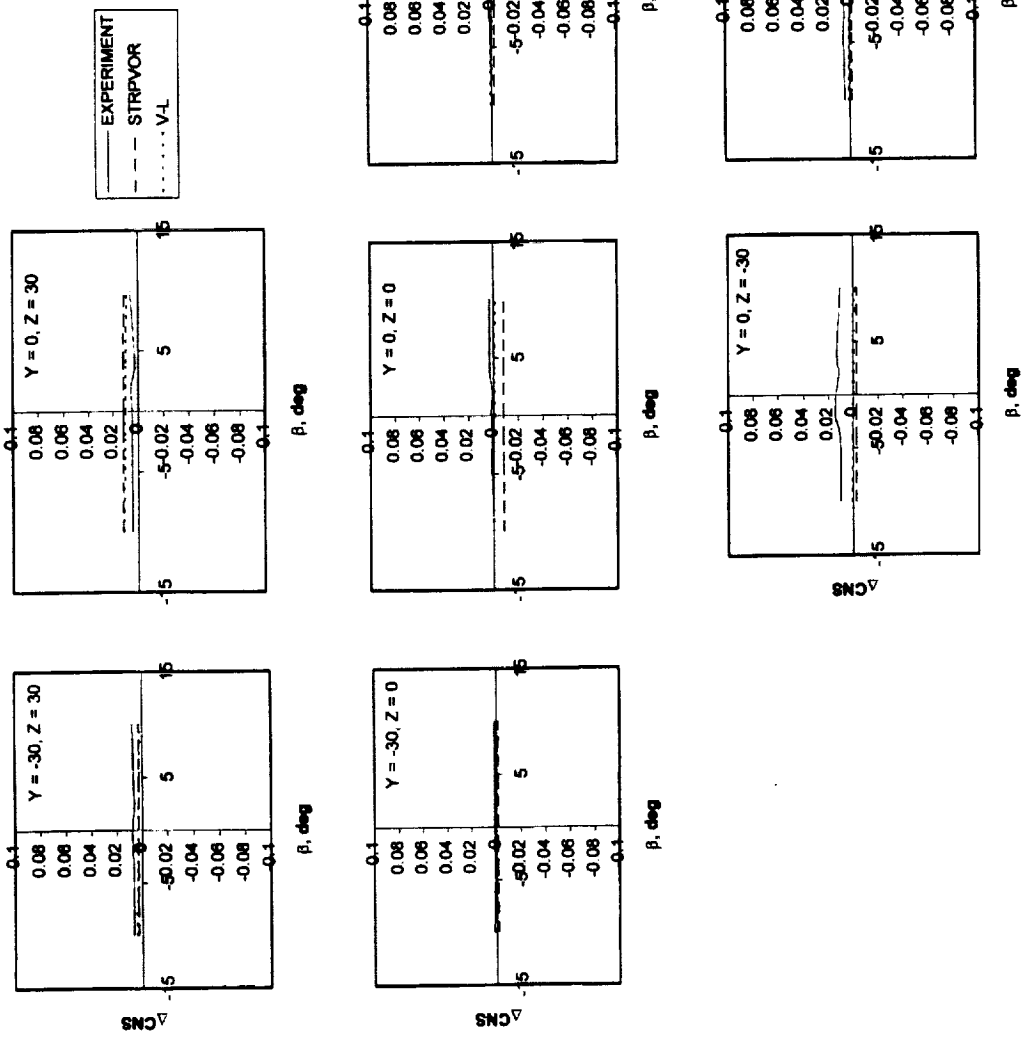

Figure 28: Change in Yawing Moment - large wing 30'x60' static test (CL=0.56, $\alpha = 4$)

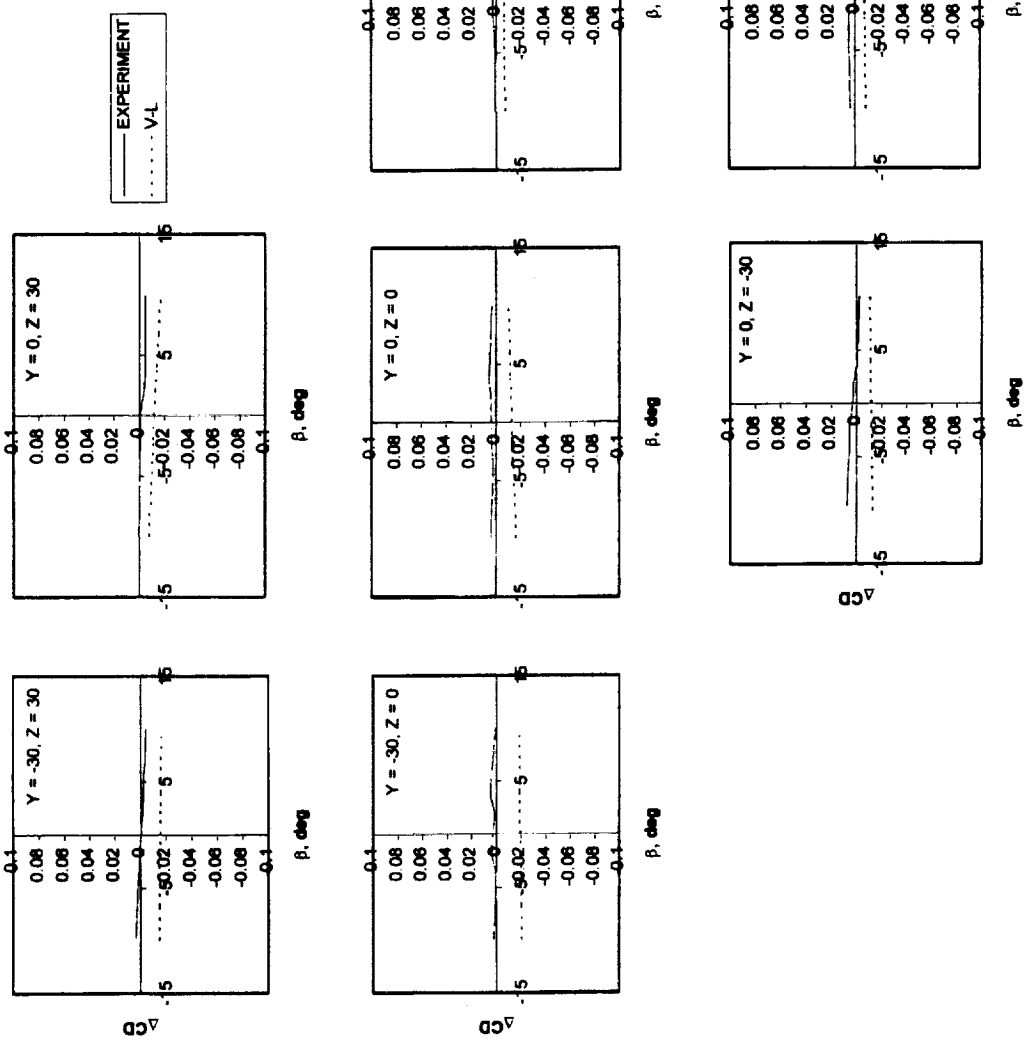

Figure 29: Change in Drag Coefficient - large wing 30'x60' static test (CL=0.56, $\alpha = 4$)

For the large wing comparisons will be made to determine how much geometrical information is needed for the models to still produce accurate results. To begin with comparisons will be in which the horizontal stabilizer and vertical tails have been removed from both the strip theory model and vortex-lattice model. These comparisons will be made for an alpha sweep. When examining the change in the sideforce coefficient, shown in Figure 30, along the z-axis the models agree with the experimental data when all tails were on. The strip theory model is less accurate at higher angles of attack for (0,0), but vortex-lattice remains in good agreement. For (0,-30), (30,-30), (0,30), and (–30,30) there is a significant difference between both models and the experimental data when the tails were on, but the models are in good agreement with experimental data when the tails were removed.

Modeling of the pitching moment, which is controlled by the horizontal stabilizer that has now been removed, shows a great inaccuracy when compared to the experimental data. In Figure 31 the models show a linear relation to the angle of attack. When alpha equals four degrees, both models accurately model the experiment. As the angle increases and decreases from four degrees the error in the modeling shows the same behavior. These results are consistent at all locations. When looking at the change in lift, Figure 32, it can be seen that there are great inaccuracies in the models. Figure 33 shows the change in drag where the vortex-lattice model accurately models the experimental data for all locations; both when the tails are on and when the tails have been removed. The change in rolling moment is depicted in Figure 34. This figure shows that both models accurately represent the experimental data both when tails are on and when they have been removed for all locations. There is a discrepancy at higher

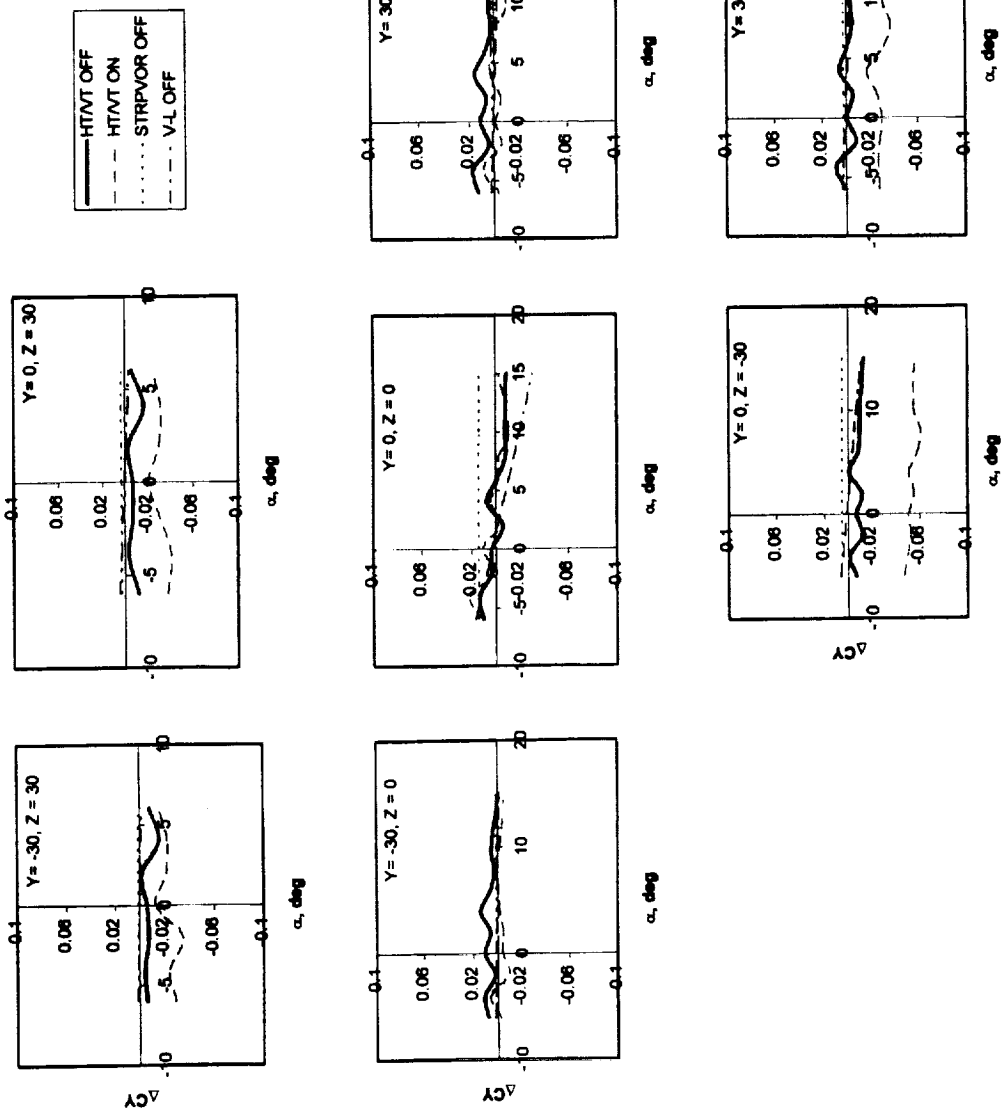

Figure 30: Change in Sideforce Coefficient - Horizontal tail and Vertical tail off - large wing 30'x60' static test (CL = 0.28, β = 0)

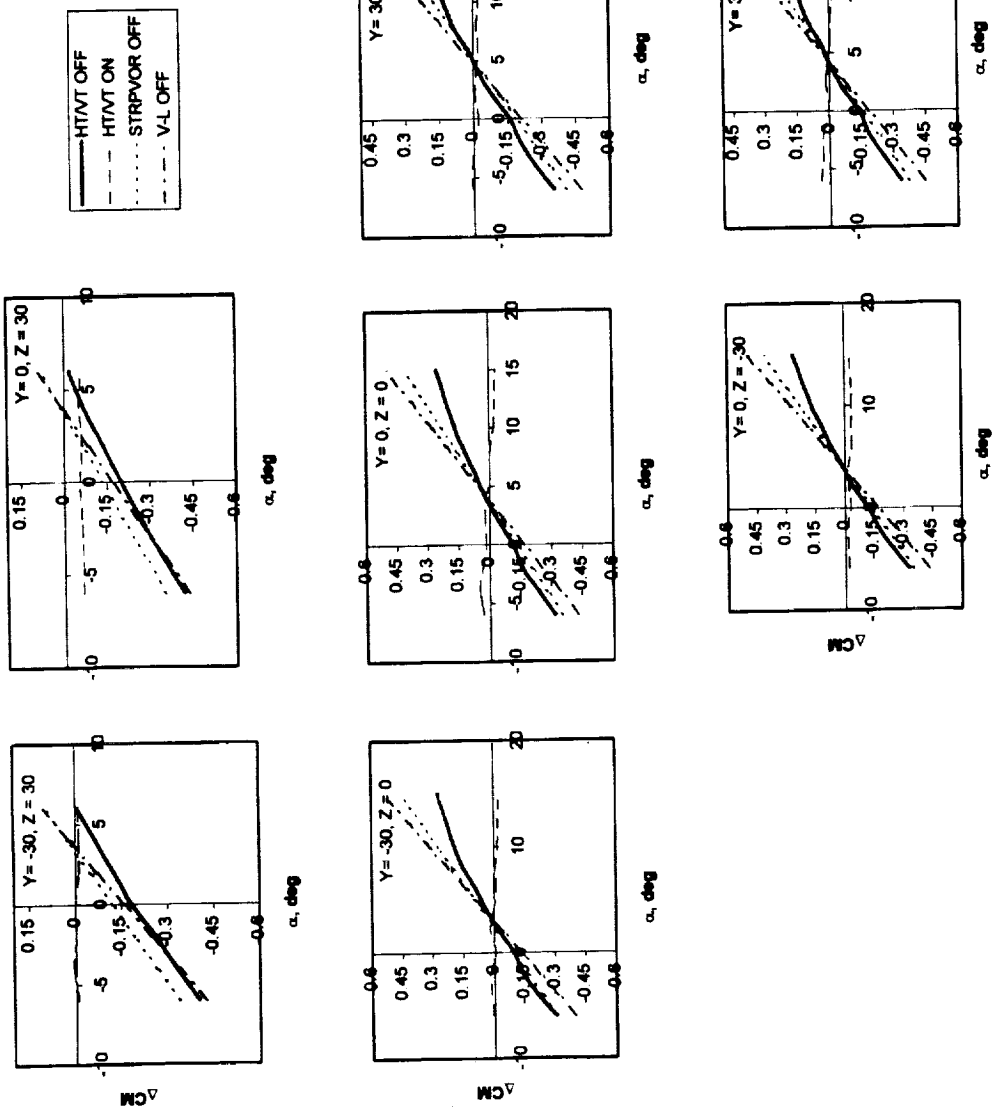

Figure 31: Change in Pitching Moment - Horizontal tail and Vertical tail off - large wing 30'x60' static test (CL = 0.28, β = 0)

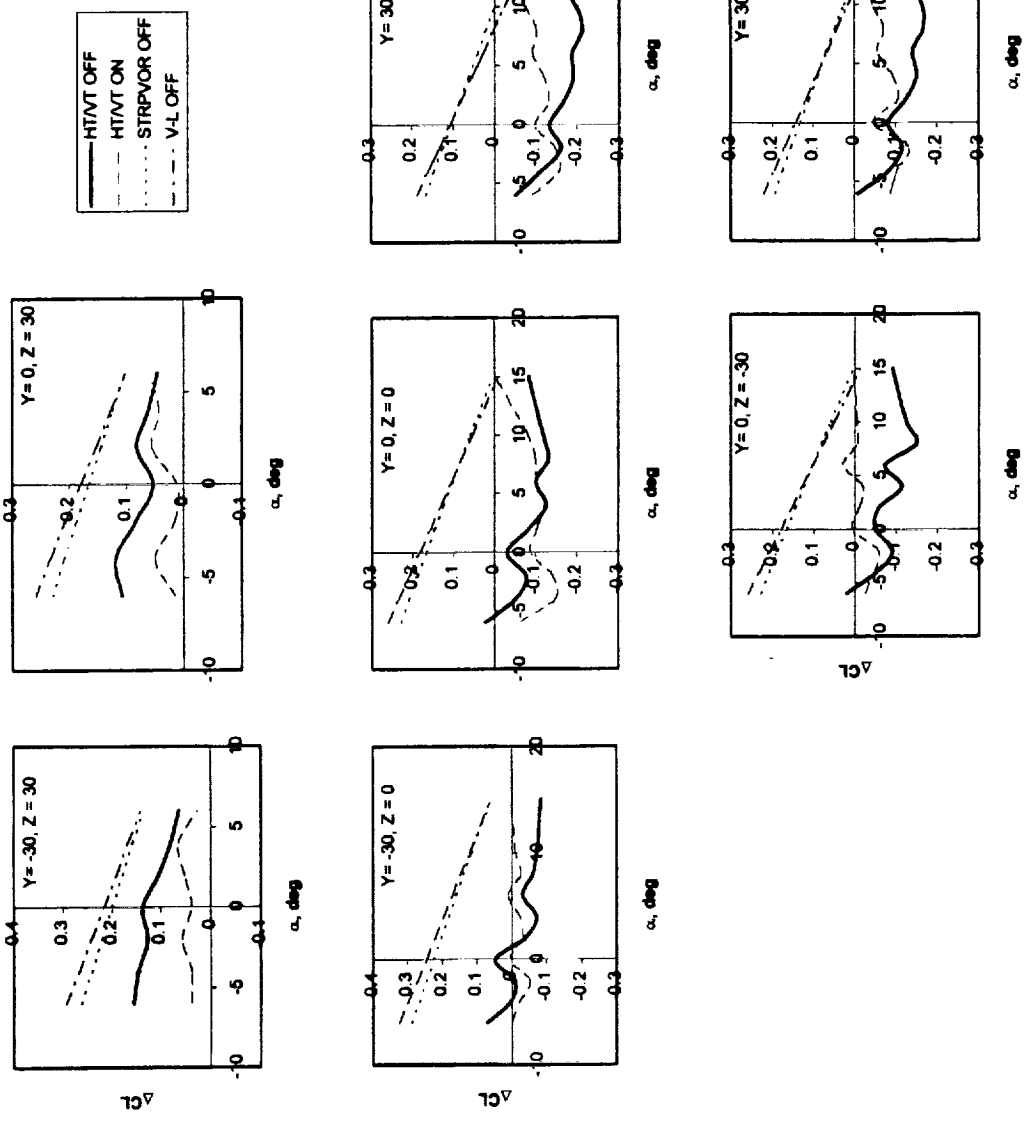

Figure 32: Change in Lift Coefficient - Horizontal tail and Vertical tail off - large wing 30'x60' static test (CL = 0.28, β = 0)

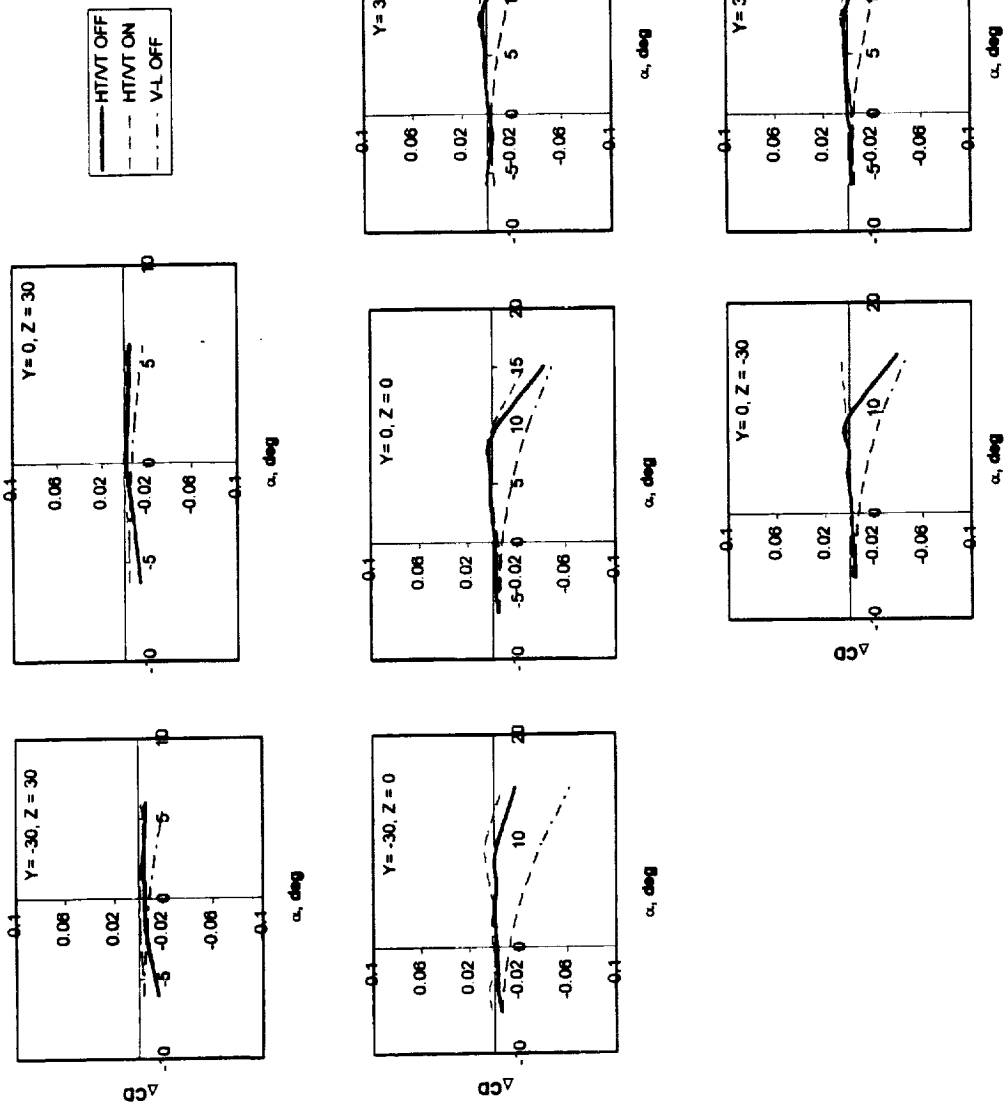

Figure 33: Change in Drag Coefficient - Horizontal tail and Vertical tail - large wing 30'x60' static test (CL = 0.28, β = 0)

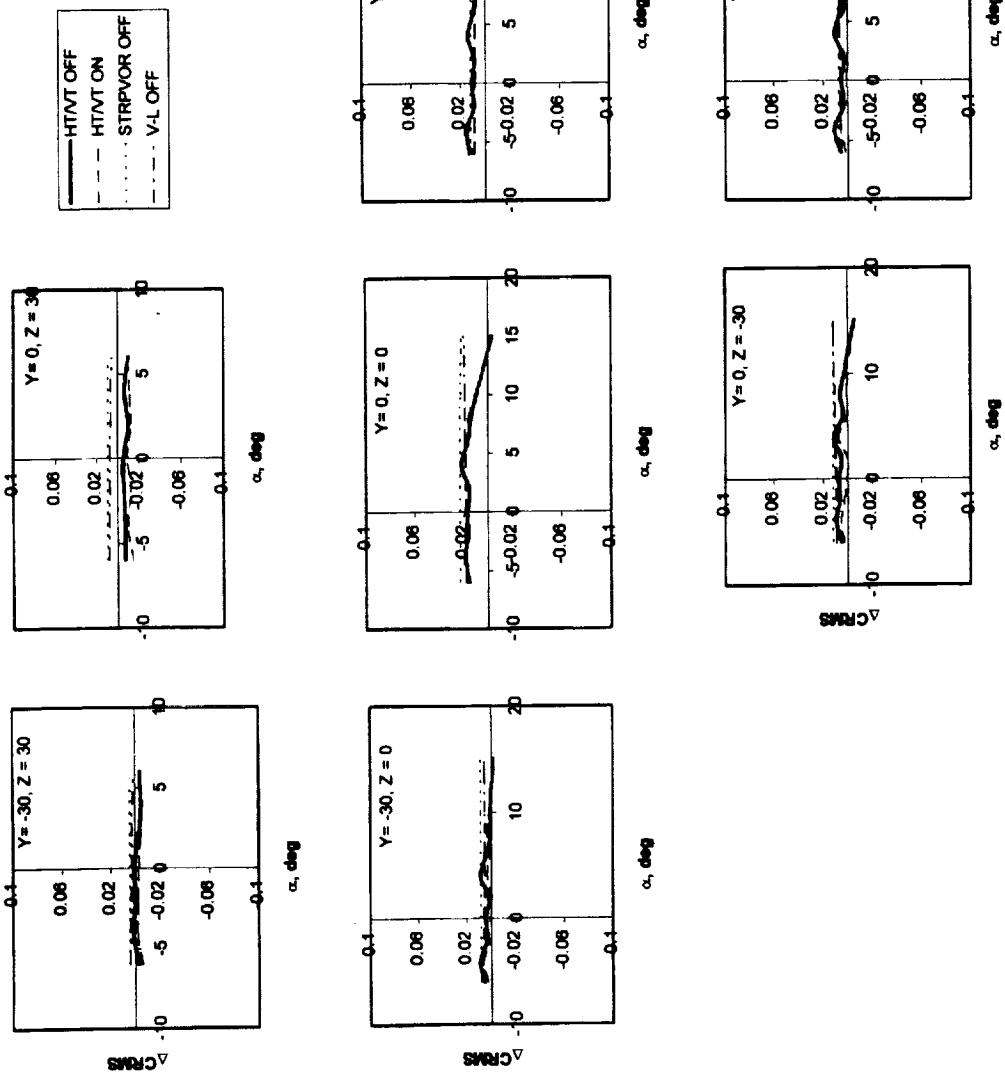

Figure 34: Change in Rolling Moment - Horizontal tail and Vertical tail off - large wing 30'x60' static test (CL = 0.28, $\beta = 0$)

angles of attack where a separation between the models and the experimental data is shown. Changes in yawing moment once again prove to be consistent at all location as see in Figure 35. Locations (0,0) and (30,0) show some discrepancy in the vortex-lattice model at large angles of attack. At all other locations both models are in good agreement with the experimental data.

Previously removing the horizontal stabilizer and vertical tail from strip theory and vortex-lattice models were discussed. Now experimental data with all tails on and experimental data with the vertical tail removed will be compared to both models in which the vertical tail has been removed. The changes in sideforce coefficient, shown in figure 36, show large discrepancies between the models and experimental data when the tail is on. This is expected since the sideforce coefficient is controlled by the vertical tail which has been removed. At an angle between –4 and 0 there is a point when the model would be able to accurately represent the experimental data. As the angle both decreases and increases the ability of the model to accurately predict the change in sideforce coefficient decreases. The change in pitching moment can accurately represented by both models when the vertical tails are removed as seen in Figure 37. This accuracy holds for all locations. Once again it appears that the results hold constant for all locations where Figure 38 is the change in the lift coefficient. Results given by the models have a slight discrepancy compared with the experiment. Change in drag coefficient can be viewed in Figure 39. Both models are in excellent agreement with the experimental data. The vortex-lattice model is slightly more accurate than the strip theory model. In Figure 40 the rolling moment has noticeable discrepancies in comparison to the experimental data. Once again there appears to be a linear relationship

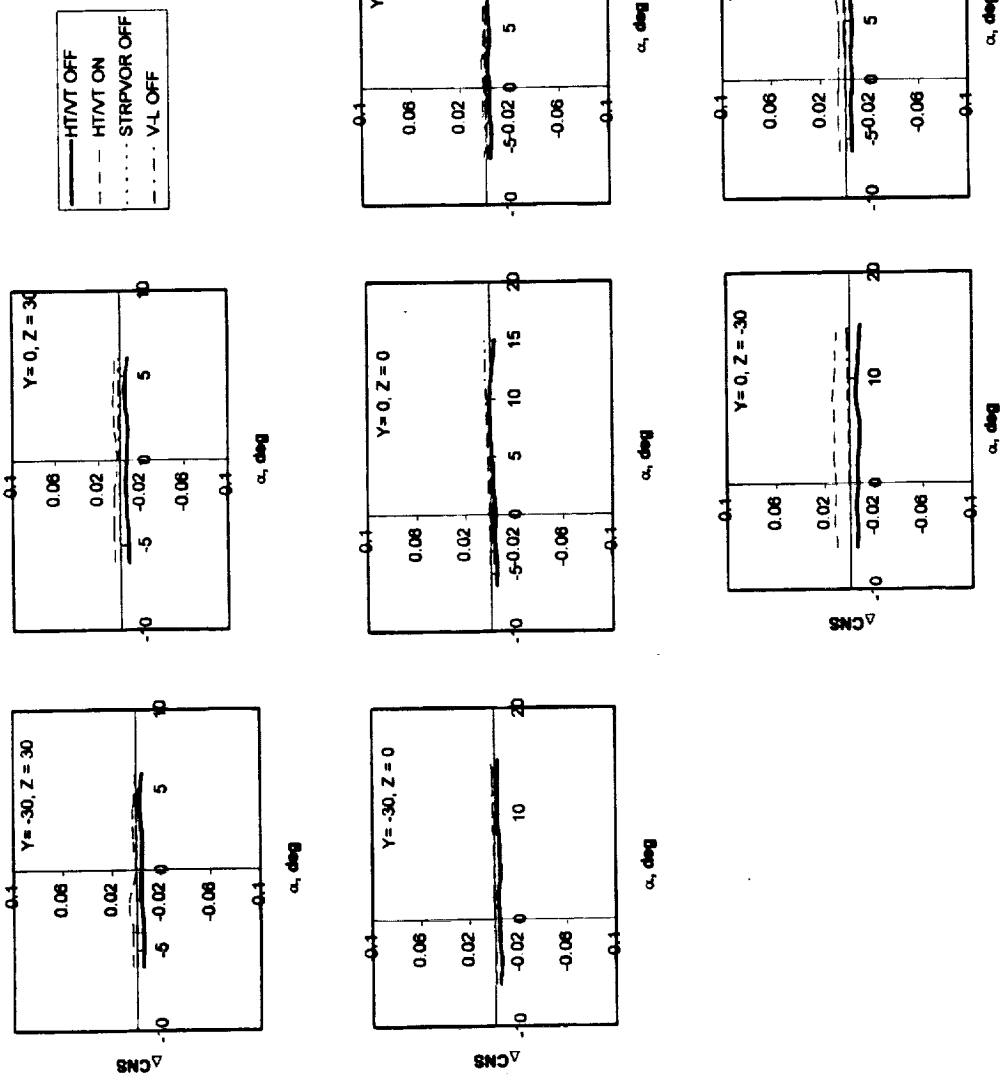

Figure 35: Change in Yawing Moment - Horizontal tail and Vertical tail off - large wing 30'x60' static test (CL = 0.28, β = 0)

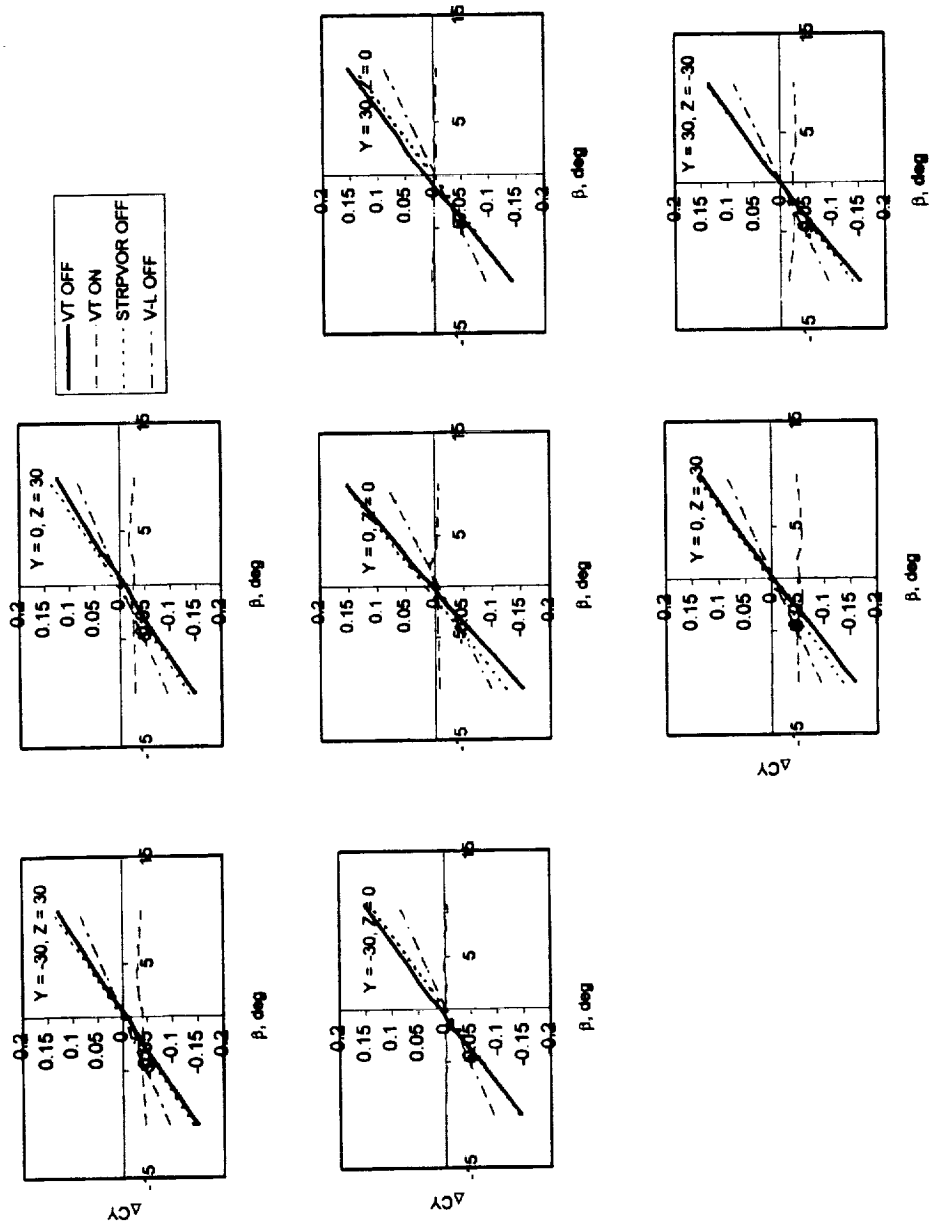

Figure 36: Change in Sideforce Coefficient - Vertical tail off - large wing 30'x60' static test (CL=0.28, $\alpha = 4$)

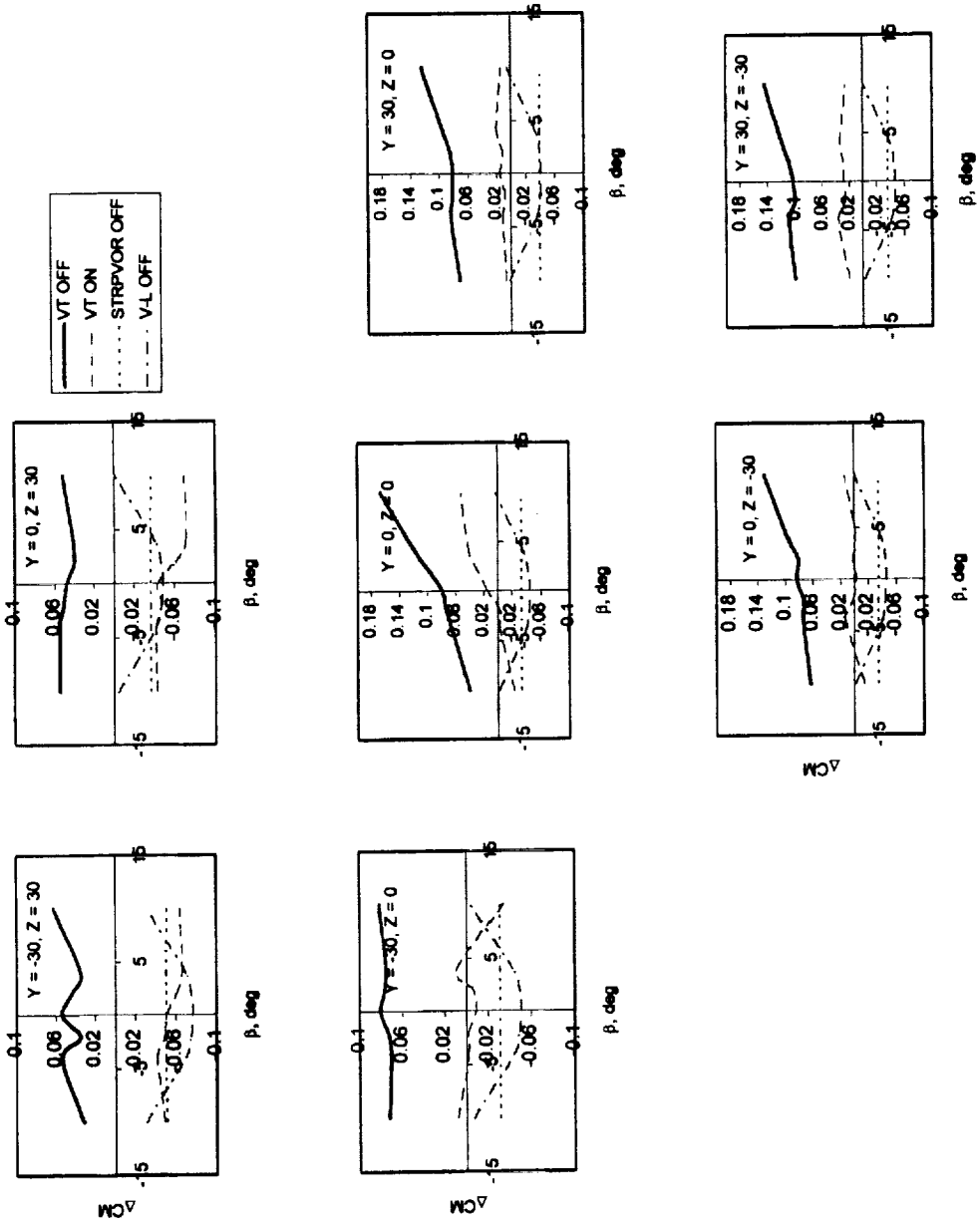

Figure 37: Change in Pitching Moment - Vertical tail off - large wing 30'x60' static test (CL=0.28, $\alpha = 4$)

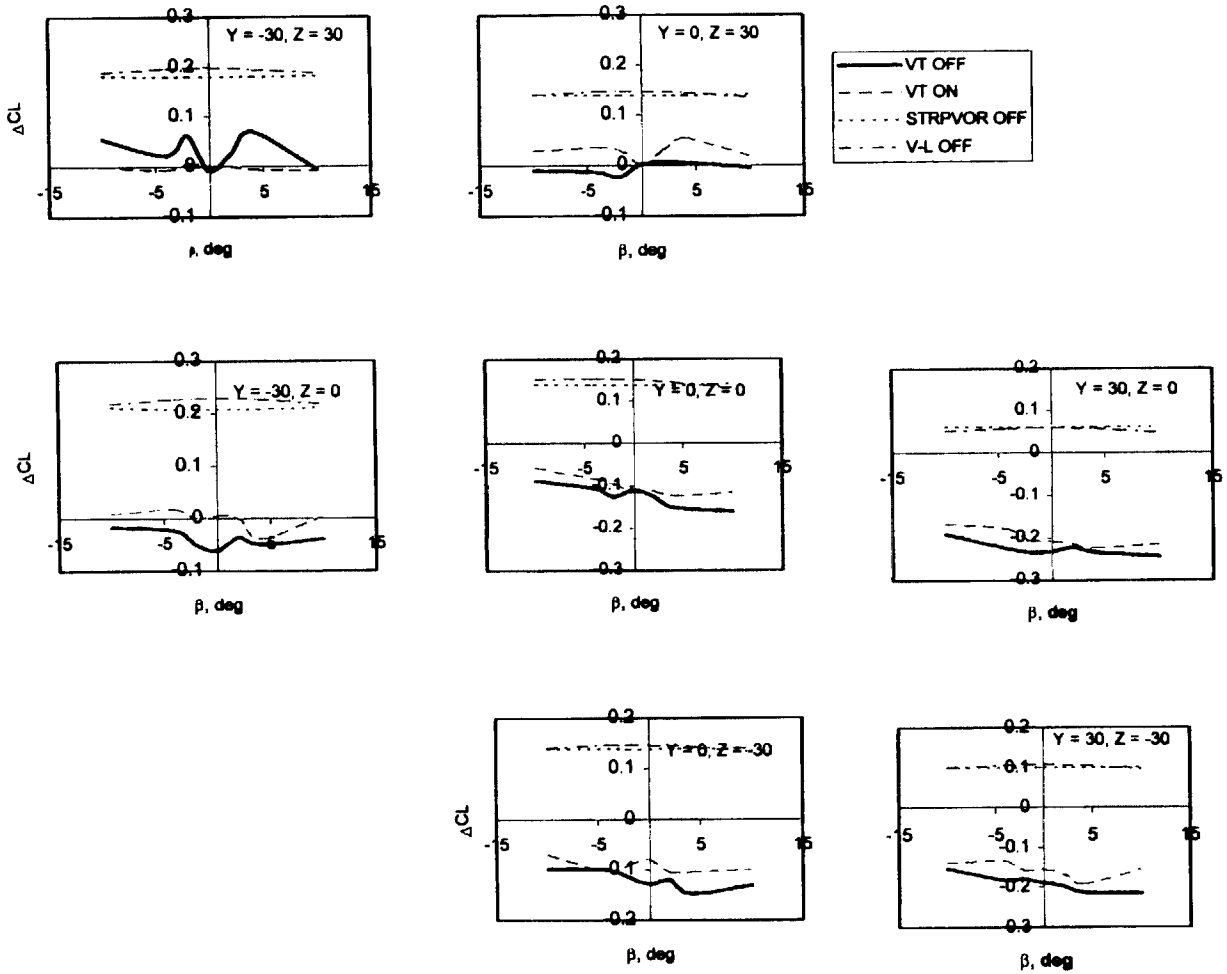

Figure 38: Change in Lift Coefficient - Vertical tail off - large wing 30'x60' static test (CL=0.28, $\alpha = 4$)

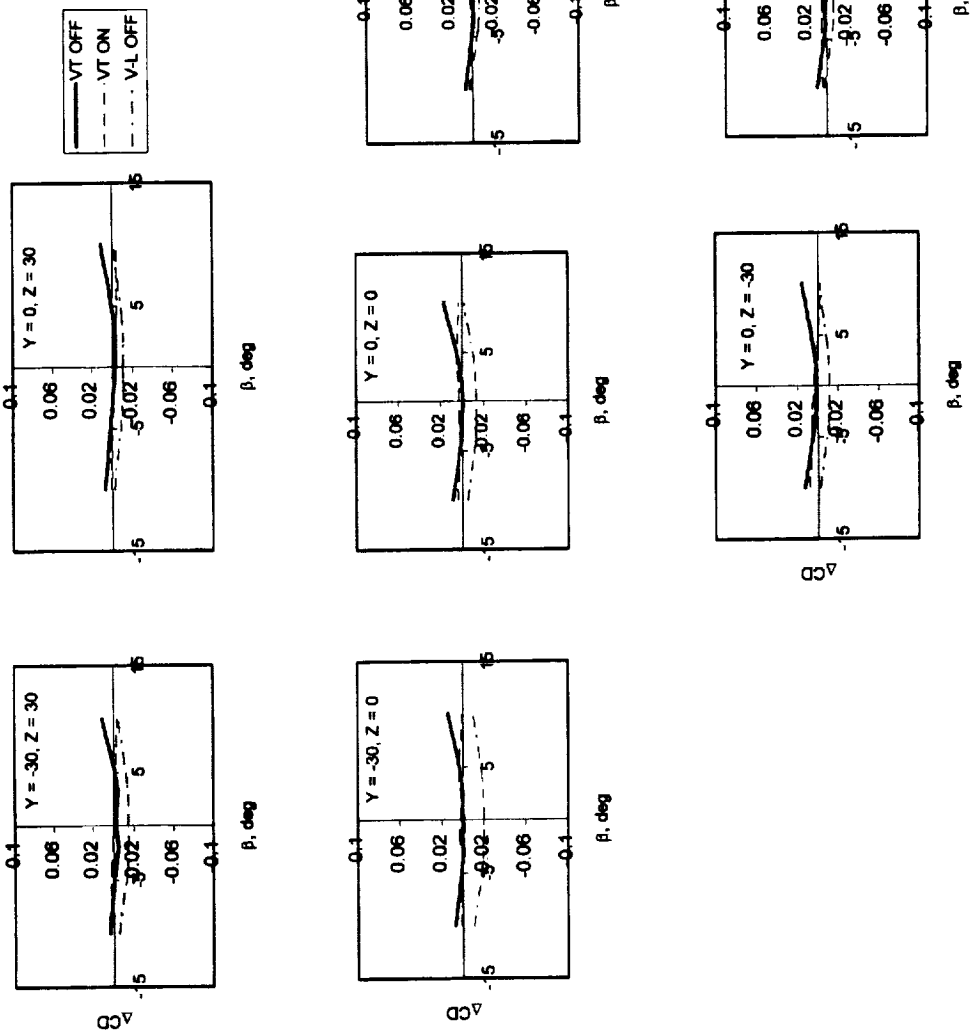

Figure 39: Change in Drag Coefficient - Vertical tail off - large wing 30'x60' static test (CL=0.28, $\alpha = 4$)

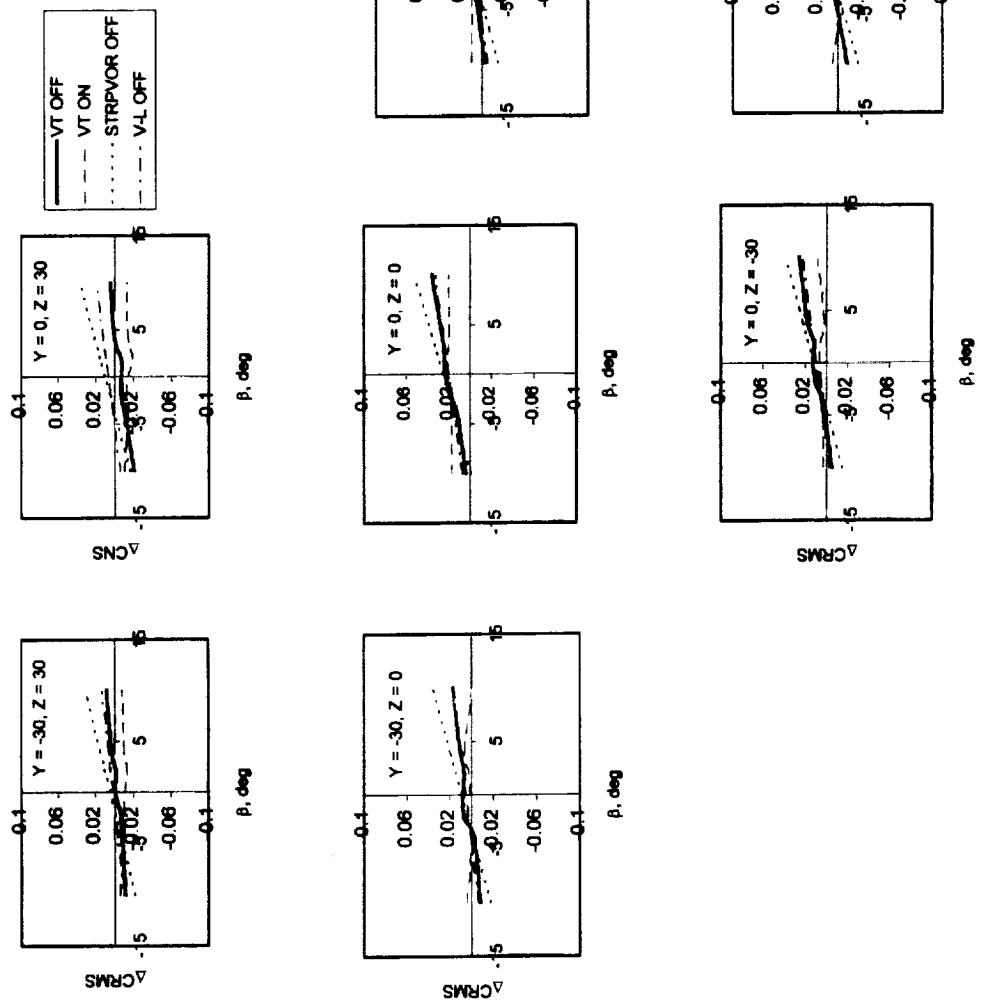

Figure 40: Change in Rolling Moment - Vertical tail off - large wing 30'x60' static test (CL=0.28, $\alpha = 4$)

in the plotted results. Since at large angles and small angles the difference is greatest between the model and the experimental data. This can be seen for all locations. Figure 41 shows the changes in yawing moment, which exhibits the same relationship in the data except the slope of the line is reversed.

It appears that when dealing purely with the alpha sweep and beta sweep, when all tails are on both models along with the experimental model, that the location of the model with respect to the vortex has a large impact on the reaction of the aircraft. Theoretically most disturbance should occur at location (0,0). Although, from the graphs it looks as though most disturbances occur on the y- axis and at points to the right of the y-axis. Omitting the vortex center the graphs on the y-axis are in a region dominated almost purely by crossflow. Directly to the right of the center is the region mainly dominated by downwash due to the counter rotating vortices. It can also be seen that overall the models are able to accurately model the experimental data, with vortex-lattice usually being more accurate than the strip theory model in most cases.

In determining the accuracy of the models when certain tails are removed, for the most part the models still are able to represent the experimental data well. Exceptions are for the change in pitching moment for both models when the horizontal stabilizer and vertical tails are removed. Secondly, exceptions lie with the change in yawing moment, rolling moment, and sideforce coefficient when the vertical tail is removed. Using a combination of the two geometries would cover all of the forces and moments and would be able to give accurate results of each. The surprising aspect about the removal of the tails is that it did not appear that location has much effect on how the forces and moments of the aircraft react to the vortex. Once again the vortex-lattice model appears

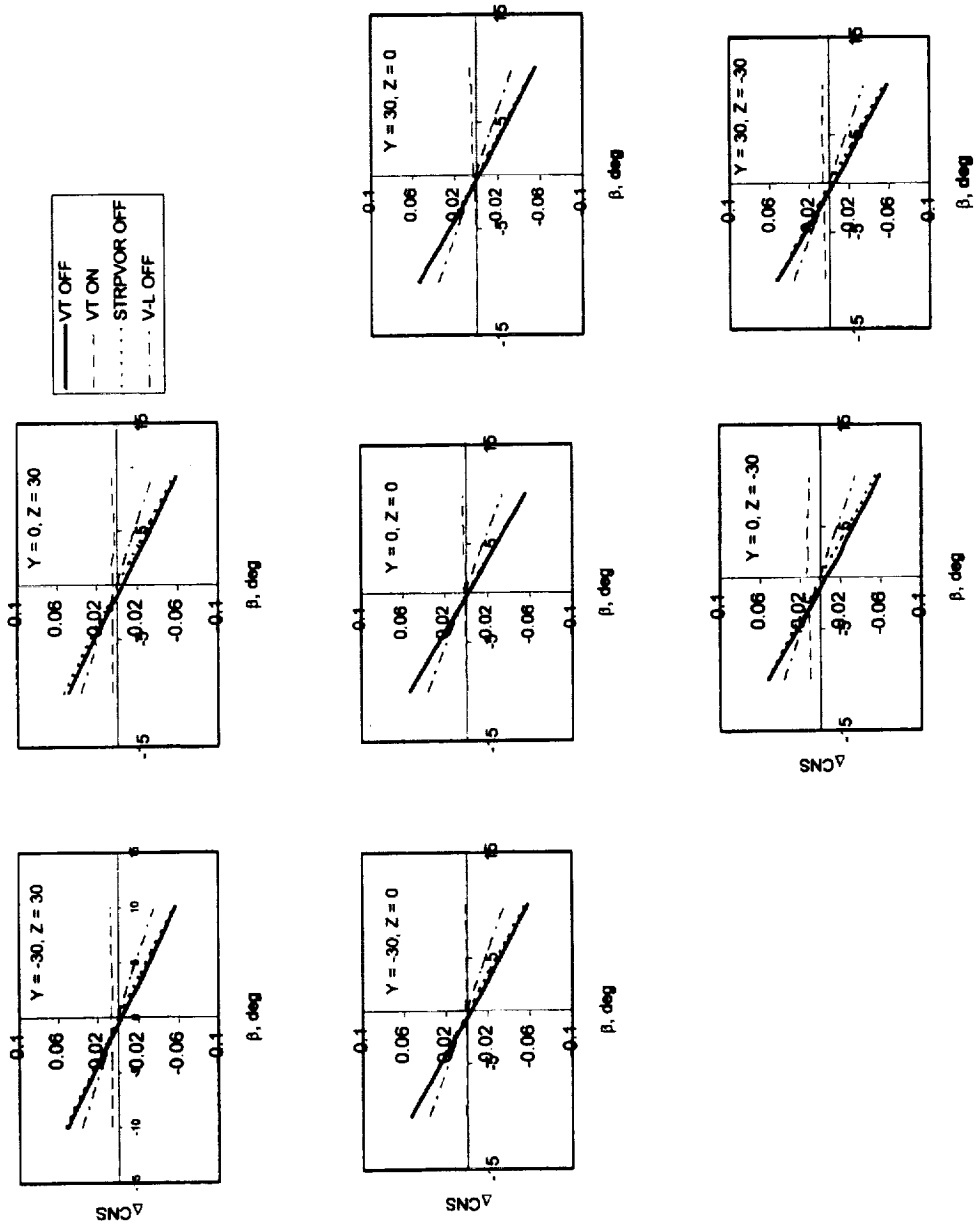

Figure 41: Change in Yawing Moment - Vertical tail off - large wing 30'x60' static test (CL=0.28, $\alpha = 4$)

to be more accurate than the strip theory model.

3.2 Small Wing

Initially alpha and beta sweeps will be viewed to determine whether the models will give accurate results when compared to experimental data. The changes in the sideforce coefficient are shown in Figure 42. At (0,0) the strip theory results deviate from the experimental data at higher angles of attack. Locations (0,-30) and (-30,30) show large discrepancies in accuracy for both models. Figure 43 shows that the models have accurately predicted the changes in pitching moment at all locations. The changes in the lift coefficient also show good agreement with experimental data for all locations as shown in Figure 44. For all locations the changes in the drag coefficient are also in good agreement with the experimental data. The only model for drag is the vortex-lattice model. At high angles of attack there is a slight separation between the model data and the experimental data. The difference in the results viewed is very small. Again both models are in good agreement with the experimental data when looking at the rolling moment, Figure 45. It appears that the vortex-lattice model is more accurate than the strip theory model. The changes in yawing moment located in Figure 46 show agreement for both models at (-30,0), (0,30), (30,0) and (-30,30). For locations (0,0) the vortex-lattice model is in good agreement, but the strip theory model has discrepancies. Further, at locations (0,-30) and (30,-30) the models do not accurately reflect the experimental data. Figure 47 shows large inaccuracies in the modeling of the rolling moment. The results show that the sideforce coefficient and the yawing moment are the more sensitive of the forces and moments for the alpha sweep. These sensitivities also

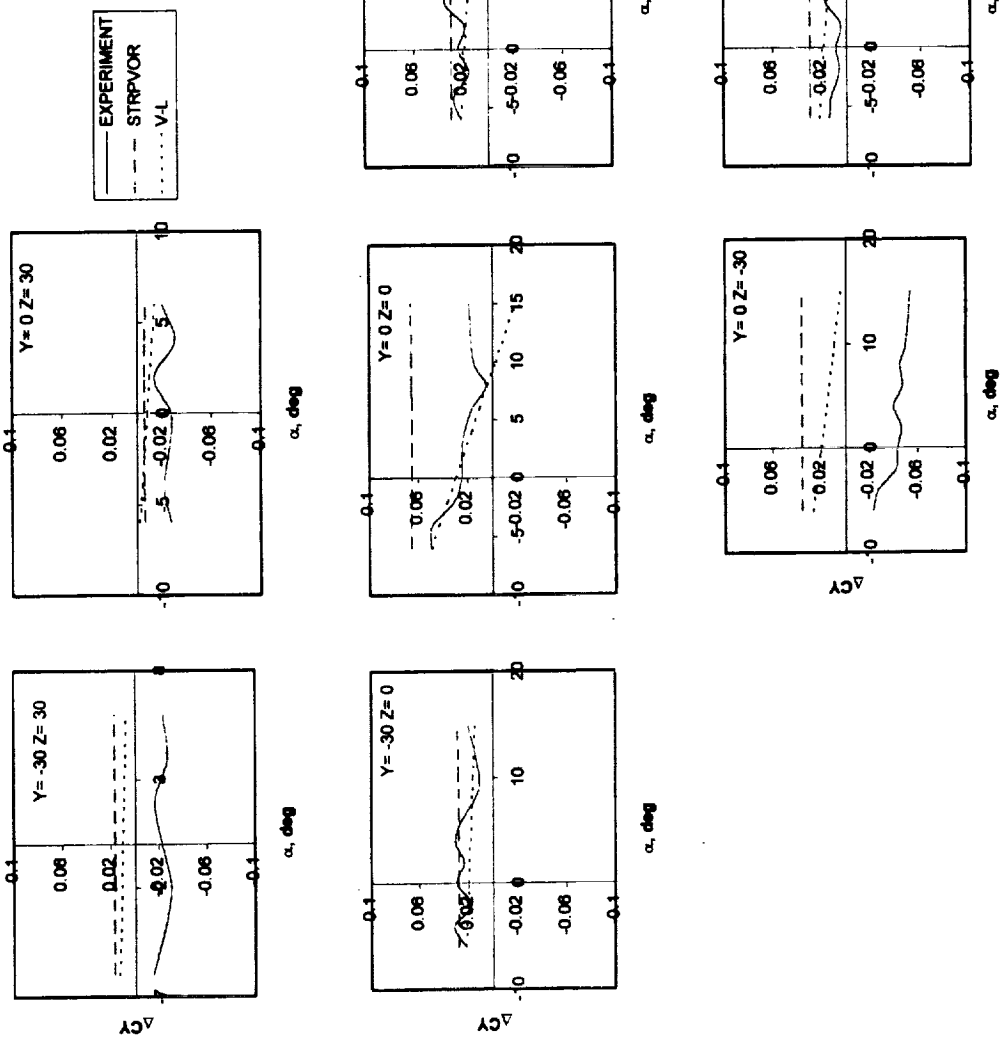

Figure 42: Change in Sideforce Coefficient - small wing 30'x60' static test (CL = 0.56, β = 0)

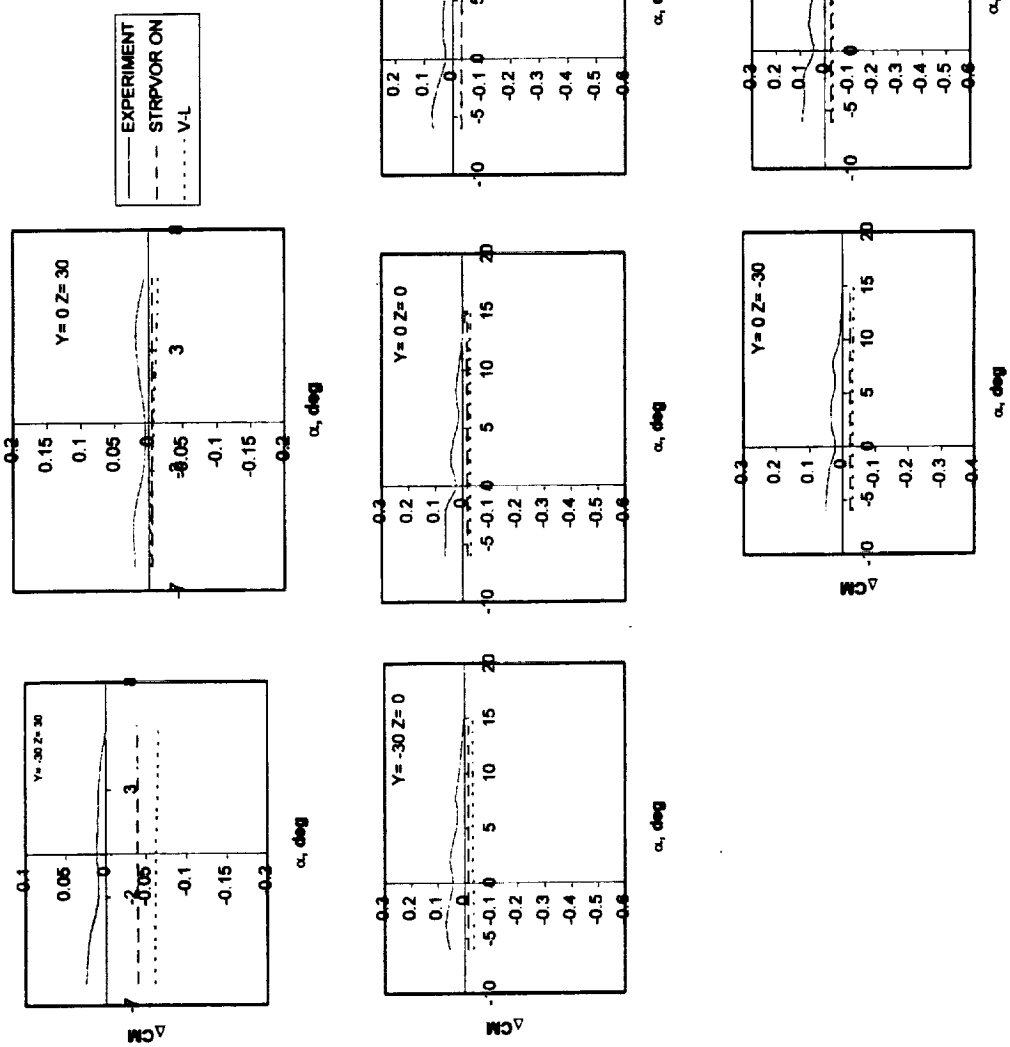

Figure 43: Change in Pitching Moment - small wing 30'x60' static test (CL = 0.56, $\beta = 0$)

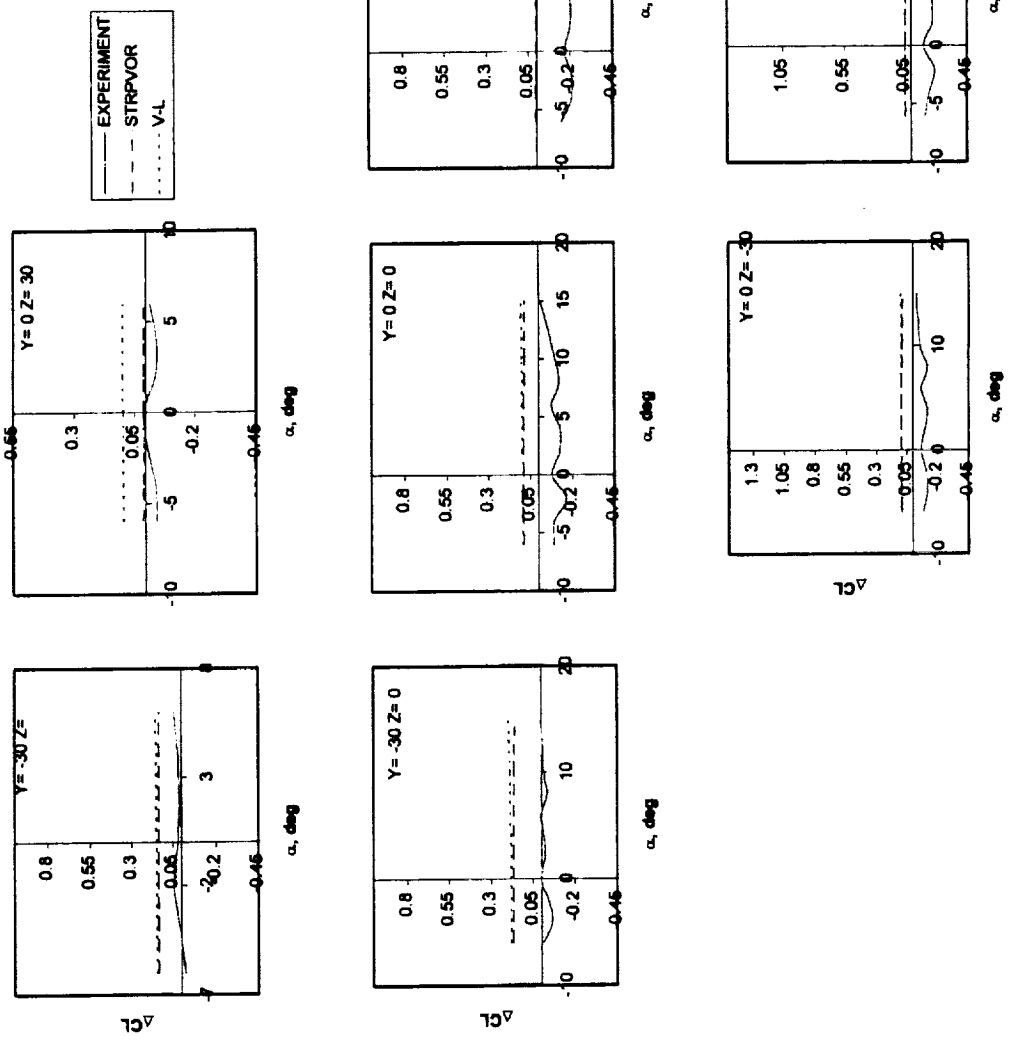

Figure 44: Change in Lift Coefficient - small wing 30'x60' static test (CL = 0.56, β = 0)

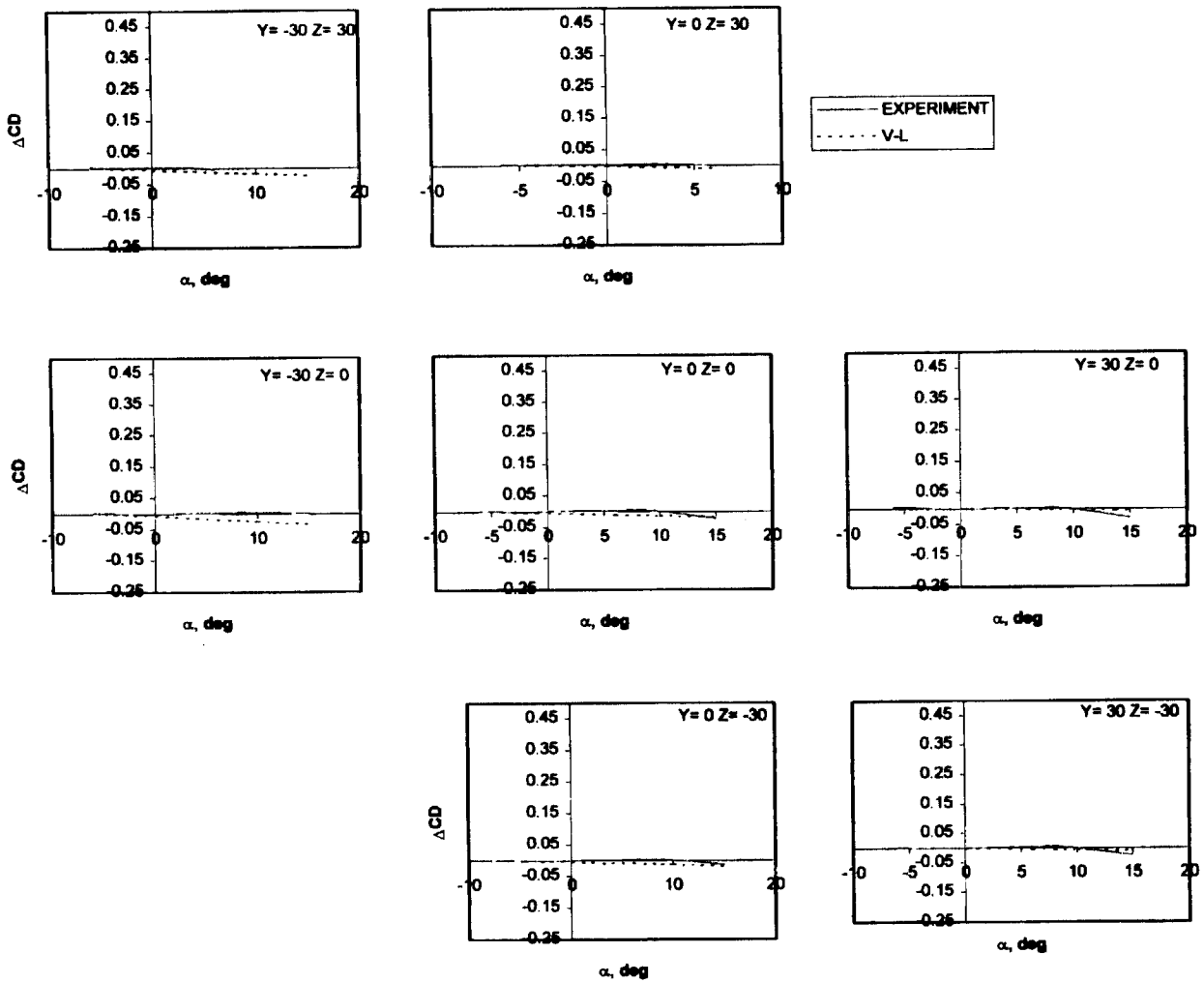

Figure 45: Change in Drag Coefficient - small wing 30'x60' static test (CL = 0.56, $\beta = 0$)

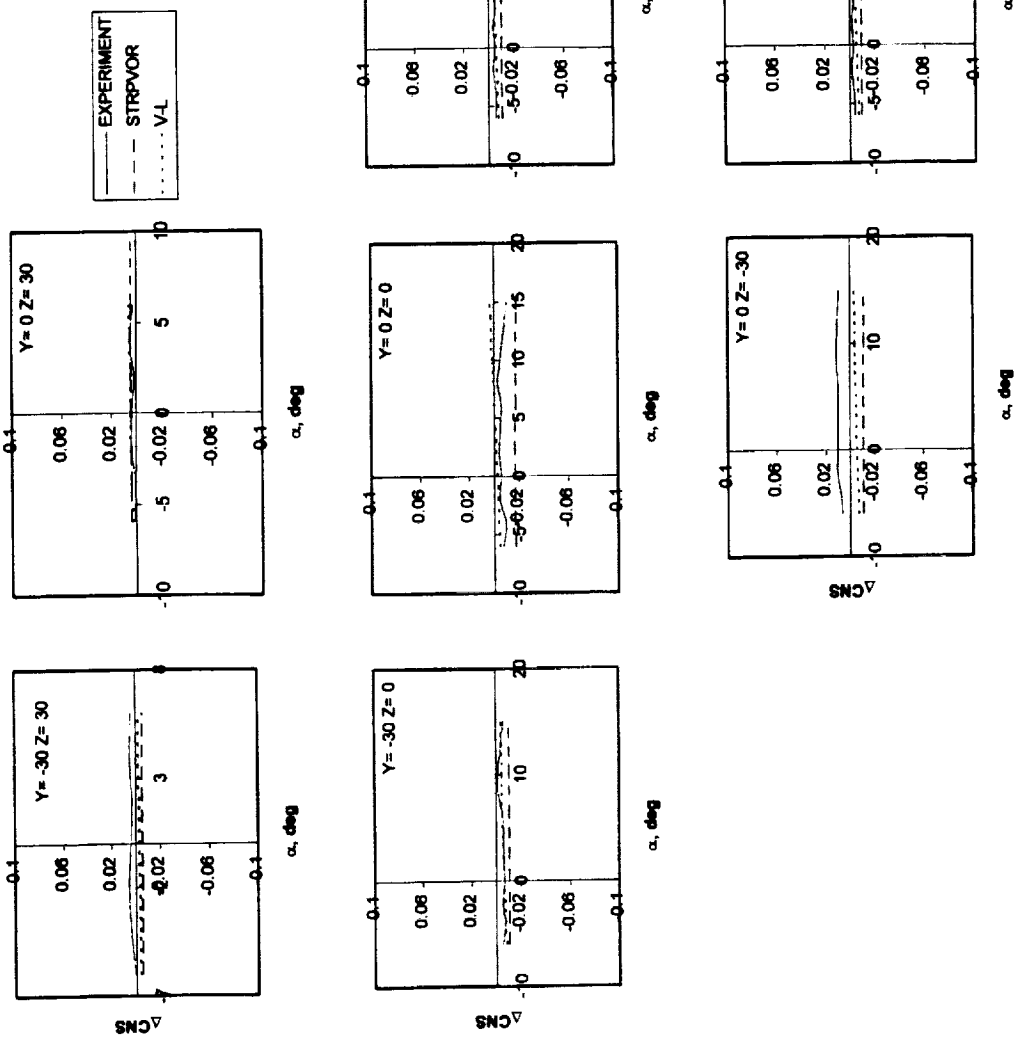

Figure 46: Change in Yawing Moment - small wing 30'x60' static test (CL = 0.56, $\beta = 0$)

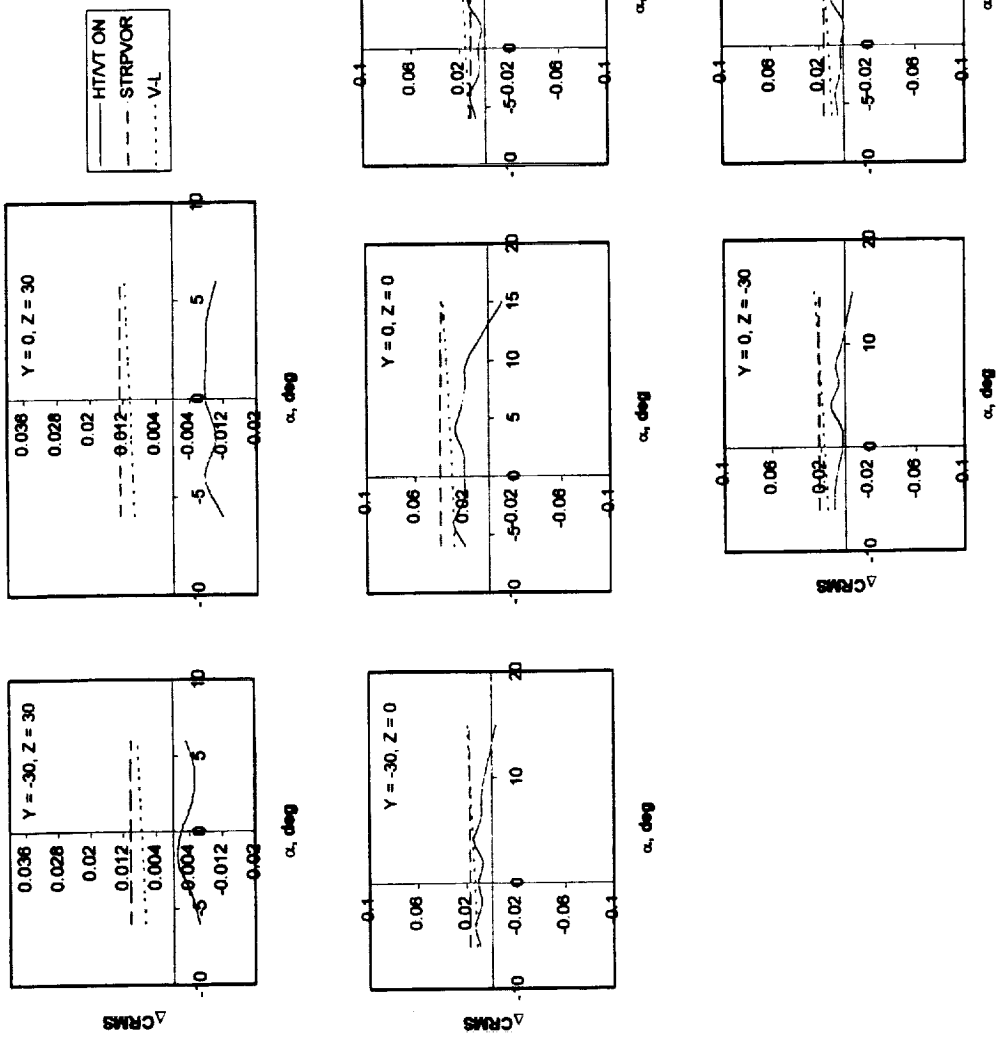

Figure 47: Change in Rolling Moment - small wing 30'x60' static test (CL = 0.56, $\beta = 0$)

appear to depend on location.

Beta sweep results for the case where the strip theory and vortex-lattice models and the experimental model have full geometry will also be compared to determine accuracy of the strip theory model and the vortex-lattice model. The sideforce coefficient shows inaccuracies at (0,0) in that the strip theory model does not resemble the experimental data, but the vortex-lattice model shows reasonable accuracy as the angle is increased. This is shown in Figure 48. Locations (0,-30) and (-30,30) also show inaccuracies, and for location (0,-30) at high sideslip angles the vortex-lattice model again approaches the experimental data. The remaining locations are also in good agreement with experimental data. The changes in the pitching moment, Figure 49, show inaccuracies in both models at all locations. Location (0,0) initially has good agreement at low angles, however in Figure 50 it can be seen that the models do not resemble the change in lift coefficient. This is consistent at all locations. Consistency is also achieved in Figure 51 where the changes in drag coefficient are compared. The vortex-lattice model shows excellent agreement with the experimental data. Although, at high angles there is a separation between the two data sets, but the separation is so small it can be neglected. When comparing the changes in rolling moment it was determined that all data was in good agreement with experimental data except for location (0,30) which can be seen in Figure 52. It has also shows that the vortex-lattice model is more accurate than the strip theory model. Changes in yawing moment found in Figure 53 show good agreement for both models, location (0,-30) shows some discrepancies. For the beta sweep inaccuracies occurred mainly with the sideforce coefficient and the lift coefficient.

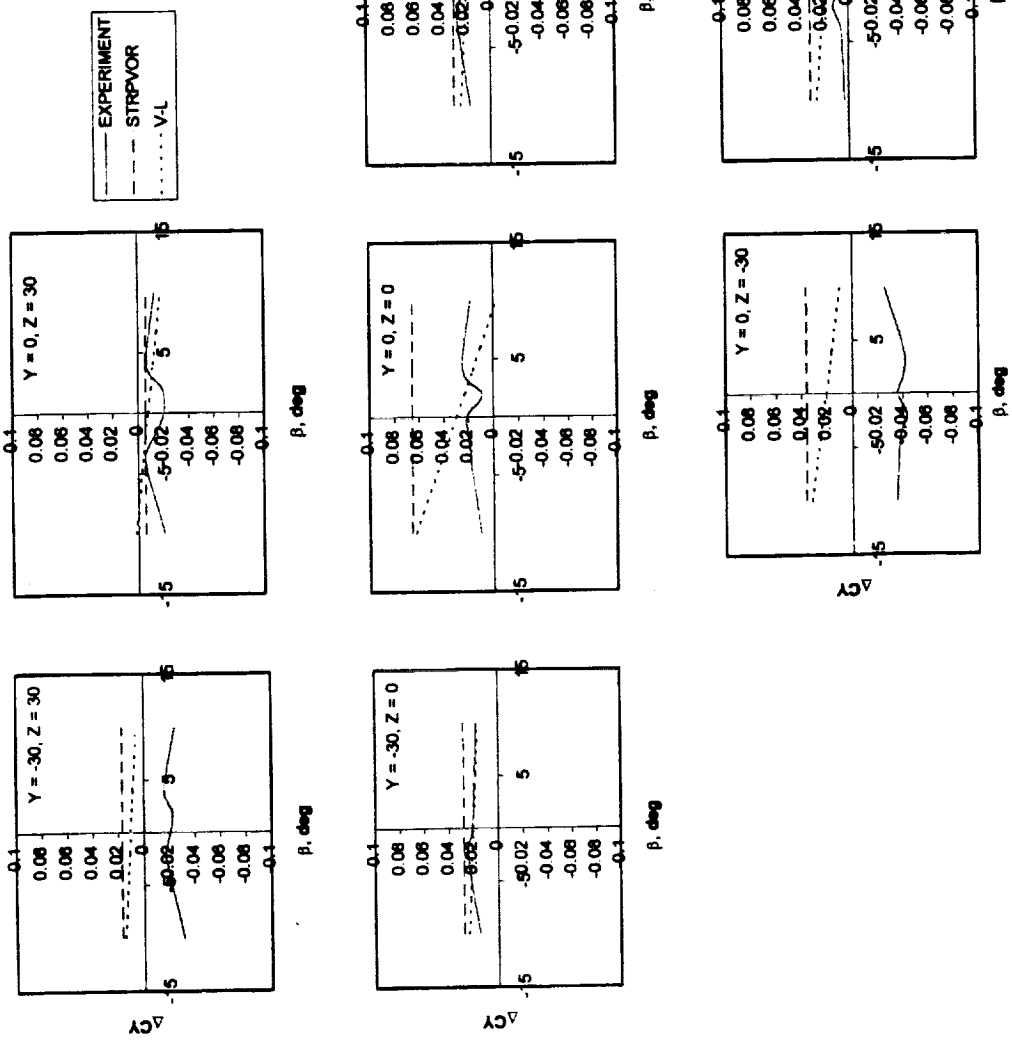

Figure 48: Change in Sideforce Coefficient - small wing 30'x60' static test (CL=0.56, $\alpha = 4$)

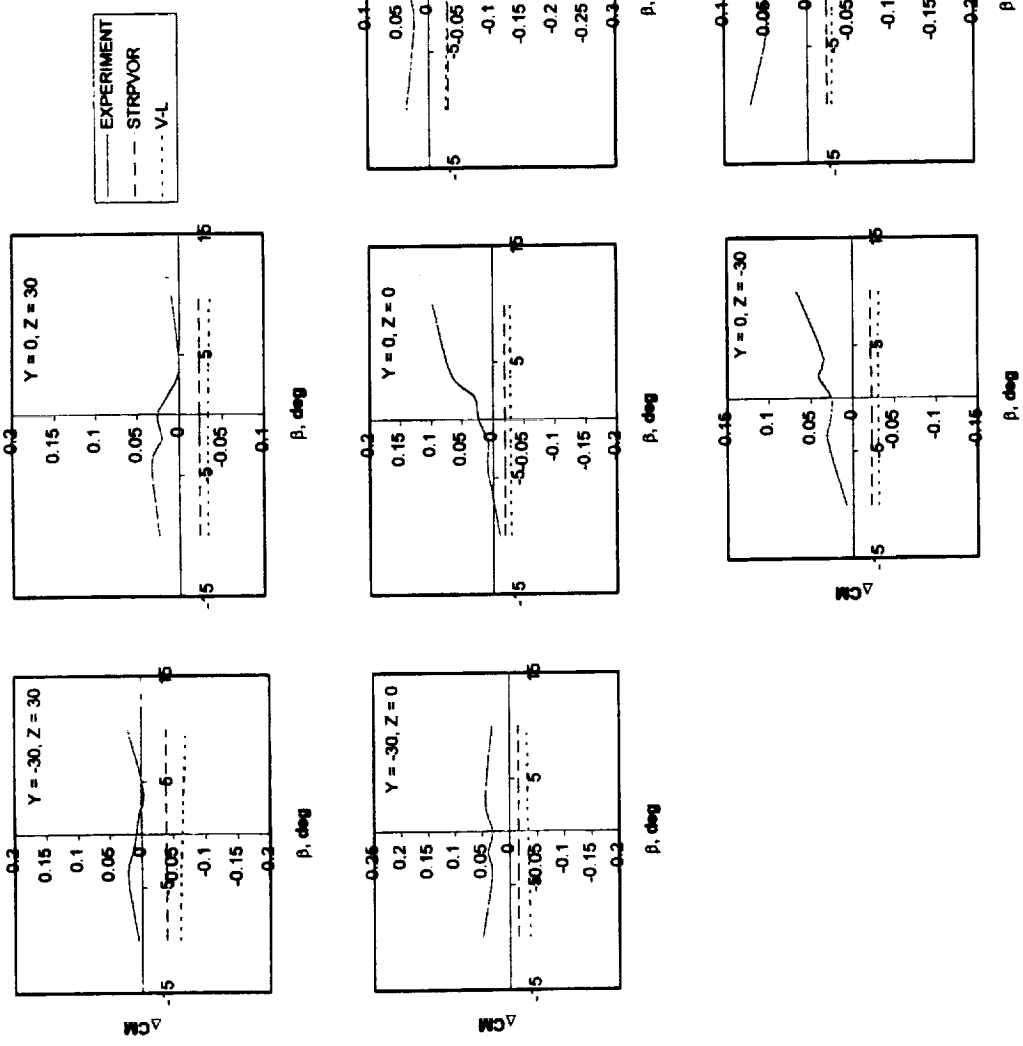

Figure 49: Change in Pitching Moment - small wing 30'x60' static test (CL=0.56, $\alpha = 4$)

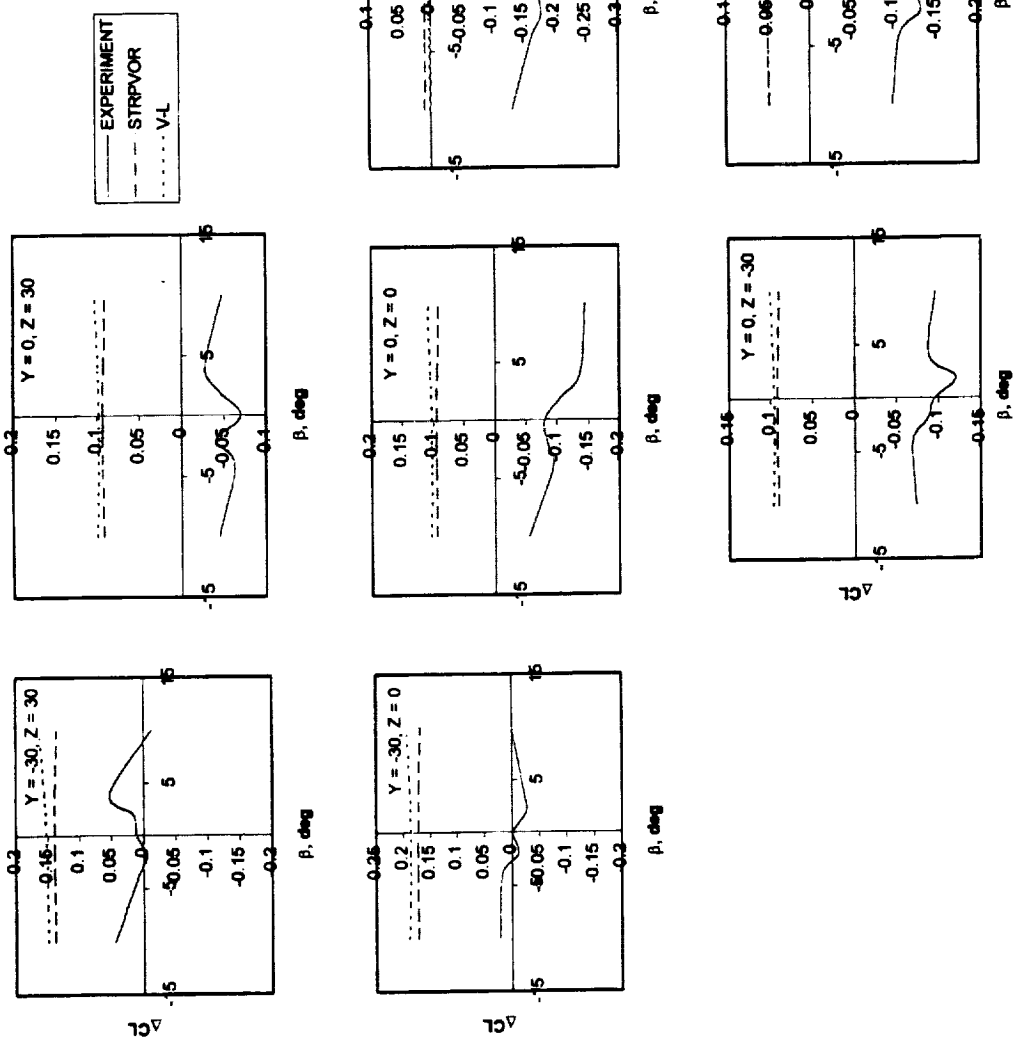

Figure 50: Change in Lift Coefficient - small wing 30'x60' static test (CL=0.56, $\alpha = 4$)

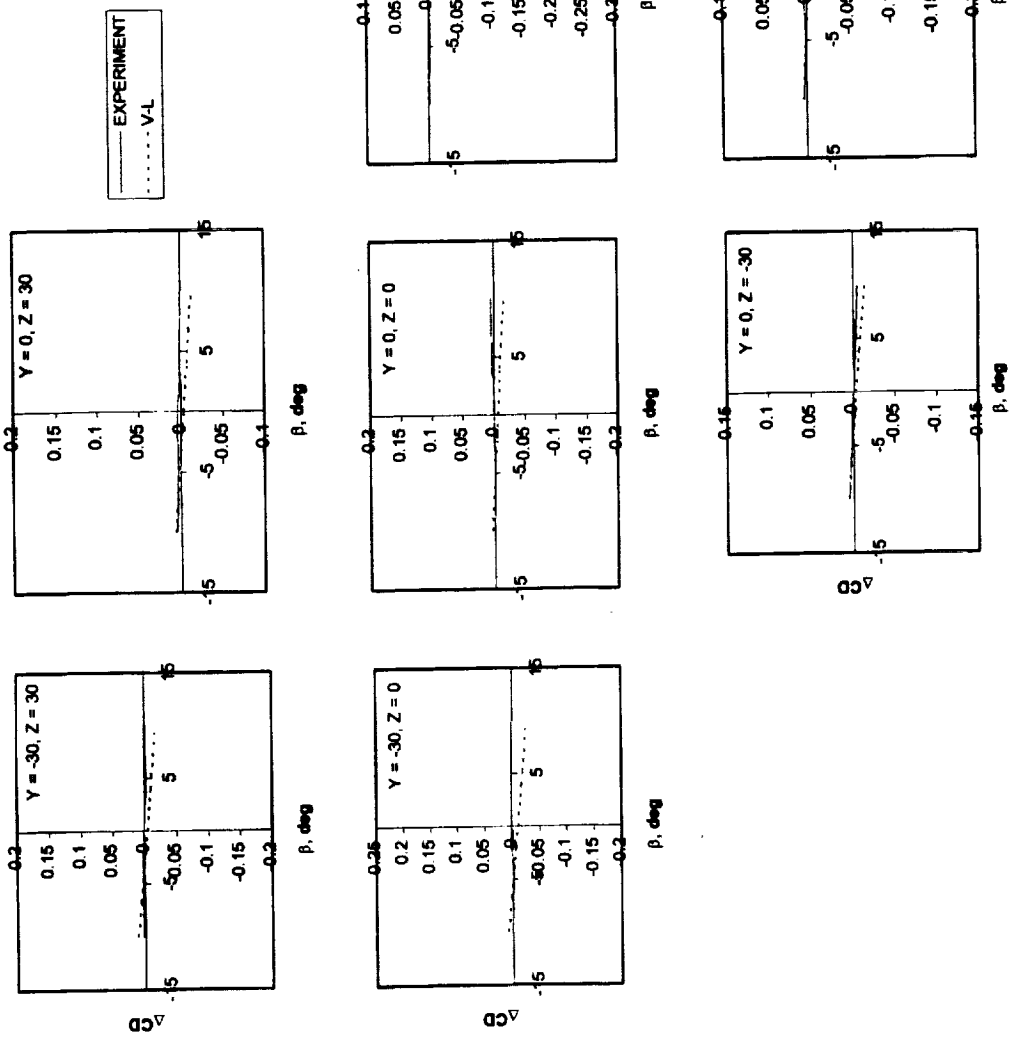

Figure 51: Change in Drag Coefficient - small wing 30'x60' static test (CL=0.56, α = 4)

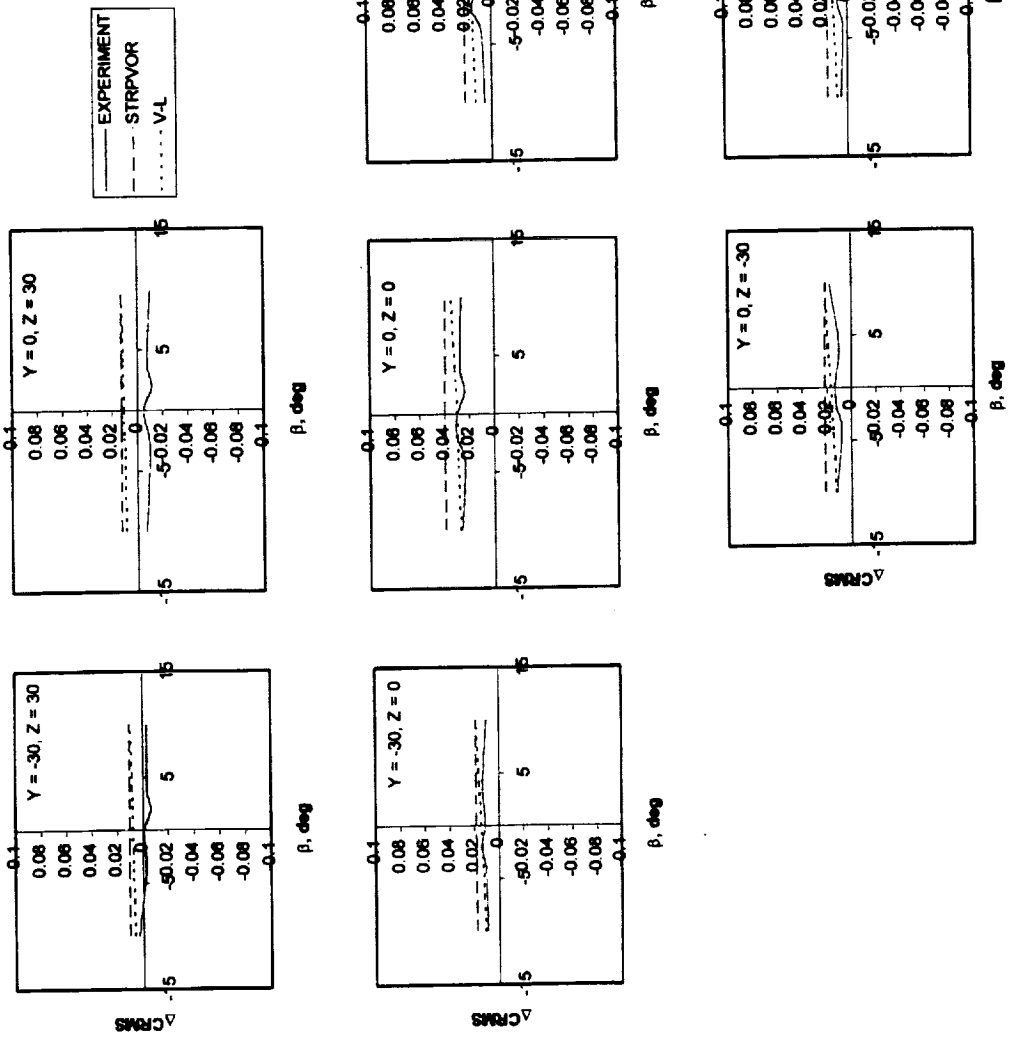

Figure 52: Change in Rolling Moment - small wing 30'x60' static test (CL=0.56, $\alpha = 4$)

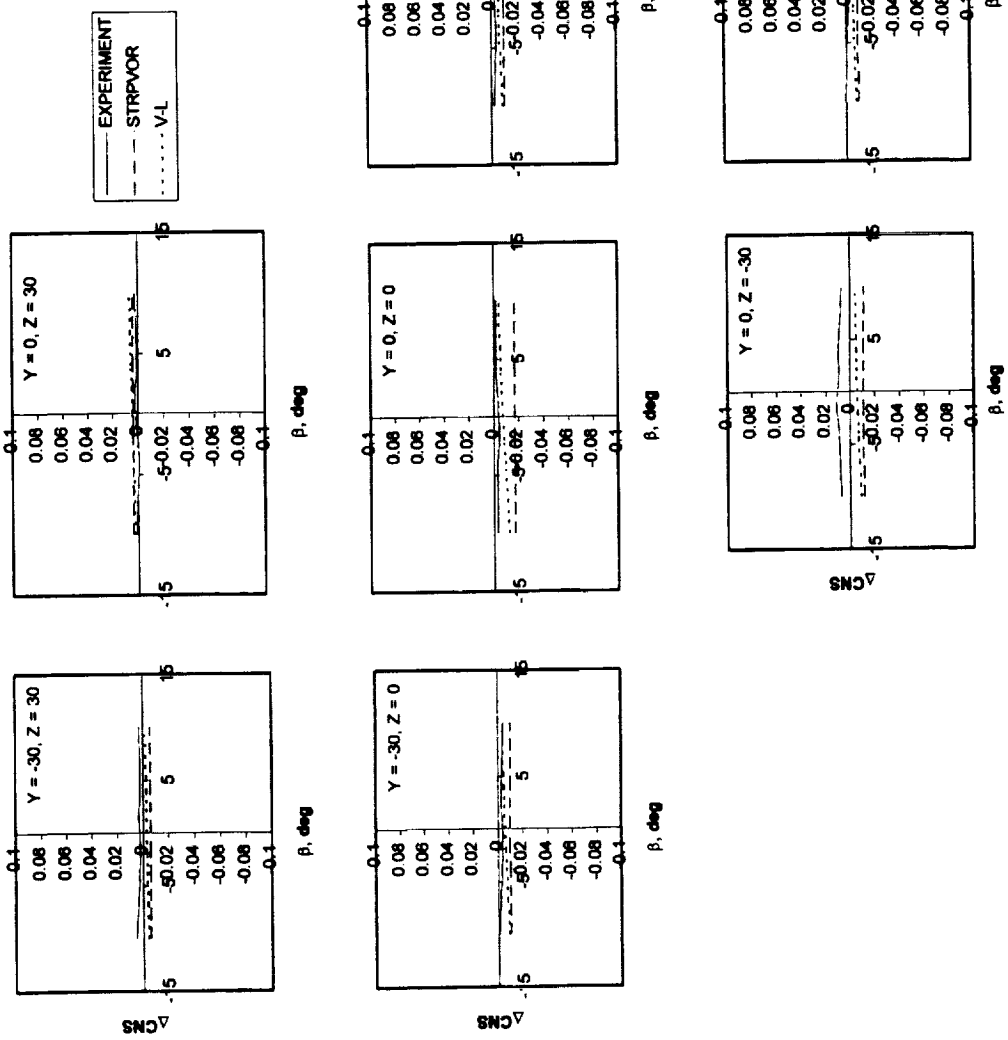

Figure 53: Change in Yawing Moment - small wing 30'x60' static test (CL=0.56, $\alpha = 4$)

For the small generating wing, comparisons will again be made for partial geometry. The only available experimental data is for the case of an alpha sweep where the horizontal stabilizer and vertical tails are removed. Beginning with the changes in sideforce coefficient, discrepancies can be seen in four of the seven locations, as shown in Figure 54. The inaccuracies are for locations (0,-30), (30,-30), (0,30), and (-30,30). The remaining positions show fairly accurate results. Once again the vortex-lattice model is more accurate than the strip model. Changes in pitching moment, Figure 55, can be seen to follow the now familiar linear relation to the angle of attack. The change increases with the angle of attack and will accurately model the experiment at one specific angle. The modeling of the changes in lift coefficient are accurate at (30,-30), (30,0), (0,30), and (-30,30). All locations in Figure 56 show a separation in the data at low angles of attack, but for these locations the separation is small. All other locations do not accurately model the experimental data. The data for all locations are similar for the change in drag coefficient (Figure 57). The model is in excellent agreement with experimental data. For location (0,30) the models do not accurately represent the experimental data. All other locations are accurately modeled. Finally the changes in yawing moment in Figure 58 are in good agreement with the experimental data except for position (0,-30) and vortex-lattice more accurately models the data than strip theory. Figure 59, the change in rolling moment, shows that the models are able to accurately model the experimental data. Location (0,30) does show some discrepancies between the experimental data and the models. When removing the horizontal stabilizer and vertical tail large discrepancies arouse in the changes of the sideforce coefficient and the changes in lift. There was some separation, which appeared, but they were either at large of small

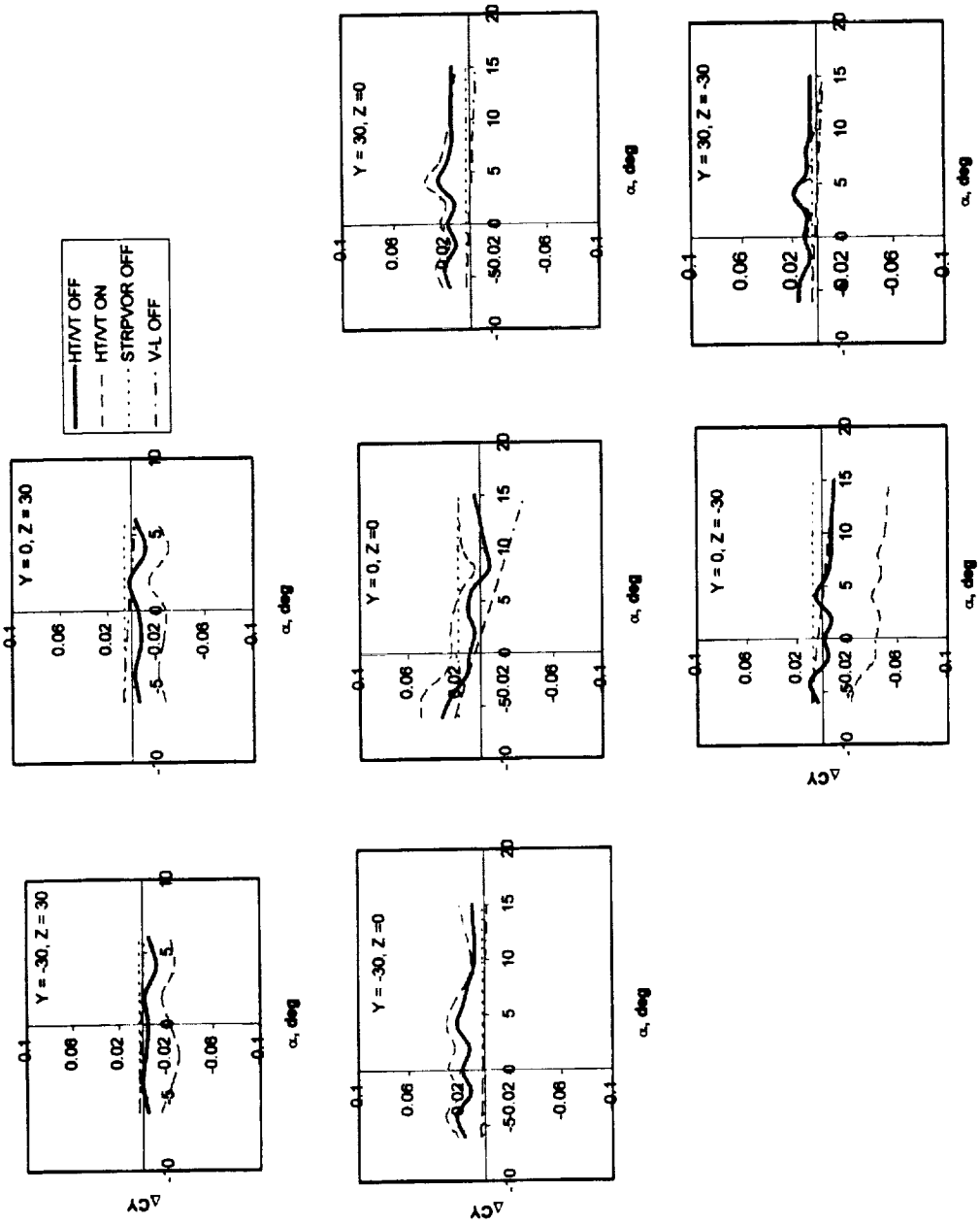

Figure 54: Change in Sideforce Coefficient - Horizontal tail and Vertical tail off - small wing 30'x60' Static Test (CL=0.56, β = 0)

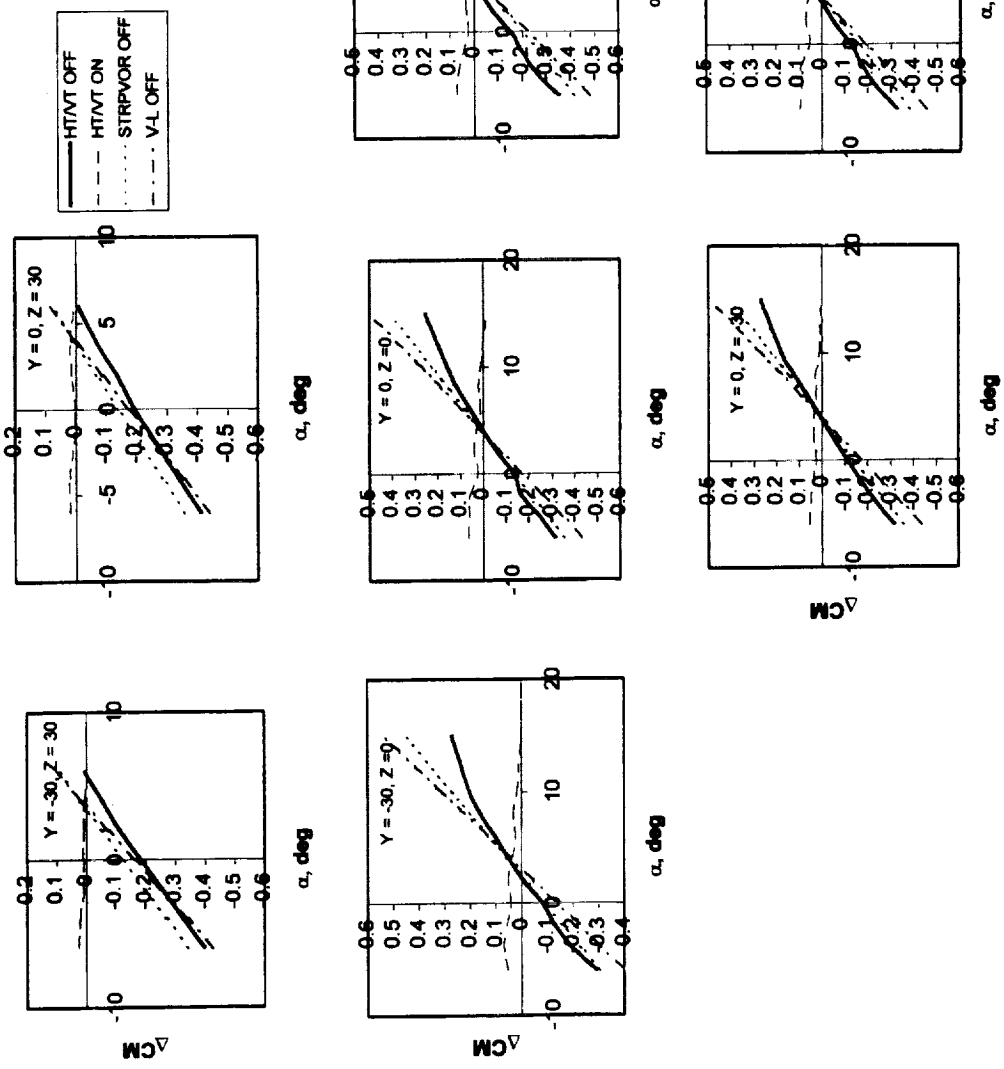

Figure 55: Change in Pitching Moment - Horizontal tail and Vertical tail off - small wing 30'x60' Static Test (CL=0.56, $\beta = 0$)

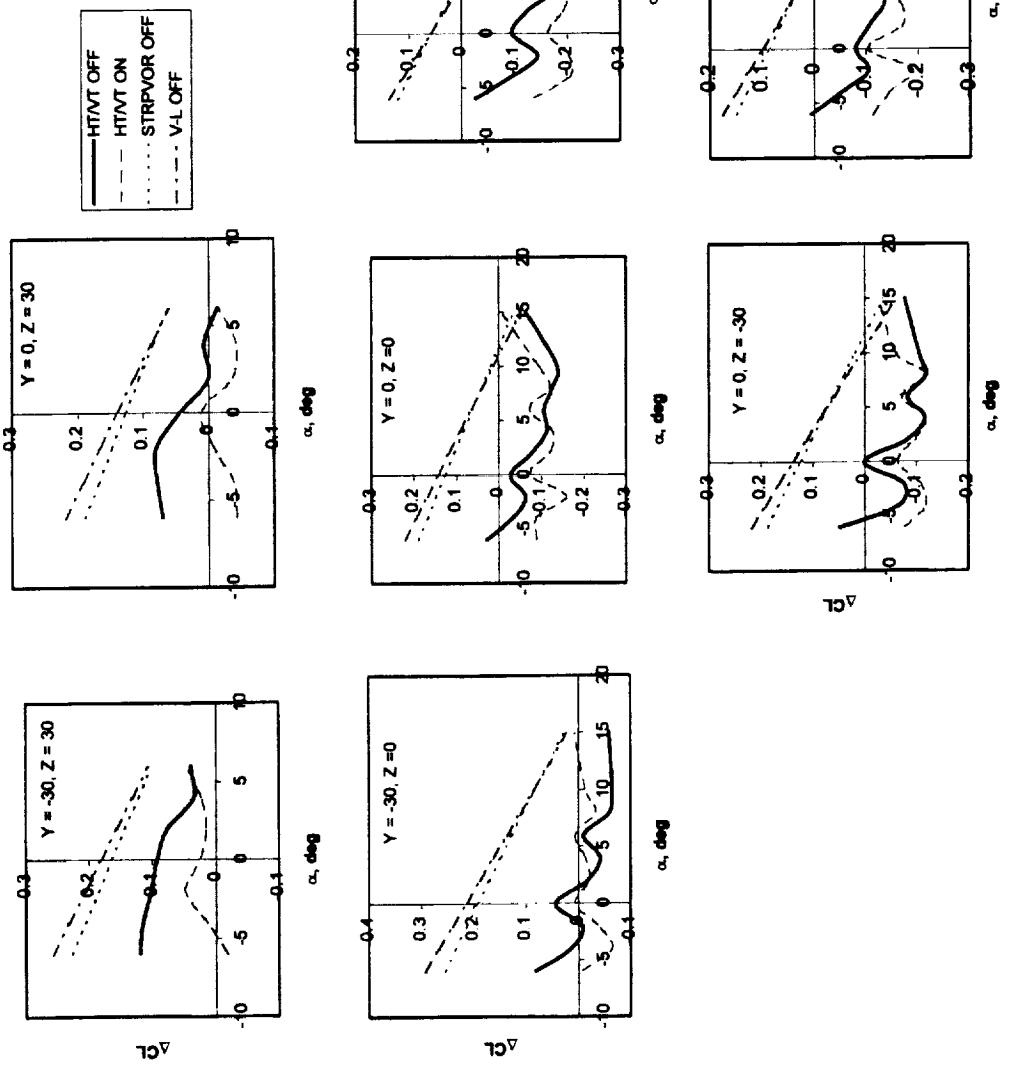

Figure 56: Change in Lift Coefficient - Horizontal tail and Vertical tail off - small wing 30'x60' Static Test (CL=0.56, β = 0)

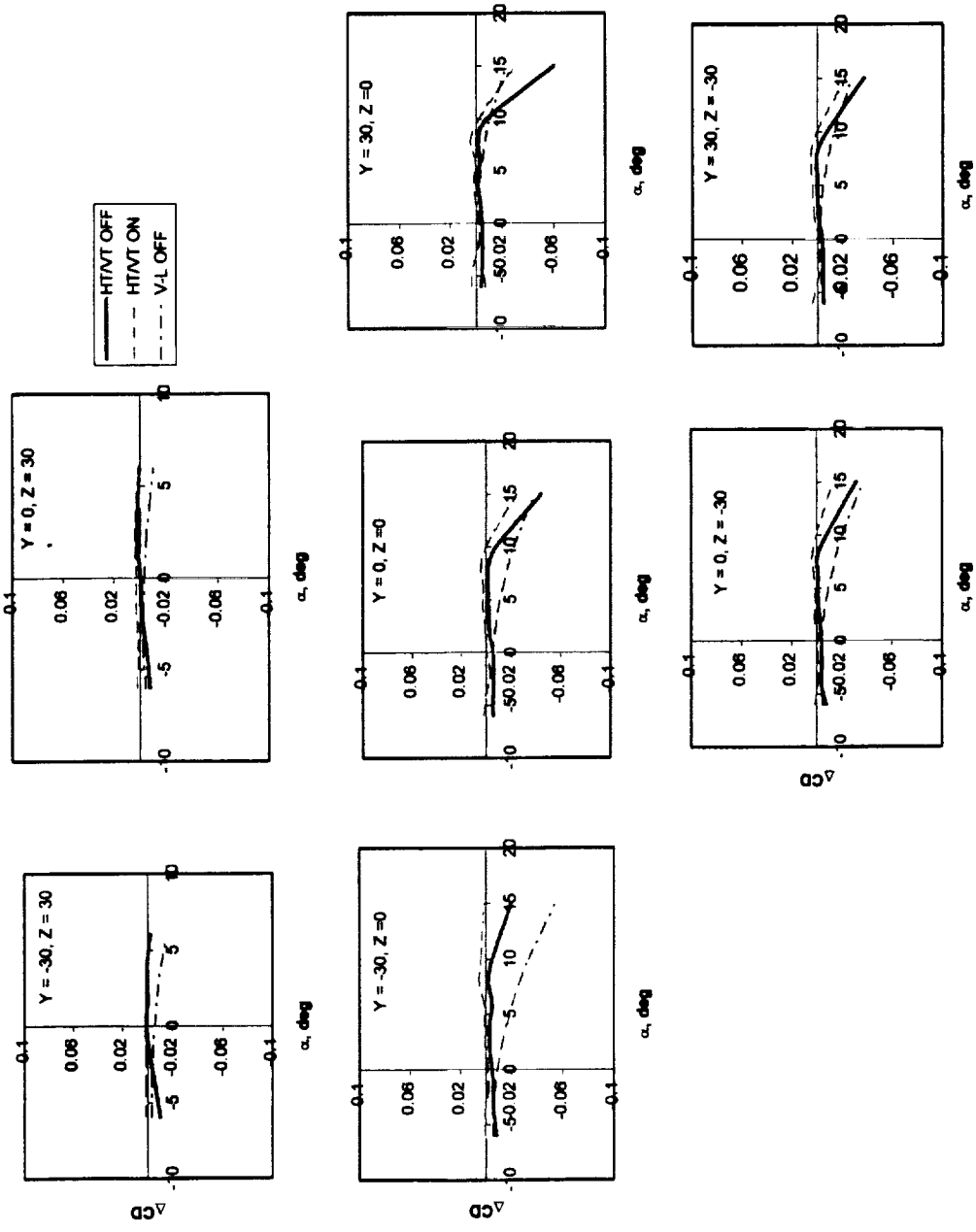

Figure 57: Change in Drag Coefficient - Horizontal tail and Vertical tail off - small wing 30'x60' Static Test (CL=0.56, β = 0)

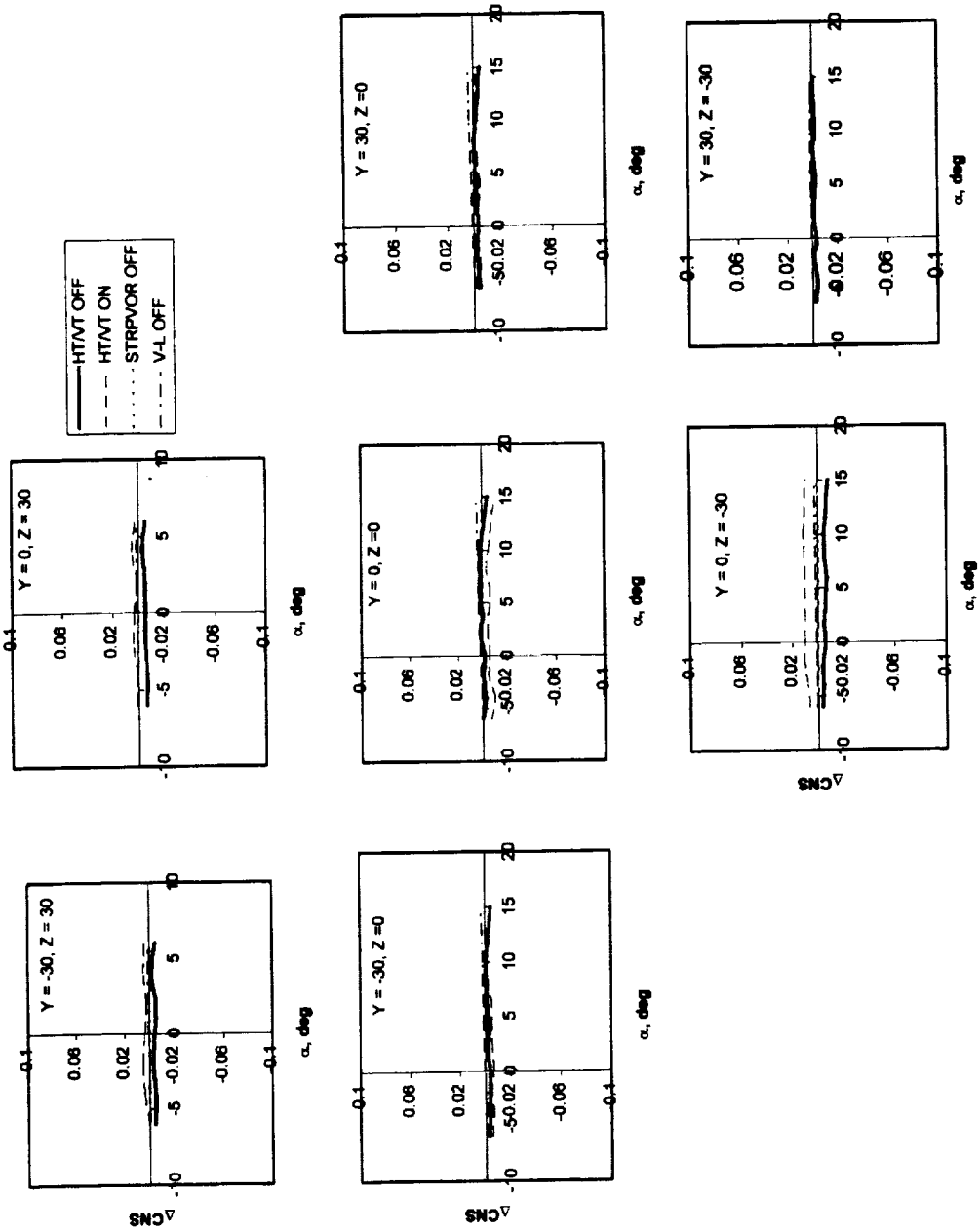

Figure 58: Change in Yawing Moment - Horizontal tail and Vertical tail off - small wing 30'x60' Static Test (CL=0.56, β = 0)

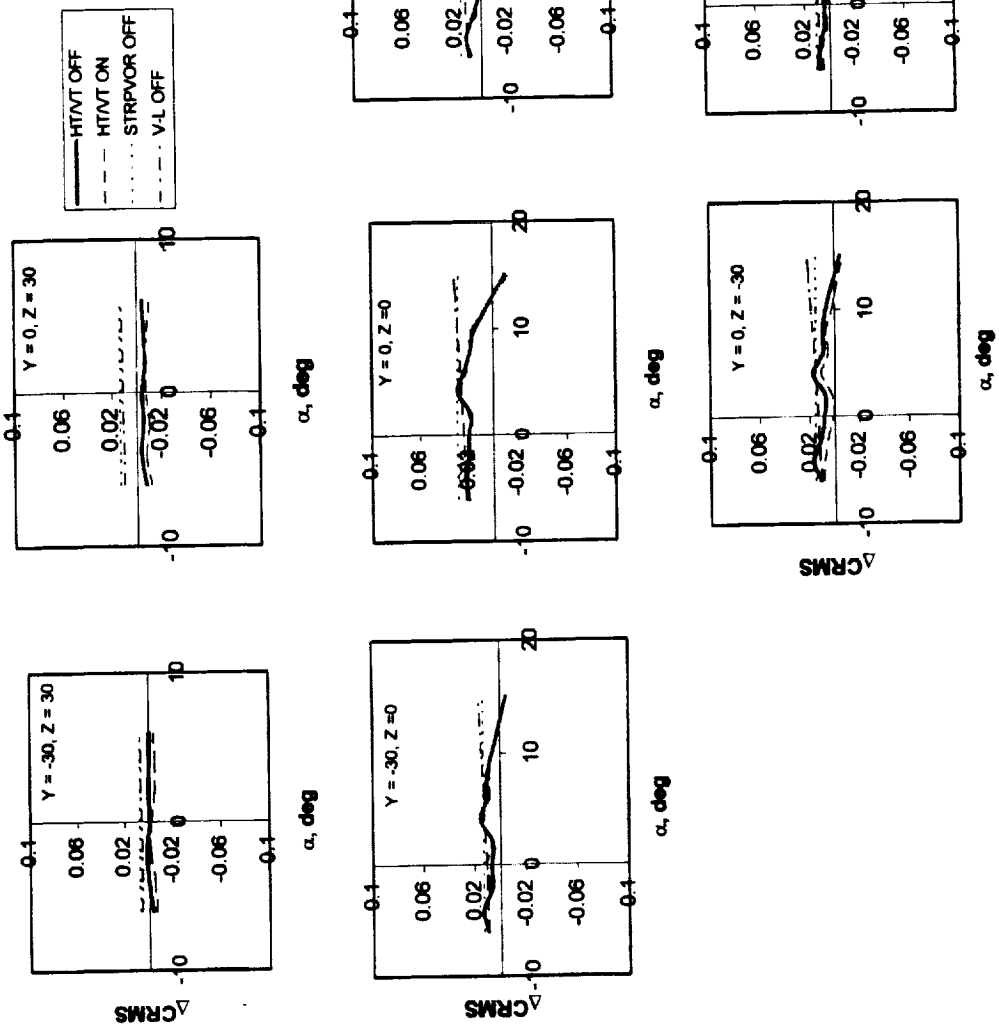

Figure 59: Change in Rolling Moment - Horizontal tail and Vertical tail - small wing 30'x60' static test (CL=0.56, β = 0)

angles of attack. This was due to the separation in the flow.

Previously, when results from the large generation wing and small generating wing was compared, the data from the two generating wings did not appear to show consistent results with each other. The results from the small generating wing actually are similar to the results for the large generating wing. The comparisons are not similar in magnitude for most cases, and the strip theory model and vortex-lattice model are not of the same magnitudes. Most modeling problems appear along the y-axis. Removal of the horizontal stabilizer and vertical tail returned better results than the removal of only the vertical tail.

3.3 Sensitivity Analysis

The sensitivity analysis is used to take a closer look at the strip theory and vortex-lattice models. In performing this analysis it will be determined how much the model will deviate from the calculated results with a 10% error in the input data. Graphs where 10% of the calculated results was added and subtracted from the models have been created. Only sideforce coefficient and pitching moment for the large generating wing with alpha sweep and pitching moment for beta sweep will be observed. In Figure 60 for the sideforce coefficient we see there is virtually no deviation from the calculated results and the 10% increase and decrease. Figure 61 shows the same results as in Figure 60, but at location (-30,30) we can see that with a larger change in the reaction the increase and decrease from the measured results are slightly greater. After viewing Figure 62 it can be seen once again that with increased magnitudes, the 10% variations also increase.

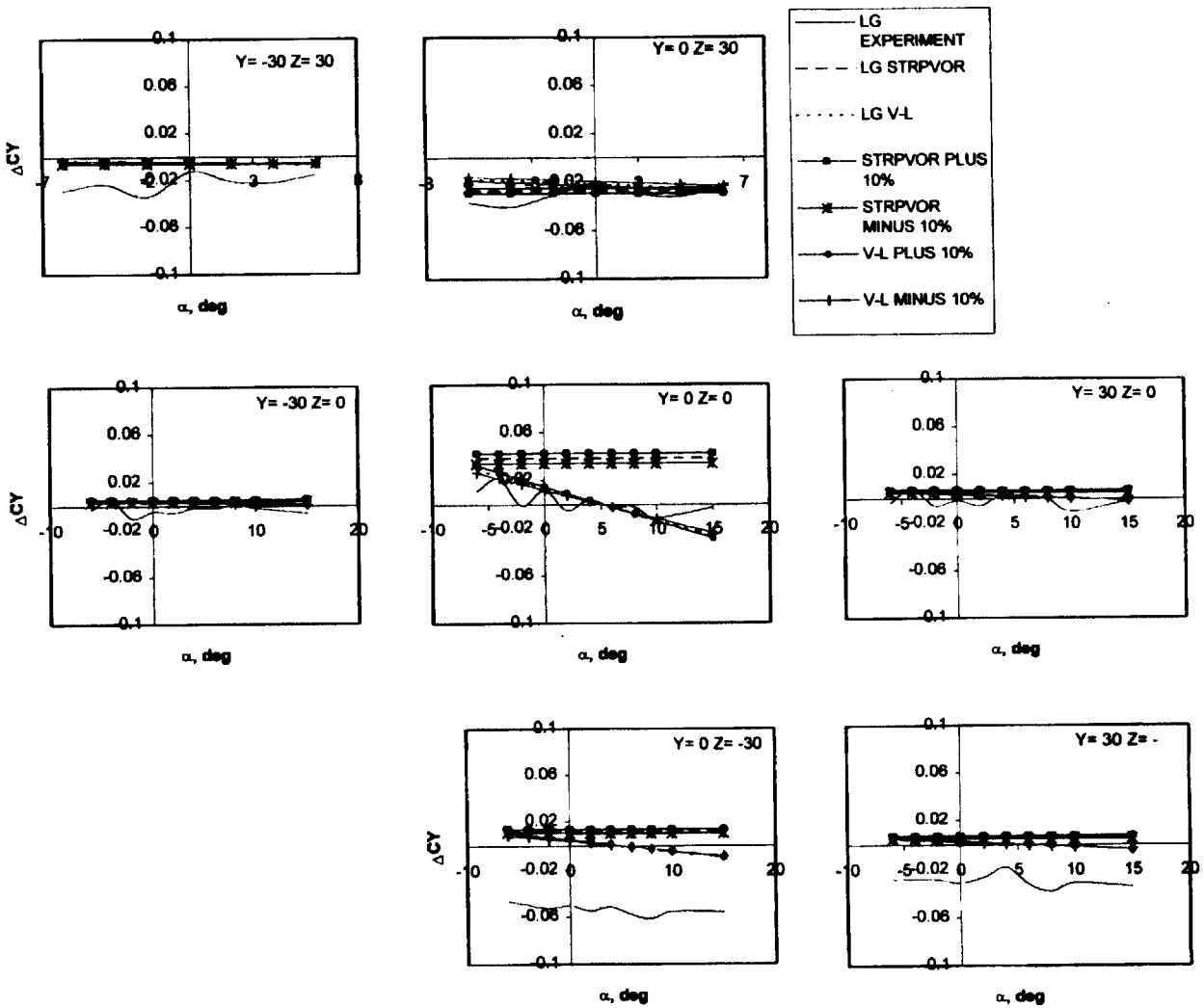

Figure 60: Change in Sideforce Coefficient - Sensitivley Analysis - large wing 30'x60' static test (CL = 0.28)

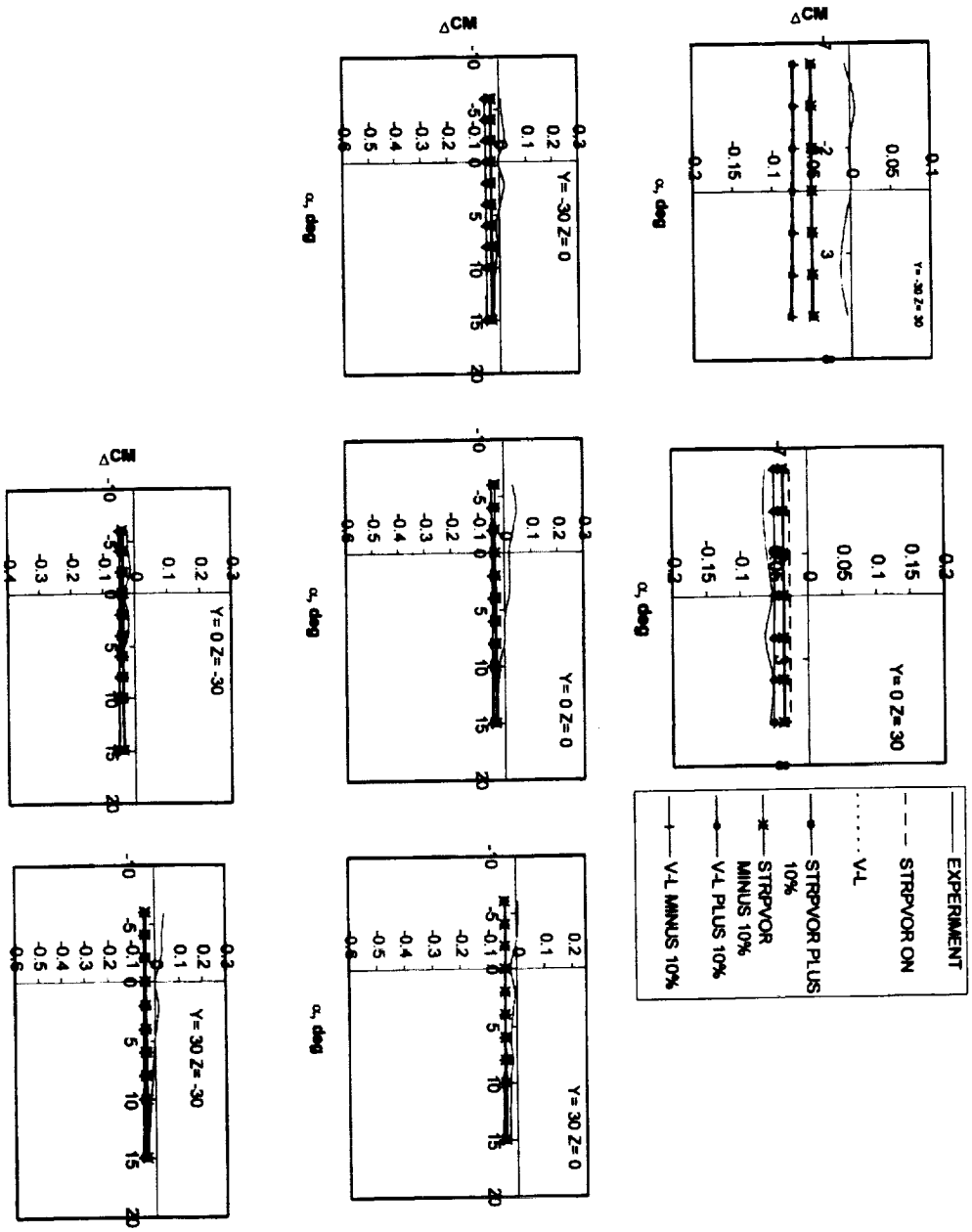

Figure 61: Change in Pitching Moment - Sensitivity Analysis - large wing 30'x60' static test (CL = 0.28)

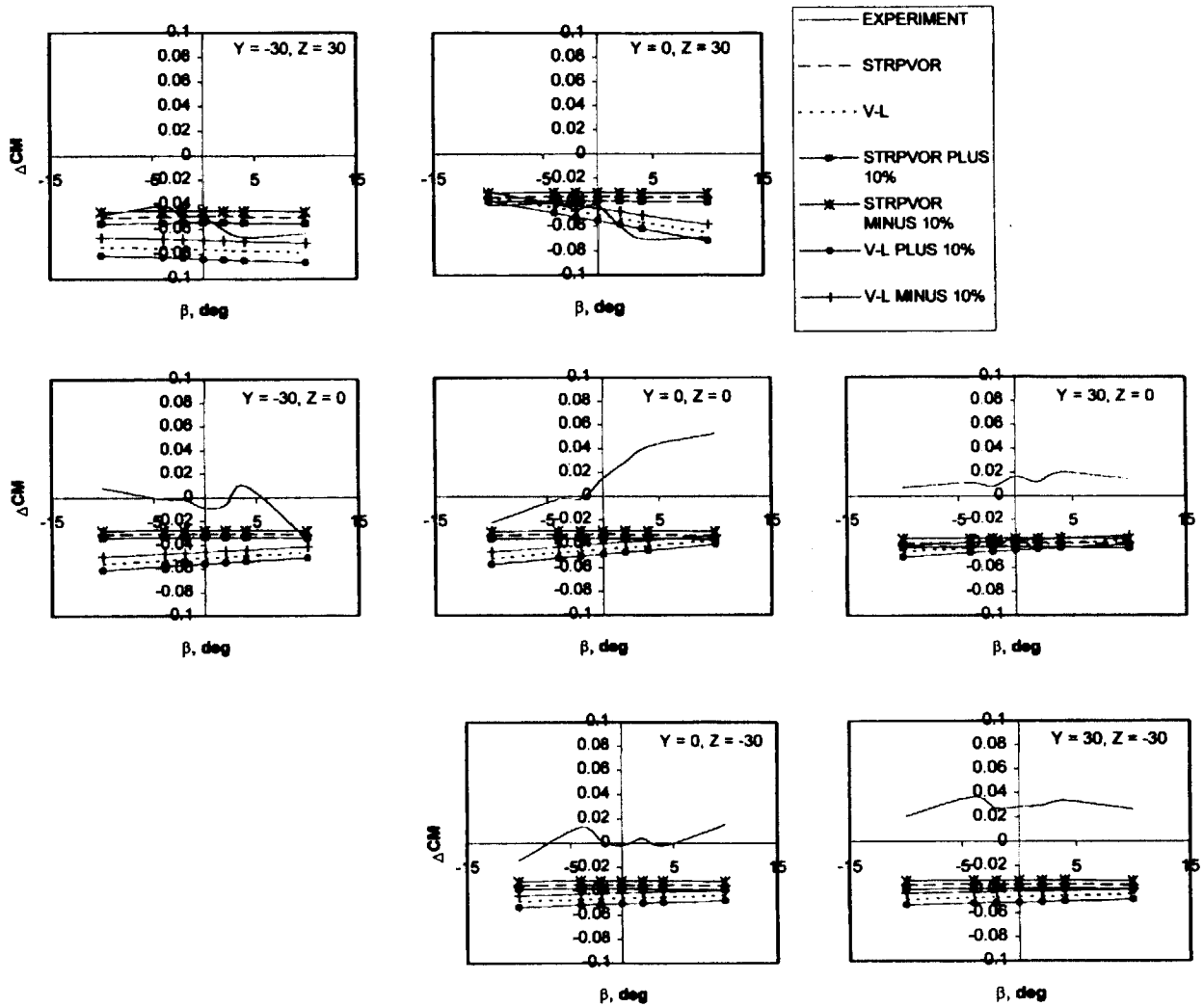

Figure 62: Change in Pitching Moment - Sensitivity Analysis -large wing 30'x60' static test (CL=0.28)

These three graphs were chosen, because they show results with large deviations from experimental data one shows small deviations from experimental data. It can also be seen that the pattern is consistent. With the larger magnitudes, the 10% deviation shows some difference from the computed results, but the difference appears to be insignificant.

CHAPTER 4: CONCLUSION

The purpose of this research was to validate the strip theory and vortex-lattice modeling techniques. As previously stated the models have been used in the past, but they have never been validated with experimental data. In the past they were tested by pilot subjective evaluation. The pilots were asked their opinion as to whether a simulation encounter was hazardous or acceptable, and the results aided in the development of the separation distances used today. This testing of the models was acceptable for the period when aircraft could be easily categorized as small, large, and heavy. With the increase in civil transport and changing aircraft design it is becoming more difficult to categorize the aircrafts by the old standards, therefore more rigorous testing must be accomplished in order to create more precise separation distances. Strip theory and vortex-lattice modeling techniques would be ideal to aid in the development of new separation distances because they are simple enough to be used in piloted simulations. The models will save time and money compared to designing an experiment for each encounter situation.

There were three objectives to this research. Initially alpha sweeps and beta sweeps were observed. The strip theory model and vortex-lattice model both had full geometries which consist of the wing, the horizontal stabilizer, and the vertical tail. The experimental model was also comprised of its full geometry. Both models were compared to the experimental data for both sweeps. This was done in order to determine if the models could accurately regenerate the force and moment data that was recorded in the wind tunnel experiment. Next, an alpha sweep was done when the horizontal

stabilizer and vertical tail was removed from both models and the experimental model. Comparisons were then made with the strip theory model, the vortex-lattice model, the experimental model. The experimental model with the horizontal stabilizer and vertical tail still on was also compared. A beta sweep was then performed when only the vertical tail was removed from the models and the experimental model. These comparisons were made to determine if, with the removal of the tails, the computational models could still accurately predict the experimental data. With this capability, computer time and cost would be decreased. Finally, a sensitivity analysis was performed. With this analysis it could be observed how accurately the models could predict the experimental data if there was a 10% error in the model input data. This was needed to view how mis-modeling the reaction would effect the final results.

Experimental data was taken for a large generating wing and a small generating wing. Comparisons were initially performed between the forces and moments for the large and small generating wings. If the forces and moments between the two were observed to be approximately the same for the experimental data, the strip theory model, and vortex-lattice model then concentration would have been given only to the large generating wing. From the comparison the two did not show enough consistency in the experimental results to be able to omit one of the generating wings.

For the alpha sweep, that consisted of the full geometry (wing, horizontal stabilizer, and vertical tail), both models as well as the experimental model showed good results for pitching moment, drag coefficient, and yawing moment. Model calculations of the sideforce coefficient and rolling moment had problems for locations along the y-axis. The lift coefficient showed poor results. In the beta sweep with full geometry

rolling moment, yawing moment, and drag coefficient could be accurately modeled. Pitching moment, lift coefficient, and sideforce coefficient showed discrepancies.

With the removal of the horizontal stabilizer and the vertical tail sideforce coefficient, pitching moment, and lift coefficient could not be modeled, while drag coefficient, rolling moment, and yawing moment could. Separation at high angles of attack was viewed for drag and rolling moment. When removing only the vertical tail sideforce coefficient, lift coefficient, pitching moment, and yawing moment could not be modeled. Drag coefficient and rolling moment remained in good agreement with the experimental data, even though rolling moment showed separation at high angles of attack.

It appears that the alpha sweep with full geometry will be able to accurately model the reactions encountered by a following aircraft. Lift can not be modeled for any of the four cases. The remaining three cases jointly had problems modeling the pitching moment, lift coefficient, and sideforce coefficient. Results from the sensitivity analysis showed very little change in the strip theory and vortex-lattice results. As the change in the forces and moments were increased and decreased the difference in the sensitivity analysis slightly increased and decreased respectively, although the magnitudes were never large enough to show significant differences.

A number of the reactions appeared to show problems along the y-axis, locations directly above and below the vortex. These locations are dominated by cross flow created by the counter clockwise direction of the vortex. Directly above the vortex center the flow is moving to the right in the positive y-direction and below the vortex the flow is moving to the left in the negative y-direction. The two corner locations (-30,30) and

(30,-30) have an equal amount of crossflow and vertical flow. These were the areas that were viewed to have the most trouble when trying to model the experimental data. In comparing the results of the strip theory and vortex-lattice models it appears that the vortex-lattice model is generally more accurate than the strip theory model. The only case were strip theory models more accurately is for pitching moment. Regardless of which model appears to be more accurate either model can be used because the inaccuracies between the two are insignificant for those cases that strip theory and vortex-lattice models are able to recreate the experimental data.

Plans to further this research involve comparing the strip theory and vortex-lattice models to a free flight wind tunnel experiment. A pilot will remotely fly the 10 % scale model of the B737-100 aircraft inside the wind tunnel. In this experiment the pilot will be able to make an approach to the vortex which is a more realistic encounter of a wake-vortex. A cable will be attached to the model that will serve as the guide for the aircraft. The model will then be flown at different locations with respect to the vortex and the forces and moments that the aircraft encounter will be recorded. The last step is to compare the strip theory and vortex-lattice models to actual flight test data. This data was taken by using the full scale B737-100 aircraft.

REFERENCES

1. Dunham, R.E.; Stuever, R.A.; and Vicroy, D.D.: "The Challenges of Simulating Wake Vortex Encounters and Assessing Separation Criteria," AIAA Atmospheric Flight Mechanics Conference, August 9-11, 1993; Monterey, CA.

2. Vicroy, D.; Brandon, J.; Greene, G.; Rivers, R.; Stewart, E.; and Stuever, R.: "Characterizing the Hazard of a Wake Vortex Encounter," *AIAA 97-0055*, 35th Aerospace Sciences Meeting & Exhibit, January 9-10, 1997, Reno, NV.

3. Hinton, D. A.: "Aircraft Vortex Spacing System (AVOSS) Conceptual Design," NASA TM-110184, August 1995.

4. Sammonds, Robert I.; Stinnett, Glen W., Jr.; and Larsen, William E.: "Criteria Relating Wake Vortex Encounter Hazard to Aircraft Response," *Journal of Aircraft*, Vol. 14, No. 10, Oct. 1977, pp. 981-987.

5. Jenkins, M. W. M.; and Hackett, J. E.: "A Pilot-in-the-Loop, Visual Simulation of Trailing Vortex Encounters at Low Speed," *AIAA 75-104*, Jan. 1975.

6. Hastings, E. C.; and Keyser, G.L., Jr.: "Simulator Study of Vortex Encounters by a Twin-Engine, Commercial, Jet Transport Airplane," NASA TP 1966, Feb. 1982.

7. Hallock, J. N.; and Eberle, W. R.: "Aircraft Wake Vortices: A State-of-the-Art Review of the United States R&D Program,""FAA-RD-77-23, February 1977.

8. Vicroy, D.D.; and Nguyen, T.: "A Numerical Simulation Study to Develop an Acceptable Wake Encounter Boundary for a B737-100 Airplane." *AIAA-96-3372*, AIAA Atmospheric Flight Mechanics Conference, July 29-31, 1996, San Diego, CA.

9. Greene, G.C.: "An Approximate Model of Vortex Decay in the Atmosphere," Journal of Aircraft, Vol. 23, July 1986, pp. 566-573.

10. Stuever, R. A.; and Greene, G. C.: "An Analysis of Relative Wake Vortex Hazards for Typical Transport Aircraft," *AIAA 94-0810*, January 1994.

11. Crow, S. C.: "Stability Theory for a Pair of Trailing Vortices," *AIAA Journal*, pp.2172-2179, Vol. 8, No. 12, 1970

12. Kandil, Osama A.; Wong, Tin-Chee; and Liu, Chen-Huei: "Turbulent Flow Over a 747/747 Generator/Follower Configuration and Its Dynamic Response," *AIAA 94-2383*, 25th AIAA Fluid Dynamics Conference, June 1994.

13. Stewart, E. C.: "A Study of the Interaction between a Wake Vortex and an Encountering Airplane," *AIAA 93-3642*, AIAA Atmospheric Flight Mechanics Conference, August 9-11, 1993; Monterey, CA.

14. Rossow, Vernon J.; and Tinling, Bruce E: "Research on Aircraft/Vortex-Wake Interactions to Determine Acceptable Level of Wake Intensity," *Journal of Aircraft*, Vol. 25, No. 6, June 1988, pp. 481-492.

15. Margason, Richard J., Kjelgaard, Scott O., Sellers, William L., III, and Morris, Charles E. K., Jr.: "Subsonic Panel Methods – A Comparison of Several Production Codes," *AIAA 85-0280*, 23rd Aerospace Sciences Meeting, January 1985.

16. Walden, A.B.; van Dam, C.P.; and Brandon, J.M.: " Modeling of the Interaction Between a Lifting Wing and a Following Aircraft and Comparison with Experimental Results. *AIAA-9690771*, 34th AIAA Aerospace Sciences Meeting and Exhibit, January 1996, Reno, NV.

17. Rossow, V. J.: "Estimate of Loads During Wing-Vortex Interactions by Munk's Transverse-Flow Method," *Journal of Aircraft*, Vol. 27, No. 1, January 1990, pp.66-74.

18. Brandon, J.M.; Jordan, F.L.; Buttrill, C.W.; Stuever, R.A.: "Application of Wind Tunnel Free-Flight Technique for Wake Vortex Encounters." *NASA Technical Paper 3672*, November 1997; Hampton, VA.

19. Reimer, Heidi M.; and Vicroy, Dan D.: "A Preliminary Study of a Wake Vortex Encounter Hazard Boundary for a B737-100 Airplane," NASA TM 110223, April 1996.

20. Margason, Richard J.; and Lamar, John E.: "Vortex-Lattice Fortran Program for Estimating Subsonic Aerodynamic Characteristics of Complex Planforms," NASA TN D-6142, February 1971.

21. Vicroy, Dan D.: "Influence of Wind Shear on the Aerodynamic Characteristics of Airplanes," NASA TP-2827, DOT/FAA/PS-88/15, August 1988.